UNCLASSIFIED

IAEE REPORT 7203

REFLECTION OF MM WAVES FROM SNOW AND SEA ICE

Semi-Annual Technical Report
31 January 1972

By

William M. Sackinger, Principal Investigator
Tel: (907) 479-7137
and
Robert Clark Byrd, Graduate Research Assistant
Tel: (907) 479-7771

Institute of Arctic Environmental Engineering
University of Alaska
Fairbanks, Alaska
99701
Tel: (907) 479-7330

Effective Contract Date: 1 June 1971
Contract Expiration Date: 1 June 1972
Amount of Contract: $40,000

Sponsored by
Advanced Research Projects Agency
ARPA Order No. 1783
Program Code Number: 04B282
Contract Number: N00014-71-A-0365-0001

The views and conclusions contained in this document are those of the authors and should not be interpreted as necessarily representing the official policies, either expressed or implied, of the Advanced Research Projects Agency or the U. S. Government.

SCIENTIFIC OFFICER: Mr. R. K. McGregor, Code 415
Office of Naval Research
800 North Quincy Street
Arlington, Virginia 22217

UNCLASSIFIED

REFLECTION OF MM WAVES FROM SNOW AND SEA ICE

Semi-Annual Technical Report
31 January 1972

By

William M. Sackinger, Principal Investigator
Tel: (907) 479-7137
and
Robert Clark Byrd, Graduate Research Assistant
Tel: (907) 479-7771

Institute of Arctic Environmental Engineering
University of Alaska
Fairbanks, Alaska
99701
Tel: (907) 479-7330

Effective Contract Date: 1 June 1971
Contract Expiration Date: 1 June 1972
Amount of Contract: $40,000

Sponsored by
Advanced Research Projects Agency
ARPA Order No. 1783
Contract Number: N00014-71-A-0365-0001

APPROVED:

William M. Sackinger,
Principal Investigator

APPROVED:

Tunis Wentink Jr.,
Associate Director

The views and conclusions contained in this document are those of the authors and should not be interpreted as necessarily representing the official policies, either expressed or implied, of the Advanced Research Projects Agency or the U.S. Goverment.

SCIENTIFIC OFFICER: Mr. R.K. McGregor, Code 415
Office of Naval Research
Arlington, Virginia 22217

CONTENTS

Unclassified

Security Classification

DOCUMENT CONTROL DATA – R & D

(Security classification of title, body of abstract and indexing annotation must be entered when the overall report is classified)

1. ORIGINATING ACTIVITY *(Corporate author)*
Institute of Arctic Environmental Engineering
University of Alaska
Fairbanks, Alaska 99701

2a. REPORT SECURITY CLASSIFICATION
Unclassified

2b. GROUP
---

3. REPORT TITLE
Reflection of MM Waves from Snow and Sea Ice

4. DESCRIPTIVE NOTES *(Type of report and inclusive dates)*
Semi-annual Technical Report, 1 June 1971 - 31 January 1972

5. AUTHOR(S) *(First name, middle initial, last name)*
Sackinger, William M. and Byrd, Robert C.

6. REPORT DATE
31 January 1972

7a. TOTAL NO. OF PAGES
∿ 100

7b. NO. OF REFS
3 + 15 in Appendix

8a. CONTRACT OR GRANT NO.
N00014-71-A-0365-0001

b. PROJECT NO. ARPA Order 1783

c.
Program Code 04B282

d.

9a. ORIGINATOR'S REPORT NUMBER(S)
IAEE Report 7203

9b. OTHER REPORT NO(S) *(Any other numbers that may be assigned this report)*

10. DISTRIBUTION STATEMENT
Distribution unlimited. [redacted]

11. SUPPLEMENTARY NOTES
Office of Naval Research, Code 415
Contract Monitoring

12. SPONSORING MILITARY ACTIVITY
Advanced Research Projects Agency
Washington, D.C. 20305

13. ABSTRACT

This report relates to utility of imaging radars for arctic surface guidance. The program involves field measurements of backscatter from snow, ice and sea ice for a wide variety of meteorological and surface conditions. Laboratory measurements of the complex dielectric constant are presented also, to enable the separation of the roughness contribution to the backscatter. During the first seven months of the program, the dielectric properties of sea ice were measured in the laboratory from 26 to 40 GHz, over a representative range of temperatures, salinities, and orientation. As reported in the detailed Appendix, which is a Master's thesis, the real part of the dielectric constant is close to 3 for most conditions, but the loss tangent can vary over three orders of magnitude, depending upon the temperature and salinity. Under most conditions, an incident wave of 1 cm wavelength would penetrate less than one meter into the sea ice. Strong distinction of freshly-formed sea ice from old sea ice appears likely. Backscatter from sea ice is currently being measured. Distinction of rough and smooth surfaces is possible, based upon preliminary interpretation of the data. A continuation of laboratory and field measurements is recommended, to include arctic conditions throughout the year.

DD FORM 1 NOV 65 1473

Unclassified

Security Classification

14. KEY WORDS	LINK A		LINK B		LINK C	
	ROLE	WT	ROLE	WT	ROLE	WT
Millimeter waves						
Reflectivity, mm waves						
Snow						
Ice						
Sea Ice						
Arctic						

SUMMARY

Defense operations in the Arctic must be capable of action during the conditions of poor visibility usually encountered. Imaging radars can provide such guidance, but the returns must be easily related to the topography of the snow-covered land and sea ice. In such interpretation, the relative contributions of the dielectric properties and of the surface roughness should be separated. For resolution cell sizes of the order of a few meters, and reasonable antenna dimensions, wavelengths in the 1 cm range or smaller are necessary. The present program involves field measurements of backscatter from snow, ice, and sea ice for a wide variety of meteorological and surface conditions. Laboratory measurements of the complex dielectric constant are also included, to enable the separation of the roughness contribution to the backscatter.

During the first seven months of the program, the dielectric properties of sea ice were measured in the laboratory from 26 - 40 GHz, over a representative range of temperatures, salinities, and orientation. As reported in the detailed Appendix, the real part of the dielectric constant is close to 3 for most conditions, but the loss tangent can vary over three orders of magnitude, depending upon the temperature and salinity. Under most conditions, an incident wave of 1 cm wavelength would penetrate less than one meter into the sea ice. Strong distinction of freshly-formed sea ice from old sea ice appears likely.

During the reporting period, a fixture for field testing was designed, fabricated, and tested. It made possible the backscatter measurements on snow-covered land which were obtained and which are being analyzed. Backscatter from sea ice is currently being measured. Distinction of rough and smooth surfaces is certainly possible, based upon preliminary interpretation of the data. A continuation of laboratory and field measurements is recommended, to include Arctic conditions throughout the year. Further comparisons of laboratory and field data are also recommended.

I. INTRODUCTION

For many decades, man's operations in the Arctic have been hindered by the extreme cold and lack of visibility. Immersed in darkness for several months of the year, the Arctic ice cap presents deadly obstacles to surface operations, in the form of irregular pressure ridges of ice and open-water leads. Fog and blowing snow often obscure this topography. Defense operations, which must be capable of action under all weather conditions, can still retain surface mobility if equipped with a high-resolution imaging radar system which can penetrate through the fog and blowing snow, giving a radar map of the snow and ice features. In the interpretation of the image information contained in the radar return signal, one would like to separate out the effects of surface roughness and geometrical irregularities from changes in the dielectric properties of the reflecting surface. Preliminary consideration of required distances, resolution cell sizes, and limits on the physical size of antennas lead quickly to the conclusion that millimeter wavelengths are necessary. Very little is known about the millimeter wave reflectivity of snow, ice, and sea ice. The present engineering research program is directed towards the measurement of the backscatter from actual Arctic terrain; the laboratory measurement of the dielectric constant and loss tangent of snow, ice, and sea ice; and the correlation of the field and laboratory measurements. The surface roughness will be separated out as an independent effect, and finally, suggestions

will be made for the design of obstacle avoidance systems which can perform this separation on a continuous, on-line basis.

During the first seven months of the program, laboratory measurements have been made of the dielectric properties of sea ice in the frequency range of 26 - 40 GHz. Preparations for field measurements during the winter were completed, and field measurements of snow-covered land were begun. In the Appendix, a detailed report of the laboratory measurements on sea ice is presented. The following sections describe some of the major findings and their implications.

II. DIELECTRIC PROPERTIES AND RADAR REFLECTIONS FROM SEA ICE.

During the past seven months, Mr. R. C. Byrd has measured the complex dielectric constant of representative samples of naturally-occurring sea ice, as a function of temperature, salinity, and orientation. Details are reported in his M.S. thesis of December 1971, which constitutes the appendix of this report. Preliminary results were presented by Mr. Byrd at the 1971 IEEE Conference on Engineering in the Ocean Environment, San Diego, September 21-24, 1971, in his paper entitled, "Interpretation of Radar Returns from Sea Ice."

Sea ice may be considered to be a mixture of dielectrics, if the size of the inhomogenieties is small compared to a wavelength. (Some samples, which contained entrapped air bubbles of dimensions comparable to a quarter-wavelength, demonstrated erratic behavior due to resonant-cell scattering effects.) At temperatures warmer than -21°C, the sea ice can be regarded as a two-phase mixture of relatively saline brine inclusions. At temperatures colder than -21°C, the

brine inclusions begin to freeze, and a simplified model of two solid phases (ice crystals with frozen brine inclusions) may be used. The dielectric loss in the frequency range under consideration, 26 - 40 GHz, is due to a rotational degree of freedom of the water molecule in the gaseous or liquid state. In the measurements reported in the Appendix, a distinct decrease in dielectric loss was observed for temperatures colder than -21°C, as expected. Furthermore, an anistropy was observed in the loss tangent, depending upon whether the electric field was parallel or perpendicular to the brine inclusions. This anistropy may give some insight into the details of the dielectric loss process. However, in the case of a radar beam striking a resolution element area several feet square, a random combination of brine inclusion directions at the surface is likely, so that the polarization anistropy is not likely to be observed in the radar return because of this particular effect. This does not rule out the possibility of an anistropy in the return due to other causes; future field measurements will determine whether this occurs.

Some insight into the scattering and absorption of incident radar waves by sea ice can be obtained by numerically evaluating the attenuation distance $1/\alpha$, the distance into the sea ice through which the wave penetrates before it decays to $1/e = 0.368$ of its original value. Von Hippel[1] has given the expression for $1/\alpha$ as:

$$\frac{1}{\alpha} = \frac{\lambda_0}{2\pi} \cdot \left[\frac{2}{\epsilon'/\epsilon \left(\sqrt{1 + \tan^2 \delta} - 1 \right)} \right]^{1/2} \qquad (1)$$

Assuming an average frequency of 34 GHz, and an average salinity of 4.48 °/oo, the dielectric constant ($\varepsilon'/\varepsilon_0$) is 3.08, 3.01, and 3.30 at -7°C, -25°C, and -32°C, respectively, while the loss tangent (tan δ) is 0.16, 0.028, and 0.007, respectively, at those temperatures. Numerically evaluating Equation 1, we find an attenuation distance $1/\alpha$ of 1.03 cm., 5.76 cm., and 22 cm., at temperatures of -7°C, -25°C, and -32°C, respectively. A common winter condition is a temperature gradient from the cold ambient air temperature at the surface of the sea ice to the -1.8°C temperature established by the sea at the water-ice boundary. A 34 GHz wave penetrating the ice, launched from an airborne SLAR at nearly normal incidence, would only penetrate to a depth exceeding a meter if extensive brine drainage had occurred, and the air temperature was very cold. Because of the high attenuation of sea ice at temperatures warmer than -10°C, it is extremely unlikely that such a wave could penetrate to the water-sea ice interface. An abrupt discontinuity in salinity near the water-sea ice interface could lead to a reflected wave, however, which (if detectable) might give a measure of ice thickness. Further analysis and field measurements are required to resolve this question.

From Fresnel's equations, the amplitude reflection coefficient, r_E, for the electric vector is (normal incidence case)[1]

$$r_E = \frac{Z_2 - Z_1}{Z_2 + Z_1} \qquad (2)$$

where a wave penetrates from a material of intrinsic impedance (Z_1) into a material of intrinsic impedance (Z_2). If the first material is free space, then algebra shows that

$$r_E = \frac{1 - \sqrt{\epsilon^*/\epsilon_\bullet}}{1 + \sqrt{\epsilon^*/\epsilon_\bullet}} \qquad (3)$$

This is, in general, a complex number. One extreme case is sea ice that is several years old, which has been subjected to considerable brine drainage and is of very low salinity. Under very cold winter conditions, the loss tangent of the ice at the air-ice interface may be neglected. Then the relative dielectric constant is near 3.1, and $|r_E| \cong .275$. The coefficient of energy reflection (R) is

$$R = |r_E|^2 \qquad (4)$$

which numerically is R = .0758, for the particular example taken. This represents the power reflected at normal incidence from very old, very cold ice. A pressure ridge in winter has some small fractional area of its rough surface which is normal to the incident wave, and the backscatter from an old pressure ridge would be reduced by this effective cross-section factor. This model of backscattering is drastically oversimplified, however; when one encounters higher temperatures, the loss tangent increases, increasing R. The viewpoint of "small specular-reflecting surface area" should then be replaced by a more complete analysis[2,3] which shows the existence of a diffuse

scattered component with, in general, a different polarization than the incident wave. Field measurements will be taken to determine the extent of this effect, and correlation of that data with Beckmann's theory is planned.

It appears that a large distinction exists between an open or a freshly frozen lead and older, colder flat ice surrounding it, when viewed at normal incidence. Future analysis will quantify this distinction.

III. FIELD MEASUREMENT PROGRAM

As indicated in the preceding section, field measurements of backscatter are planned for sea ice of varying temperature, salinity, and topography. Similar measurements are planned for snow-covered sea ice, pure ice, and soil, so that a comprehensive picture of the millimeter-wave radar reflectivity of arctic surfaces may be known.

During the past seven months, several representative sites for these measurements were selected and photographed. A test fixture was fabricated which would position the transmitting and receiving horn antennas exactly, and upon which they could be moved to vary the angle of incidence of the wave.

This fixture is in the form of a track extending over a 90° arc, upon which is mounted a sliding traveler which holds the antennas. Both transmitting and receiving horns can be independently rotated, making possible the measurement of backscatter for horizontal, vertical, and crossed polarization. Considerable ingenuity was embodied in the fixture design so that all mechanical positions required could be achieved easily in the field, with positive positioning. No mechanical

measurements on the fixture are required in the field, reducing sources of error. Tolerances on dimensions and angles are in every case those obtainable during the machining process.

A simple transmission and reflection measurement technique is used, in which an r.f. signal is amplitude-modulated before transmission, and the received r.f. energy is demodulated and detected with a phase-locked receiver. A received signal 60 db below the transmitted signal could easily be distinguished using this approach, which proved adequate to detect reflected power in the first measurements on snow-covered soil.

Complete data was obtained for a particular site near the end of the reporting period. This site had approximately 28 inches of dry powder snow covering the soil, with an ambient temperature in the range of -25°C to -45°C. Analysis of the data is in progress, and the data will be presented and discussed fully in the next technical report.

During the next quarter, data will be obtained on sea ice at Barrow, and on snow-covered ice and terrain at other locations near Barrow and Fairbanks.

IV. CONCLUSIONS AND RECOMMENDATIONS

The dielectric properties of sea ice have been measured in the frequency range 26-40GHz. A comprehensive report on this subject is included as the Appendix. The fixtures for field measurements have been designed, fabricated, and tested. The backscatter from snow-covered soil at one site has been measured as a function of incidence

angle and polarization.

During the next reporting period, additional field measurements of backscatter will be taken for sea ice, fresh-water ice and land, both snow-covered and exposed. Laboratory measurements of the dielectric properties of snow and pure ice will commence. A continuation of this research is recommended to measure backscatter during the summer and early winter, and to analyze field measurements. This should lead to an understanding of the relative contributions of the surface roughness and of the surface dielectric properties.

REFERENCES

1. A. R. Von Hippel, Dielectrics and Waves, Wiley, New York (1954).

2. P. Beckmann and A. Spizzichino, The Scattering of Electromagnetic Waves from Rough Surfaces, Pergamon, Oxford (1963).

3. P. Beckmann, The Depolarization of Electromagnetic Waves, Golem Press, Boulder (1968).

THE DIELECTRIC PROPERTIES OF SEA ICE IN THE FREQUENCY RANGE FROM 26GHz to 40GHz

A Thesis
Presented to the Faculty of the Graduate
School of the University of Alaska for
the Degree of
Master of Science

by
Robert Clark Byrd

December 1971

BIOGRAPHY

The author was born on July 26, 1944, in Brookhaven, Mississippi. He attended Brookhaven High School and was graduated in 1962. From 1962 he majored in marine engineering at the United States Coast Guard Academy, receiving the Bachelor of Science in June 1966. From 1966 through 1970 he served as an engineering officer in the U. S. Coast Guard. He entered the Graduate School of the University of Alaska in September 1970.

In 1966 he received honors for the outstanding power engineering thesis in his graduating class. In 1969 he was the diving officer for the first trip by the S.S. Manhattan through the Northwest Passage.

He is a member of the Society of Naval Architects and Marine Engineers.

ACKNOWLEDGMENTS

It is a pleasure to thank Dr. W. M. Sackinger for suggesting the topic and for stimulating discussions and guidance during the course of this research, Dr. Charles E. Behlke for providing the opportunity for participation in this program, and Dr. T. E. Osterkamp for assistance in obtaining and analyzing samples.

This research was supported by the Advanced Research Projects Agency through the Office of Naval Research, Contract No. N00014-71-A-0365-001.

CONTENTS

ABSTRACT

The dielectric properties of sea ice are measured for frequencies from 26 GHz to 40 GHz. The effect of temperature and salinity on the complex permittivity are determined. The orientation of the brine cells within the sea ice is found to have an effect on the loss tangent of the ice. An average value for the real part of the complex permittivity is derived along with an empirical expression for determining loss tangent.

I. INTRODUCTION

With the increase in interest in recent years in recovering natural resources from the Arctic region, new and better methods of transport through and over the Arctic Ocean ice cover are being sought. To facilitate routing of icebreakers and surface-effect vehicles, better ice navigation systems and methods of predicting ice surface topography are needed. One area of major emphasis is in the development of radar systems which produce a graphic representation of the ice surface, both for large area prediction, as in the case of airborne side-looking radars, and for navigational radar carried by the vessels themselves. Because of the nature of the surface to be represented and the information that is being sought from the radar presentations, high degrees of resolution are desired. This will necessitate use of systems at frequencies in excess of 20 GHz. One problem which has not been satisfactorily solved, involving the design of sea ice radar systems is development of a method of interpreting the return signals received by such systems. A radar impulse returning from a sea surface having partial ice cover may represent reflections from fresh water, fresh water ice, sea water, and sea water ice in a variety of combinations--all having somewhat different reflectivity characteristics. The return signal is the result of a complex

interaction of the electromagnetic field of the impulse with the sea ice profile. The dielectric constant and loss tangent of the sea cover components partly determine the reflection coefficient at each boundary. The differences in reflective characteristics between different sea ice profiles will be better understood when more information is available about the dielectric properties of sea ice. This study seeks to determine these properties for natural sea ice in the frequency from 26.5 GHz to 40.0 GHz, and their changes with salinity and temperature.

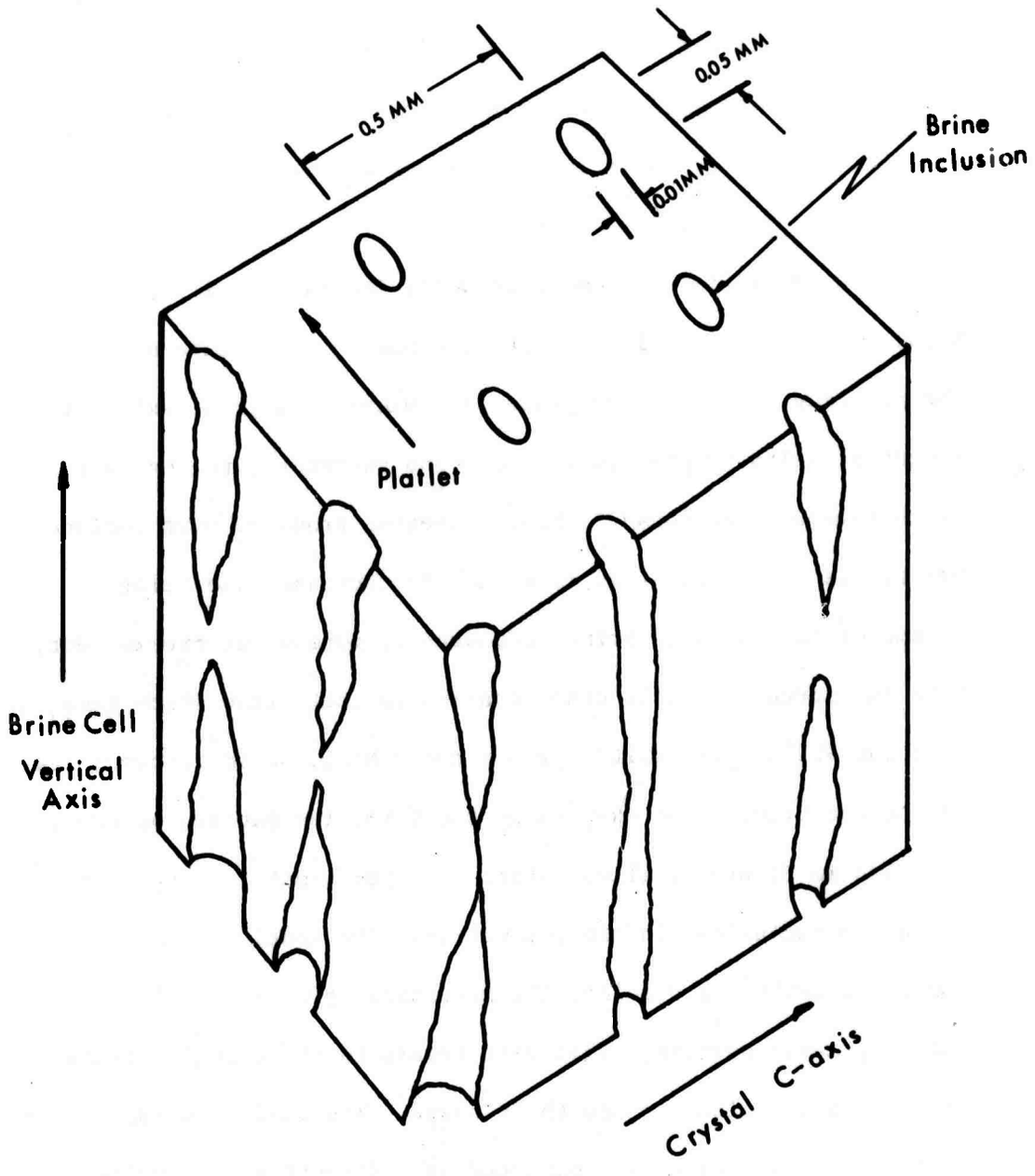

Fig.1 Sea Ice Model (after Assur & Weeks, ref. 3)

II. GENERAL PROPERTIES OF SEA ICE

In this section the physical properties of sea ice which effect its electromagnetic characteristics are discussed, along with a brief description of the relationship between reflectivity and the dielectric properties of the reflecting material.

1. Physical Properties of Sea Ice

Sea ice differs from fresh water ice in that it has liquid brine inclusions contained in its ice matrix. The rate at which the freezing process takes place determines to a great extent the amount of salts trapped in the ice, and therefore, the percent of brine volume to be found.[1] Rapid freezing produces more included brine. As the temperature continues to decrease, the relative volume of the included brine decreases as more water freezes out, with an increase in salt concentration in that brine which remains. At about -22°C solid salts, predominantly NaCl, begin to precipitate out of the brine.[2] An example of the formation pattern of sea ice is shown in Figure 1, illustrating the approximate arrangement of the brine inclusions in the ice matrix. The model was used by Assur and Weeks[3] to simulate the mechanical properties of sea ice and is greatly oversimplified with regard to the orderly arrangement of the brine inclusions and their shape. The inclusions have been observed to sometimes be connected in a direction perpendicular

to their vertical axis and their cross-sectional shape is generally not as well defined as that shown.

Once the ice has reached its minimum temperature, the process has by no means stabilized. The liquid brine inclusions tend to gravity drain to a lower point and eventually out of the ice. If the ice cycles through warming periods, the amount of trapped brine decreases more rapidly due to increased migration.[4] The maximum salinity found in young sea ice is generally around 20°/oo [5] (parts per thousand) and it may range to nearly zero in old ice. The average salinity in the sea ice which comprises the majority of ice surface disruptions is around 5°/oo.[6]

In predicting the electromagnetic properties of sea ice at microwave frequencies, the properties of its two major constituents, ice and liquid brine, must be considered. Pure ice has been found to be a low-loss dielectric at frequencies above 10^7 Hz, while water, which the brine is expected to resemble, has been predicted to have high loss in the frequency range between 10^{10} and 10^{11} Hz.[7] The percent of brine volume in sea ice varies greatly with salinity and temperature; Figure 2 shows this relationship.[2] The dielectric properties of a particular sample of sea ice will depend on its past history and, more important, on its current temperature.

2. Electromagnetic Properties of Dielectric Materials.

Before proceeding with the discussion of the measurement of the electromagnetic properties, we shall examine briefly the general

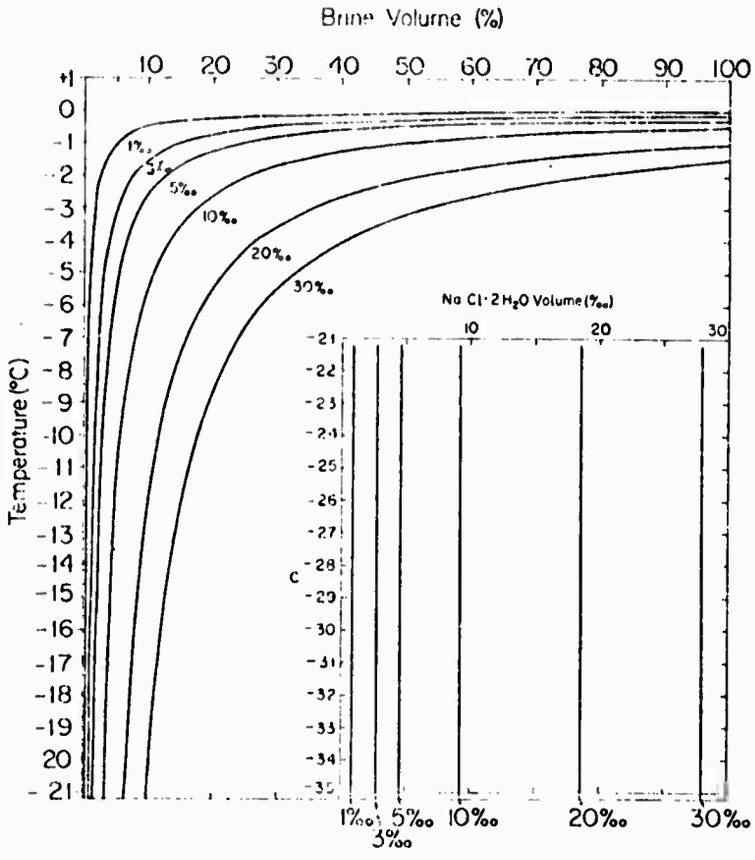

FIGURE 2: Brine Volume of NaCl Ice as a Function of Temperature & Salinity (after Weeks, ref. #2).

properties of dielectric materials and how they relate to the reflectivity of electromagnetic waves.

A simple electromagnetic wave traveling in free space can be visualized as consisting of two components, as shown in Figure 3; an electric field vector ($\overline{E}$) and a magnetic field vector ($\overline{H}$). In the undisturbed case these vectors are at right angles to each other and each is at right angles to the direction of propagation. Our problem is to define the information necessary to determine how the wave reacts when confronted with substances other than free space. When this occurs, the incident wave is broken into two additional waves; the reflected wave--that portion which is returned from the boundary of the dielectric, and the transmitted wave--that portion which proceeds through the dielectric. The three waves are interconnected by the boundary condition that the tangential component of $\overline{E}$ and $\overline{H}$ must be continuous in traversing the interface between two media. This, in fact, is two conditions, since the amplitudes as well as the phases must be continuous. Figure 4 shows the simple case of a plane wave at normal incidence from one dielectric media to another. We are generally not interested in the absolute value of the reflected or transmitted wave amplitudes, but are interested in the ratios of the different amplitude components, the reflection coefficient (r) and the transmission coefficient (t). These may be defined in terms of the intrinsic impedances of the media.[8]

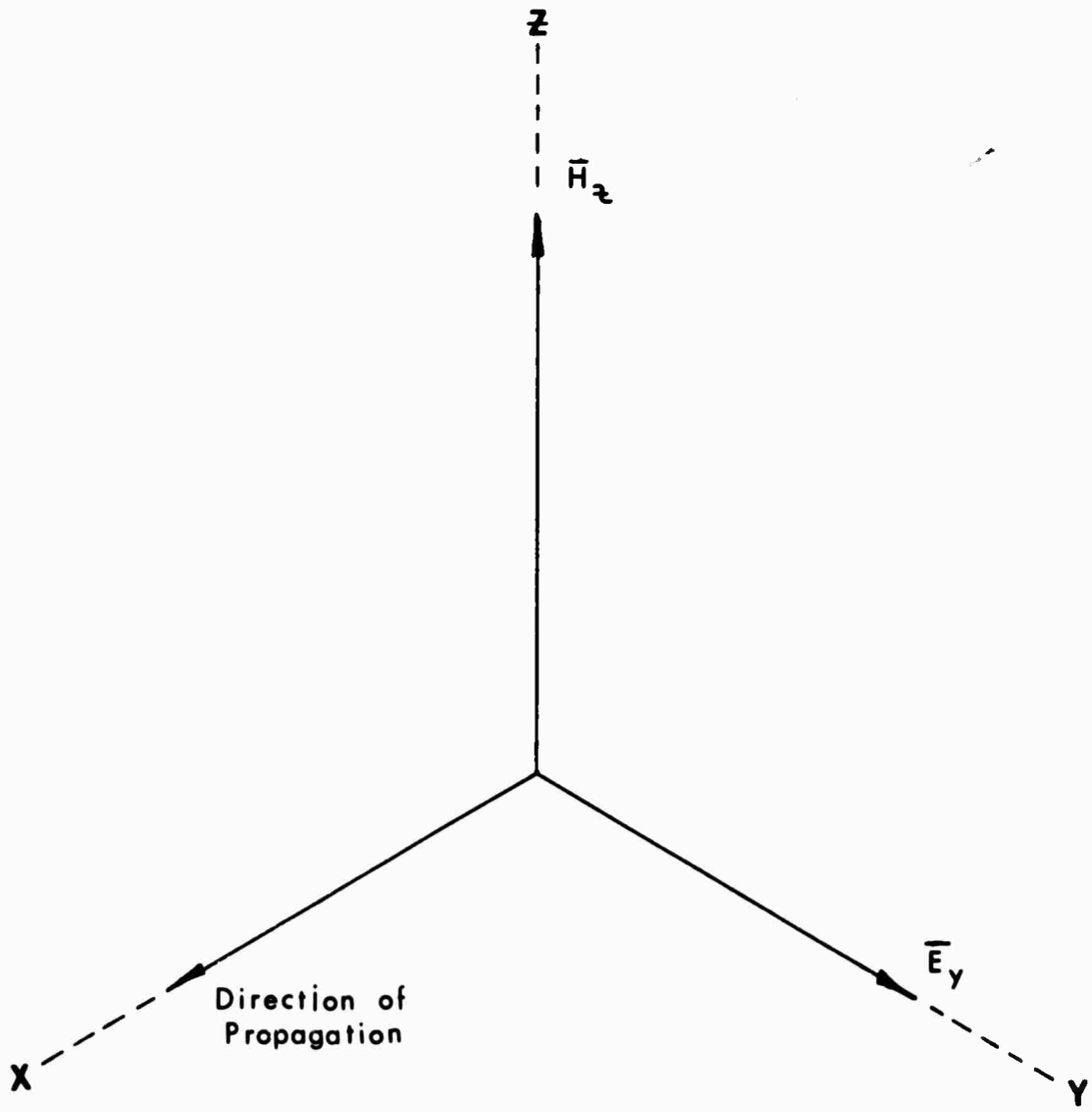

Fig, 3 Traveling Transverse Electromagnetic Wave

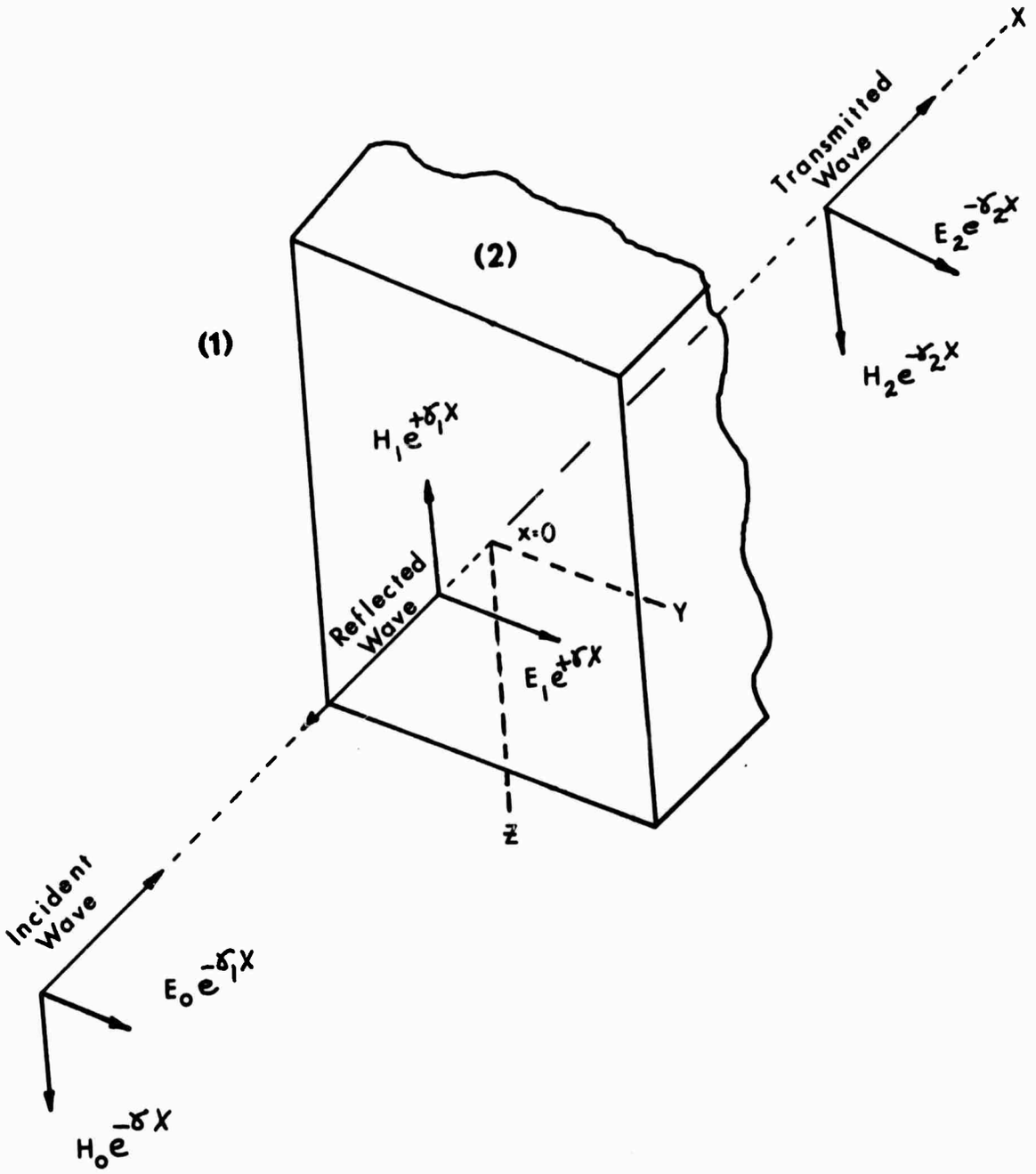

Fig. 4 · Plane Wave Reflection at Normal Incidence

$$r_E = \frac{Z_2 - Z_1}{Z_2 + Z_1} = -r_H = \frac{\bar{E}_1}{\bar{E}_2} \qquad (1)$$

$$t_E = \frac{2Z_2}{Z_2 + Z_1} = \frac{Z_2}{Z_1} \cdot t_H = \frac{\bar{E}_2}{\bar{E}_o} \qquad (2)$$

The intrinsic impedances may in turn be defined in terms of the complex permittivity (ε^*) and the complex permeability (μ^*),[8]

$$Z = \frac{\gamma}{j\omega\varepsilon^*} = \frac{\mu^*}{\varepsilon^*} = \frac{j\omega\mu^*}{\gamma} \qquad (3)$$

where the complex propagation constant (γ) is defined

$$\gamma = j\omega(\varepsilon^*\mu^*)^{\frac{1}{2}} = \alpha + j\beta \qquad (4)$$

where: ω = radian frequency of the wave.

Figure 5 illustrates a wave at other than normal incidence. The relationship of the different wave components to intrinsic impedances and angles of incidence and refractions are given by von Hippel.[8] (see the equations contained in drawing #5 as illustration). These figures and expressions are somewhat simplified, but serve to illustrate the point that the characteristics of electromagnetic waves reflected and refracted by dielectrics are dependent on the complex permittivity and permeability of the substances on

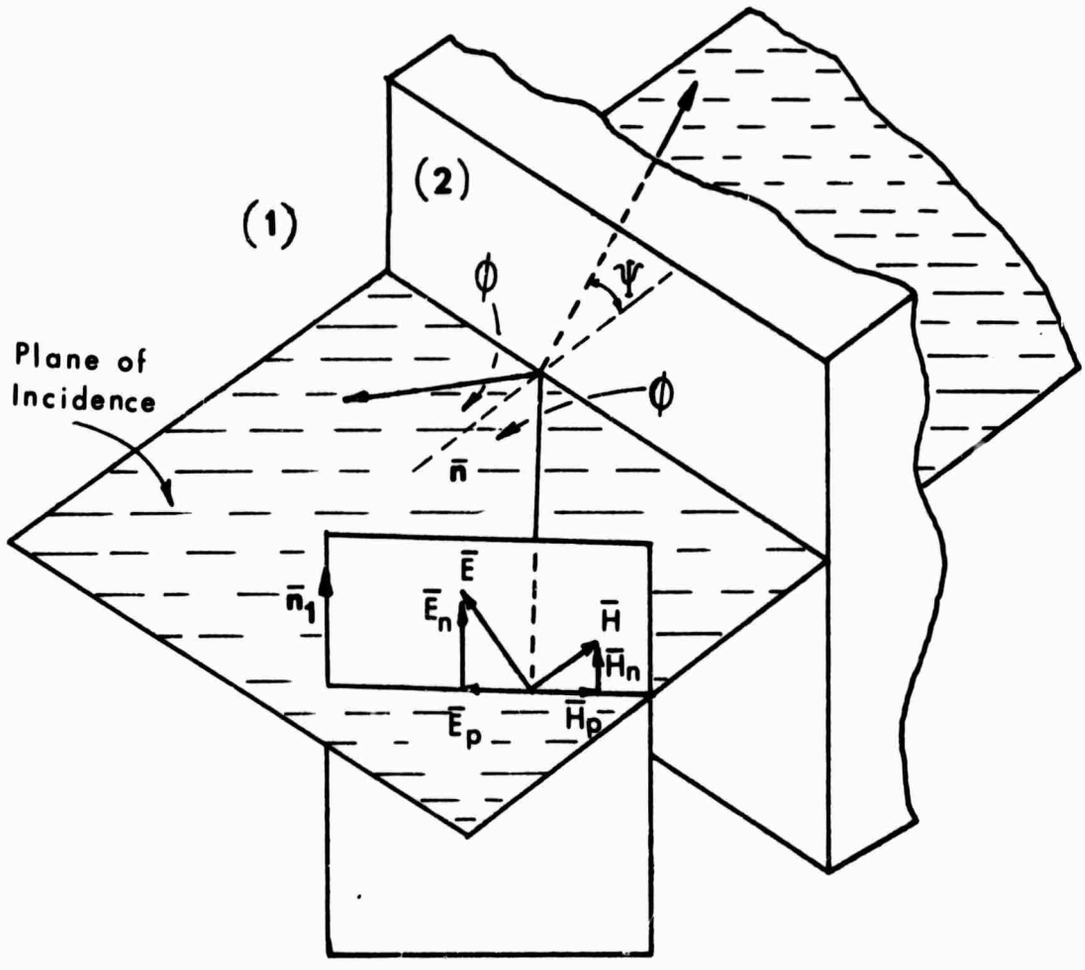

$$r_{E_n} = \left(\frac{E_1}{E_0}\right)_n = \frac{z_2 \cos\phi - z_1 \cos\psi}{z_2 \cos\phi + z_1 \cos\psi} = -r_{H_p} \qquad (5)$$

$$r_{E_p} = \left(\frac{E_1}{E_0}\right)_p = \frac{z_2 \cos\psi - z_1 \cos\phi}{z_2 \cos\psi + z_1 \cos\phi} = -r_{H_n} \qquad (6)$$

Fig. 5 T.E.M. Wave at Non-normal Incidence

which the waves are incident. Most dielectrics of interest are for all practical purposes non-magnetic, therefore, $\mu^* = \mu_o$, the permeability of free space. Therefore, the first step in understanding the reflective characteristics of a particular dielectric material comes with knowing its complex permittivity (ε^*) for the frequencies of interest.

III. COMPLEX PERMITTIVITY DETERMINATION

Methods for measuring the dielectric properties of materials at high frequencies have been described by a number of authors and vary greatly in the specific details, depending on the range of accuracy for which they may be used and the physical properties of the materials to be measured.[8, 9, 10, 11] Most of the methods described are intended for use in homogeneous materials where a high degree of accuracy is possible; they require a high degree of control of sample dimensions, measurement of absolute distances, and generally require complicated calculations for each measurement taken. A method which has been found to be particularly well suited for measurements in sea ice at the frequencies to be considered here was described by Tinga and Edwards; a swept frequency technique, it offers several advantages over other methods available.[11] This technique requires only one length measurement, that of the sample. It provides for rapid acquisition of data and can be used in samples having some inhomogeneities. It offers the opportunity for a trade of some accuracy for a great deal of simplicity.

Most conventional methods of dielectric measurements are simplified considerably if the sample length has a particular value such as an odd or even number of quarter wave-lengths in the material. However, since wavelength in the material is a function of the dielectric constant, this condition is usually difficult to achieve

in practice, since this is the characteristic to be measured. The electrical length of the sample, however, can be varied easily by changing the frequency. If the assumption is made that the dielectric properties of the material under test do not change greatly with frequency over a relatively short frequency range, then changing the electrical length, by sweeping the frequency over some band, has the effect of changing the physical length of the sample. This allows a situation to be created which makes it relatively easy to calculate the complex permittivity of the material. This approach forms the basis for the swept frequency technique. The experimental measurement is basically a reflection measurement, which relies on the interface reflections and the attenuation of the sample to give information about the complex permittivity.[11]

A block diagram of the experimental apparatus is shown in Figure 6. A leveled microwave sweep generator sends an incident wave to the sample, which will reflect and transmit some of the energy. If the total reflected signal is detected and displayed versus frequency, a characteristic pattern such as is given in Figure 7 results. This pattern contains a large amount of information about the dielectric behavior of the material under examination.

The following is an outline of the derivation of the necessary

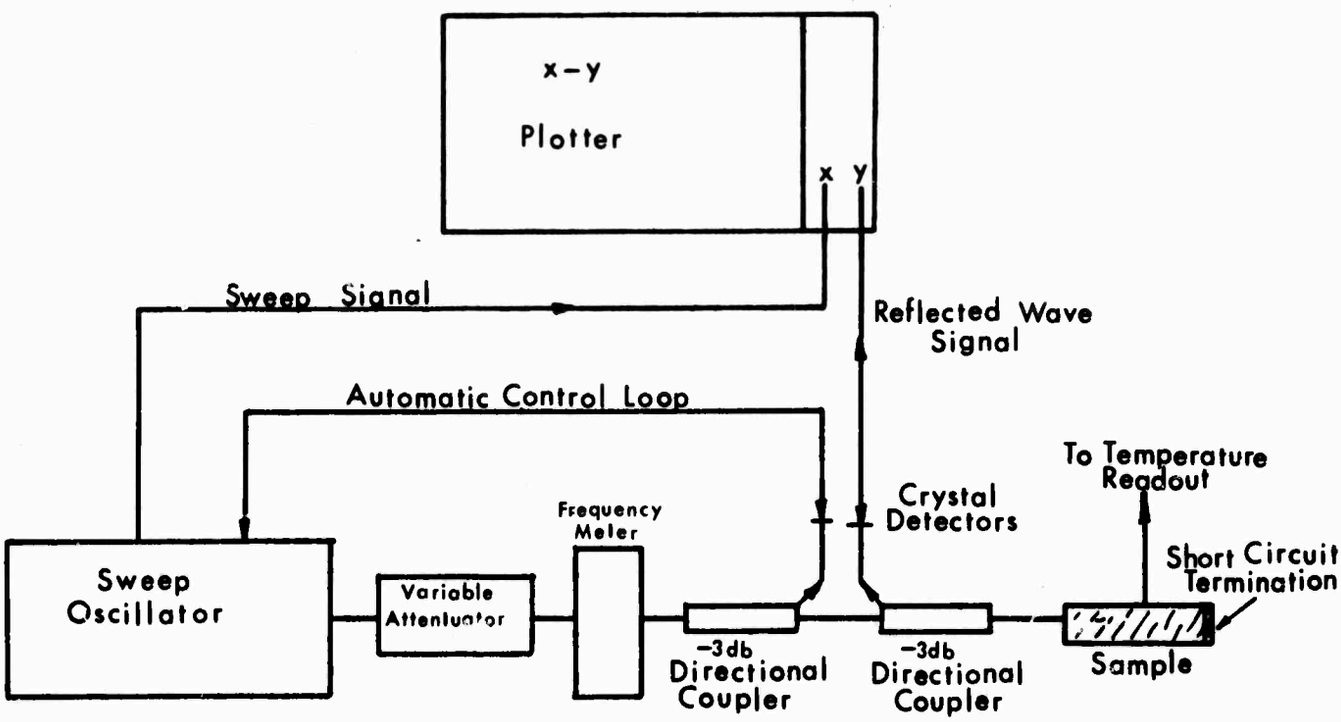

Fig. 6 Equipment Setup

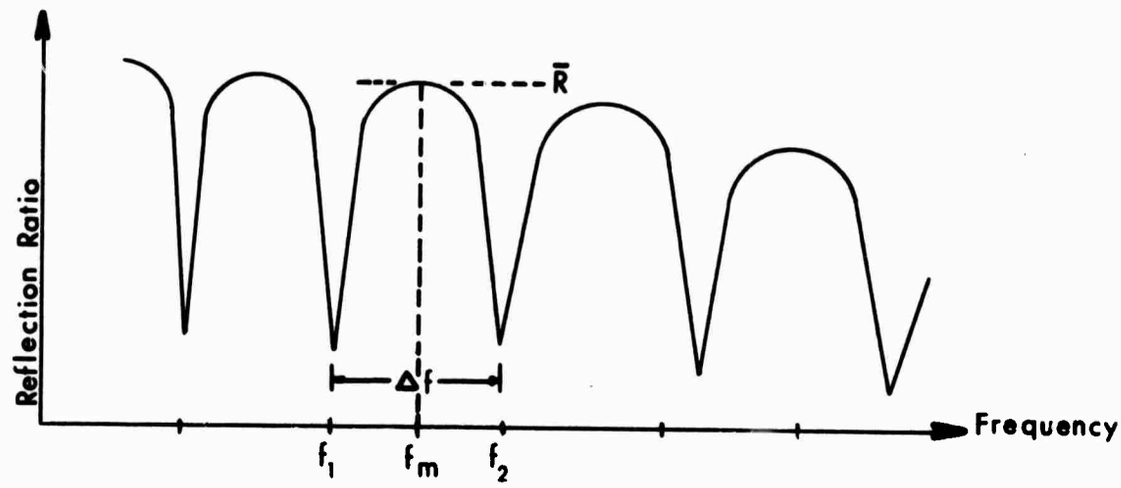

Fig. 7 Representative Data Trace

equations, taken from the detailed work of Tinga and Edwards, for the particular case of a short circuit sample holder termination, which was used in these measurements and is shown in Figure 8.

The propagation constant for a medium of arbitrary dielectric constant, ε^*, filling a rectangular wave-guide, may be expressed

$$\gamma = \alpha + j\beta = j(2\pi f/c)\sqrt{\varepsilon^* - P} \qquad (7)$$

where

$$\varepsilon^* = \varepsilon' + j\varepsilon'' \qquad \text{(complex permittivity)} \qquad (8)$$

$$P = (f_c/f)^2 \qquad (9)$$

with f_c being the cutoff frequency of the wave-guide used and f as the frequency being examined; c represents the speed of light in free space.

Squaring (7) and solving for ε' and ε'' gives

$$\varepsilon' = P + (c/2\pi f)^2 (\alpha^2 - \beta^2) \qquad (10)$$

$$\varepsilon'' = 2(c/2\pi f)^2 \alpha\beta \qquad (11)$$

To find values for α and β, referring to Figure 8,

$$R = \frac{B}{A} = \frac{r_1 + r_2 e^{-2\gamma_1 \ell}}{1 + r_1 r_2 e^{-2\gamma_1 \ell}} \qquad (12)$$

where

A = amplitude of the incident wave electric field
B = amplitude of the total reflected wave electric field
r_1 = reflectivity coefficient at face of the sample
r_2 = reflectivity coefficient at the short circuit
ℓ = length of the sample
γ_1 = propagationconstant of the sample

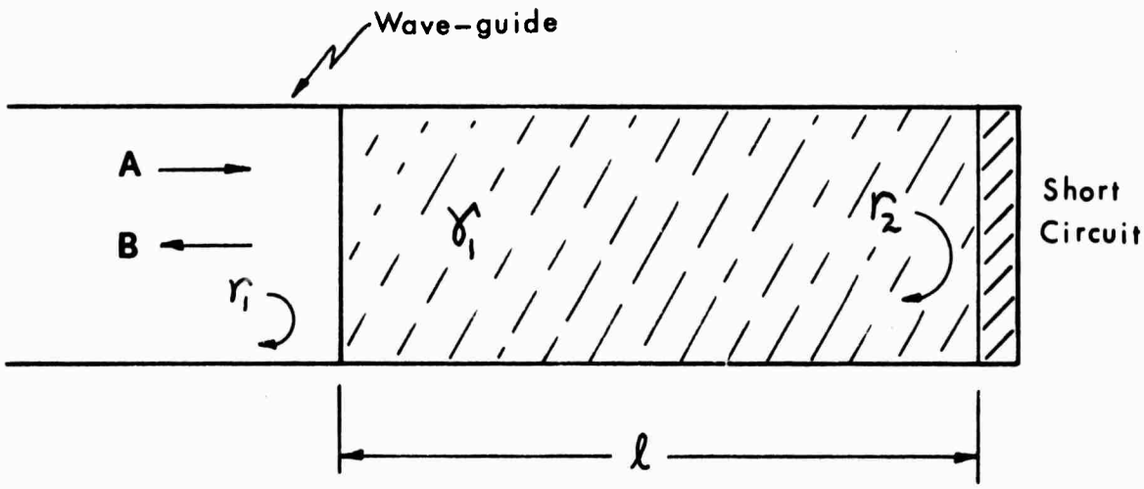

Fig. 8 Sample in Wave-guide

For the case of a short circuit termination, $r_2 = -1$, and

$$r_1 = \frac{\sqrt{1 - P} - \sqrt{\varepsilon_1^* - P}}{\sqrt{1 - P} + \sqrt{\varepsilon_1^* - P}} \qquad (13)$$

To find the points of extrema in equation (12), the condition that the first derivative with respect to frequency be equal to zero is applied. To find a first approximation to the solution, the assumptions of plane wave propagation and a lossless dielectric ($\alpha = 0$) are made, resulting in

$$\beta \simeq \frac{n\pi}{2\ell} \qquad n = \text{integer, for extrema} \qquad (14)$$

$$\Delta\beta = \beta_1 - \beta_2 = \frac{m\pi}{2\ell} \qquad m = \text{integer} \qquad (15)$$

Assuming that $\alpha^2 << \beta^2$ one may solve equation (10) for β .

$$\beta = (2\pi f/c)\sqrt{\varepsilon_1' - P} \qquad (16)$$

Assuming that ε' remains constant between two adjacent maxima or minima and taking m = 2, since the electrical length between two adjacent maxima or minima equals one-half the wave length within the sample, substitituting equation (16) into equation (15) yields

$$(c/2\ell\Delta f) = \varepsilon_1'/\sqrt{\varepsilon_1' - P} \qquad (17)$$

where $\Delta f = f_2 - f_1$ (See Figure 7)

Squaring and solving for ε_1' ,

$$\varepsilon' = 1/2\ E\ [1 + \sqrt{(1 - 4P)/E}\ ] \qquad (18)$$

where

$$P = \frac{(f_2P_2 + f_1P_1)}{f_1 + f_2}$$

$$E = (c/2\ell\Delta f)^2$$

It can be seen in equation (18) that all variable terms are available from the experimental trace and that ε' is a function of Δf only.

Now, taking equation (12) and assuming that r_1 has only a real component; i.e., the sample is lossless,

$$\overline{R} = \frac{|r_1| - e^{-2\alpha\ell}}{1 - |r_1|e^{-2\alpha\ell}} \qquad (19)$$

Solving equation (19) for α gives

$$\alpha = 1/2\ell \quad (\ln\overline{A}) \qquad (20)$$

where

$$\overline{A} = (1 - \overline{R}|r_1|)(\overline{R} - |r_1|) \qquad (21)$$

The bars over the ratios indicate that they are taken for maximum values.

Substituting equations (20) and (16) into equation (11)

$$\varepsilon_1'' = (c/2\pi f_m\ \ell)\ (\sqrt{\varepsilon_1' - P})\ \ln \overline{A} \qquad (22)$$

or

$$\tan\delta = (c/2\pi f_m \varepsilon')\ (\sqrt{\varepsilon_1' - P})\ \ln \overline{A} \qquad (23)$$

Equations (18) and (23) represent the information necessary to determine the complex permittivity for materials which approximately obey the assumptions made in arriving at these solutions.

In the formation of the expression for the dielectric constant (ε'), equation (18), plane wave propagation along with a lossless dielectric

was assumed. These conditions are not generally the case in practical laboratory experiments. However, Tinga and Edwards have shown by use of computer solutions for wave-guide propagation in lossy dielectrics that these result only in a phase shift in the value of β expressed in equation (14), but do not affect the difference expression as stated in equation (15), for a given sample length. The major assumption left to be fulfilled in satisfying equation (18) is that the dielectric constant, ε', not vary greatly between any two minima, since this expression gives the average value of this property between the frequencies where Δf is measured. The results to be presented later will show that this is a valid assumption for sea ice in the frequency range considered and that, in fact, the dielectric constant generally remains within $\pm$ 10 percent of the same value over the entire band measured, for most conditions.

In arriving at the expression for tan δ, equation (23), it was assumed that $\alpha^2 << \beta^2$, which is a good assumption for dielectric materials to which this method can be applied, since a trace as shown in Figure 7 cannot be achieved for real sample lengths unless this condition is met. It was also assumed that r_1 could be found using only the real part of the complex permittivity in arriving at a value for $\overline{A}$ in equation (21). This will result in some error if the value of tan δ is large, requiring reinteration using the full value of permittivity for greater accuracy. However, for values of tan $\delta < 0.1$, the percentage error of the calculations using only the real part of the complex permittivity in calculating r_1 has been found to be less than 5%.[11]

This is generally the case for sea ice where a usable sample trace is achieved. It was found that when the value of loss tangent was much above 0.1, the minima could not be defined on the sample trace. This occurs only at high salinities and/or high temperatures, as will be shown, and an alternate method must be used for future laboratory measurements of very lossy sea ice.

IV. EXPERIMENTAL PROCEDURE

Ice samples for this experiment were taken from the Arctic Ocean in January and March of 1971 from first-year, shore-fast ice. Care was taken to insure that the ice was kept at temperatures below -40°C until the time of use. The ice was selected at random from undisturbed pieces of pack ice at locations ranging from on the surface (under snow cover) to eighteen inches beneath the surface. All samples fell into three groups by salinity: 2.85 °/oo, 3.4 °/oo, and 7.2 °/oo.

A 3db directional coupler was selected as the ice sample holder illustrated in Figure 9. As indicated, the straight, uncoupled end section of the coupler was used as the holder. This provided a device in which the wave propagation was understood and allowed the number of components used in the experiment to be kept at a minimum. A copper shorting plate was used as a termination.

A number of temperature control mechanisms were considered and the following arrangement was found to be most convenient:

1) A temperature-sensing thermistor was mounted at the approximate mid-point of the sample on the sample holder.
2) The thermal mass of the sample holder was increased by addition of a tightly-wound casing of fine copper wire.
3) The entire apparatus was covered with polyurethane insulation approximately 6 inches thick, so that the temperature decay from -60°C to 0°C when exposed to ambient room temperature averaged less than 1.5°C per minute, and was considerably

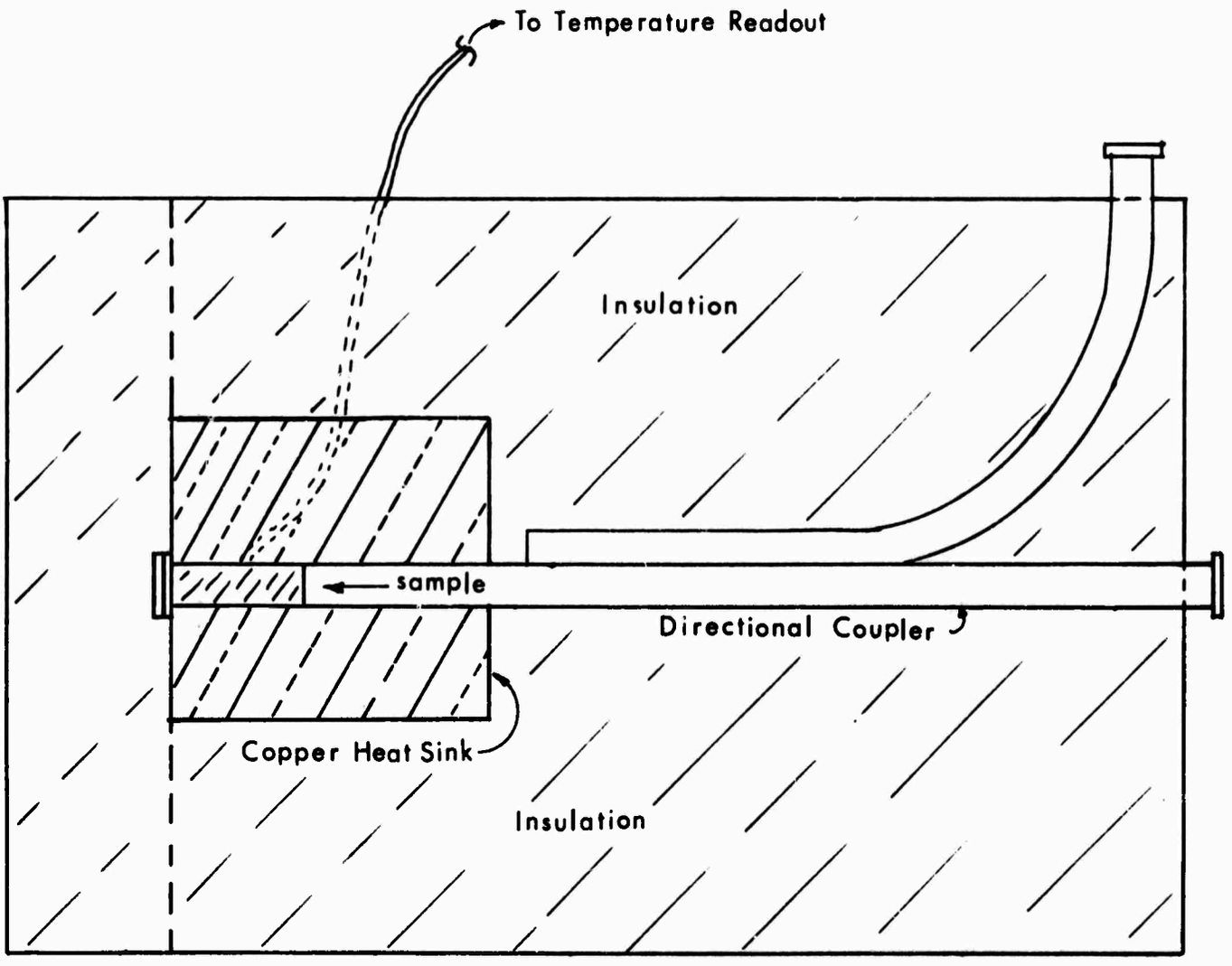

Fig. 9 Sample Holder

3) continued...
slower at the warmer temperatures where the dielectric properties were expected to change more rapidly.

Before each series of measurements, the sample and sample holder were allowed to stabilize at -60°C. The sample holder was then removed from cold storage and allowed to slowly warm, with readings being taken at intervals between -45°C and -7°C. The sample holder was returned to cold storage without allowing the sample to melt.

A swept backward wave oscillator, Hewlett-Packard Model 8690B, was used as the signal generator. A power level of approximately 5 milliwatts incident upon the sample was used for all cases. An automatic leveling control loop was used in the sweep oscillator to insure that the magnitude of the output power was the same at all frequencies. The band from 26.5 GHz to 40.0 GHz was swept in approximately five seconds on all samples. This sweep time was found to be slow enough for accurate following by the X-Y plotter, Hewlett-Packard Model 7004B, but fast enough so that less than 0.2°C change in temperature occurred during the measurement.

The reference for determining the value of the incident wave electric field was taken from the reflected wave of the shorted sample holder without a sample in place. This allowed for cancellation of effects due to the directional coupler. Reference traces were run immediately before the sample holder was chilled and again after the sample was removed, to check drift of the oscillator. Reference traces were also run on the empty sample holder while warming from -60°C to determine the effect of temperature change; none was

noted. However, it was determined that the crystal detectors used to detect the magnitude of the reflected power were sensitive to temperature and had to be protected from temperature change in order to insure consistency. This was done by allowing the detectors to come in contact with the cold apparatus only during the short intervals necessary to take readings. Removing and attaching the detectors had no noticeable effect on the measurements.

The individual sample data was recorded on an X-Y plotter, as shown in Figure 6. Figure 10 shows a data trace for a typical sample. Usable data traces were received from most samples at temperatures of -32°C, -25°C, -21.5°C, -16.5°C, and -7°C. Below -32°C and above -7°C the loss factor of the sea ice examined was not within the range of this detection technique.

The most difficult and time-consuming portion of this experiment was in preparing the sea ice samples for the sample holder. As stated earlier, care was taken to prevent the samples from being exposed to temperatures above -40°C for any appreciable length of time in order to prevent brine drainage. The raw sea ice and prepared samples were stored at -60°C in the laboratory while awaiting use. Prepared samples were sealed in airtight containers to prevent evaporation in storage. Although a number of methods of actually preparing samples were tried, no efficient method was found, and in the end, samples were prepared by manually carving with a razor blade. A simple jig was used to insure square corners, and a proper fit in the wave-guide. The samples were rectangular in cross-section, to match the wave-guide, and

7/18/71
Sample 21

Salinity : 3.40‰

Orientation: Parallel

ℓ : 2.72 CM

Fig. 10 Actual Trace Data

Temperature –16.5° C

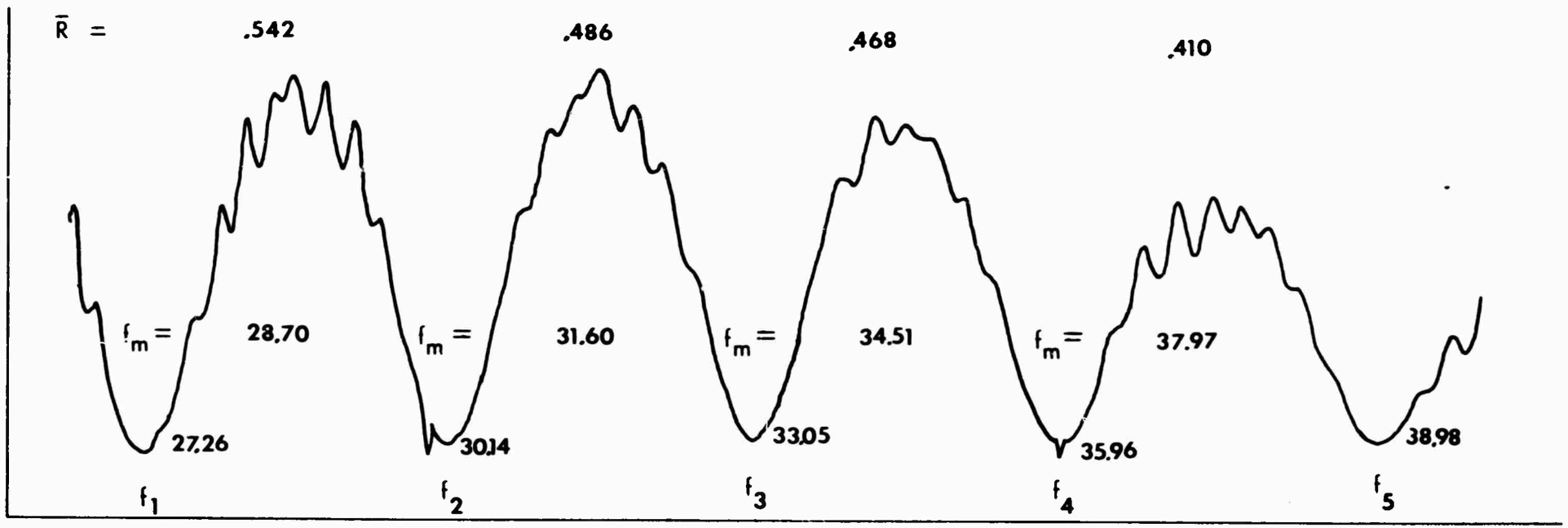

ranged in length from 1.2 to 3.5 cm. Care was taken in selecting the samples so that they contained as few cracks, bubbles and similar inhomogeneities as possible. The samples were examined under a microscope during preparation so that they could be oriented with the brine inclusions either perpendicular or parallel to the direction of the electric field in the wave-guide. Only samples with well-defined and reasonably consistent brine inclusions were used. The samples were prepared in a cold room at -22°C. Care was taken to minimize the time that the samples were subjected to this temperature to prevent brine drainage. Sample preparation time averaged about 1-1/2 hours for each sample. Thirty samples were prepared, twenty were successfully examined.

V. RESULTS

Tables AI, AII, and AIII of the Appendix show the values of individual data points obtained in this experiment for the three sea ice salinity groupings respectively. Figures A1 through A30 present a least squares, best straight line fit of the tabulated data points for the different salinities, temperatures and sample orientations examined and an average value for the individual conditions without regard to sample orientation. It will be noted that in some cases data is not available for parallel sample orientation at -7°C and perpendicular sample orientation at -32°C. Most of the samples measured were too lossy to be measured in the former condition and not lossy enough

for the latter condition. The range over which samples could be evaluated extended from a loss tangent of approximately 0.120 down to 0.001.

In evaluation of the tabulated data points, it should be kept in mind that each point represents an average value of the complex permittivity over a small band of frequencies, generally about 3×10^9 Hz, and that the frequency value listed represents the mid-point of that band; for example, a point listed for 28×10^9 represents the average value from 26.5 to 29.5×10^9 Hz.

Tables I through V show the values of the real part of the dielectric constant (ε') taken from the average value plots in the Appendix with respect to temperature and salinity for even frequencies across the band measured. In Table I the values listed for the 7.20 $^o/_{oo}$ salinity samples are those for the perpendicular orientation of the brine inclusions only. The parallel oriented samples were too lossy to be measured as noted above. The assumption is made that the effect of orientation on the real part of the complex permittivity is small. In Table V, the values listed for the 2.85 $^o/_{oo}$ salinity samples are for parallel orientation only. Again, the assumption of a small change due to orientation is made. All other values listed are for the average of the two orientations measured at a particular salinity, temperature, and frequency, taken from the data plots in the Appendix. Tables VI shows the average values of the real part of the dielectric

constant with respect to frequency and salinity alone. The results of these tables are presented graphically in Figures 11, 12, and 13.

Tables VII through XI show the values of loss tangent (tan δ) taken from the average value plots in the Appendix with respect to temperature, salinity and orientation for the even frequencies. In table VII the values listed for the average value of loss tangent at -7°C where estimated from the observation that at the warmer temperatures, the average loss approaches twice the value of that of the perpendicular orientation. The values listed for the parallel orientation were estimated from a four to one ratio between parallel and perpendicular orientation. Examination of the plotted data in the Appendix will show that this appears to be a reasonable assumption. Table XII shows the average loss tangent with respect to frequency for salinity and orientation. These tables are presented graphically in Figures 14, 15, 16, and 17.

The data which was used to produce these graphs was subject to error which should be considered in their interpretation. Error due to the assumption of constant real part of the complex permittivity with frequency made in arriving at equation (18) is calculated to be less than 1% for a given data point. The assumption of low loss made in arriving at equation (23) causes a 5% error in loss tangent at -7°C and less than 1% at -32°C. This error will cause the data to be lower than the actual value. The greatest source of error comes

from interpreting the data traces. The accuracy varies with temperature from $\pm$ 5% for -7°C through -25°C and $\pm$ 40% for values at -32°C. These errors are random in nature and tend to be cancelled by the averaging process used to arrive at the straight line plots shown in the Appendix, however, they are apparent in examination of the tabulated data points shown in Tables AI through AIII of the Appendix. Error due to the accuracy of the sample length measurement is $\pm$ 1% for the real part and $\pm$ 2% for the loss tangent.

Overall accuracy is expected to be approximately $\pm$ 2% for the real part of the complex permittivity and $\pm$ 5% for the loss tangent.

TABLE I Comparison of the Average Values of the Real Part of the Complex Permittivity

Temperature: -7°C

Frequency ($x10^9$ hz)

Salinity	28	30	32	34	36	38	40	Average
2.85	3.00	3.07	3.13	3.19	3.26	3.32	3.39	3.19
3.40	3.00	3.03	3.07	3.10	3.13	3.17	3.20	3.10
7.20	3.23*	3.14*	3.05*	2.95*	2.85*	2.75*	2.65*	2.95*
Average	3.08	3.08	3.08	3.08	3.08	3.08	3.08	3.08

*values for perpendicular orientation only

TABLE II

Temperature: -16.5°C

Frequency ($x10^9$Hz)

Salinity	28	30	32	34	36	38	40	Average
2.85	2.99	3.00	3.01	3.02	3.03	3.04	3.05	3.02
3.40	2.88	2.93	2.98	3.03	3.08	3.13	3.18	3.03
7.20	3.04	3.02	2.99	2.97	2.95	2.92	2.89	2.97
Average	2.97	2.98	2.99	3.01	3.02	3.03	3.04	3.01

Comparison of the Average Values of the Real

Part of the Complex Permittivity (Continued)

TABLE III

Temperature: -21.5°C

Frequency ($x10^9$Hz)

Salinity	28	30	32	34	36	38	40	Average
2.85	2.86	2.92	2.98	3.04	3.10	3.15	3.20	3.03
3.40	2.91	2.93	2.96	2.98	3.00	3.03	3.05	2.98
7.20	2.86	2.88	2.90	2.93	2.96	2.98	3.00	2.93
Average	2.88	2.91	2.95	2.98	3.02	3.05	3.08	2.98

TABLE IV

Temperature: -25°C

Frequency ($x10^9$Hz)

Salinity	28	30	32	34	36	38	40	Average
2.85	2.88	2.93	2.98	3.03	3.08	3.13	3.18	3.03
3.40	2.98	2.98	2.97	2.97	2.97	2.96	2.96	2.97
7.20	2.83	2.90	2.96	3.02	3.08	3.14	3.20	3.02
Average	2.90	2.94	2.97	3.01	3.04	3.08	3.11	3.01

Comparison of the Average Values of the Real Part of the Complex Permittivity (Continued)

TABLE V

Temperature: -32°C

Frequency ($x10^9$Hz)

Salinity	28	30	32	34	36	38	40	Average
2.85	3.25*	3.21*	3.16*	3.11*	3.06*	3.01*	2.96*	3.11*
3.40	2.73	2.82	2.91	3.00	3.08	3.17	3.25	2.99
7.20	2.58	2.99	3.40	3.80	4.20	4.59	4.98	3.79
Average	2.85	3.01	3.16	3.30	3.45	3.59	3.73	3.30

*values for parallel orientation only

TABLE VI

ε' versus Frequency ($x10^9$Hz)

f	Average ε'	2.85‰ ε'	3.40‰ ε'	7.20‰ ε'
28	2.94	3.00	2.90	2.91
30	2.98	3.03	2.94	2.99
32	3.03	3.05	2.98	3.06
34	3.08	3.08	3.02	3.13
36	3.12	3.11	3.06	3.21
38	3.17	3.13	3.09	3.28
40	3.21	3.16	3.12	3.34

Comparison of the Average Values
of Loss Tangent

TABLE VII

Temperature: -7°C

Frequency ($x10^9$Hz)

Salinity ‰			28	30	32	34	36	38	40	Average
	2.85	∥	.268*	.280*	.292*	.300*	.308*	.320*	.328*	.300*
		AV.								.150*
		⊥	.067	.070	.073	.075	.077	.080	.082	.075
	3.40	∥	.280 *	.292*	.308*	.320*	.332*	.348*	.360*	.320*
		AV.								.160*
		⊥	.070	.073	.077	.080	.083	.087	.090	.080
	7.20	∥	.300*	.316*	.332*	.344*	.360*	.372*	.388*	.344*
		AV.								.172*
		⊥	.075	.079	.083	.086	.090	.093	.097	.086
AV. Parallel			.284*	.296*	.312*	.320*	.332*	.348*	.360*	.322*
Overall Average			.142*	.148*	.152*	.160*	.166*	.179*	.180*	.161*
AV. Perpendicular			.071	.174	.078	.080	.083	.087	.090	.080

*values estimated from the value for Perpendicular orientation

TABLE VIII

Temperature: -16.5°C

Frequency ($x10^9$Hz)

Salinity ‰			28	30	32	34	36	38	40	Average
	2.85	∥	.054	.054	.054	.053	.053	.053	.053	.053
		AV.	.035	.037	.038	.039	.041	.042	.044	.039
		⊥	.017	.020	.023	.026	.029	.032	.035	.026
	3.40	∥	.053	.054	.054	.055	.056	.056	.057	.055
		AV.	.039	.040	.040	.041	.041	.042	.042	.041
		⊥	.029	.027	.027	.027	.026	.026	.026	.027
	7.20	∥	.130	.124	.118	.110	.104	.098	.090	.111
		AV.	.084	.079	.075	.070	.066	.060	.056	.070
		⊥	.036	.039	.032	.030	.028	.026	.023	.030
AV. Parallel			.079	.077	.075	.073	.071	.069	.067	.073
Overall Average			.053	.052	.051	.050	.049	.048	.047	.050
AV. Perpendicular			.027	.027	.027	.028	.028	.028	.028	.028

Comparison of the Average Values
of Loss Tangent

TABLE IX

Temperature: -21.5°C

Frequency ($x10^9$Hz)

			28	30	32	34	36	38	40	Average
Salinity ‰	2.85	∥	.034	.036	.038	.039	.041	.043	.044	.039
		AV.	.023	.025	.027	.029	.031	.033	.035	.029
		⊥	.010	.013	.016	.018	.021	.024	.026	.018
	3.40	∥	.036	.036	.036	.036	.036	.036	.036	.036
		AV.	.029	.029	.028	.028	.027	.027	.026	.026
		⊥	.022	.021	.020	.019	.018	.017	.016	.019
	7.20	∥	.070	.068	.067	.065	.064	.062	.060	.065
		AV.	.048	.046	.045	.043	.042	.040	.034	.043
		⊥	.025	.024	.023	.021	.020	.019	.018	.021
AV. Parallel			.047	.047	.047	.047	.047	.047	.047	.047
Overall Average			.033	.033	.033	.033	.033	.033	.033	.033
AV. Perpendicular			.019	.019	.019	.019	.019	.019	.019	.019

TABLE X

Temperature: -25°C

Frequency ($x10^9$Hz)

			28	30	32	34	36	38	40	Average
Salinity ‰	2.85	∥	.023	.025	.027	.028	.030	.032	.033	.028
		AV.	.016	.018	.020	.022	.025	.027	.029	.022
		⊥	.008	.011	.014	.017	.020	.022	.025	.017
	3.40	∥	.027	.027	.027	.028	.028	.028	.028	.028
		AV.	.024	.024	.024	.023	.023	.023	.023	.024
		⊥	.020	.020	.019	.018	.018	.018	.017	.019
	7.20	∥	.045	.044	.052	.055	.059	.062	.065	.055
		AV.	.033	.034	.035	.037	.038	.039	.041	.033
		⊥	.020	.019	.019	.018	.017	.017	.016	.018
AV. Parallel			.032	.034	.035	.037	.039	.041	.042	.037
Overall Average			.024	.025	.026	.028	.029	.030	.031	.028
AV. Perpendicualr			.016	.017	.017	.018	.018	.019	.019	.018

Comparison of the Average Values
of Loss Tangent

TABLE XI

Temperature: -32°C

Frequency ($x10^9$Hz)

Salinity ‰			28	30	32	34	36	38	40	Average
	2.85	∥	.002	.003	.004	.006	.006	.007	.008	.005
		AV.								
		⊥	.002*	.002*	.002*	.003*	.003*	.004*	004*	.003*
	3.40	∥	.007	.008	.008	.009	.009	.010	.010	.009
		AV.	.006	.007	.007	.007	.007	.007	.007	.007
		⊥	.006	.006	.006	.005	.005	.005	.005	.005
	7.20	∥	.009	.009	.010	.010	.011	.011	.012	.009
		AV.	.006	.006	.006	.007	.007	.008	.008	.007
		⊥	.003	.003	.003	.004	.004	.004	.004	.004
AV. Parallel			.006	.007	.007	.008	.009	.009	.010	.008
Overall Average			.005	.005	.006	.006	.007	.007	.008	.006
AV. Perpendicular			.004	.004	.004	.004	.004	.004	.004	.004

*estimated from values for Parallel Orient

TABLE XII

Tan δ vs Frequency

f	overall AV.	∥	⊥	∥	⊥	∥	⊥
28	.058	.076	.020	.081	.029	.111	.032
30	.060	.080	.023	.003	.029	.113	.032
32	.062	.083	.026	.087	.030	.116	.032
34	.064	.085	.028	.090	.029	.118	.032
36	.065	.088	.030	.092	.030	.120	.032
38	.067	.091	.032	.095	.031	.121	.032
40	.069	.093	.034	.098	.031	.123	.032

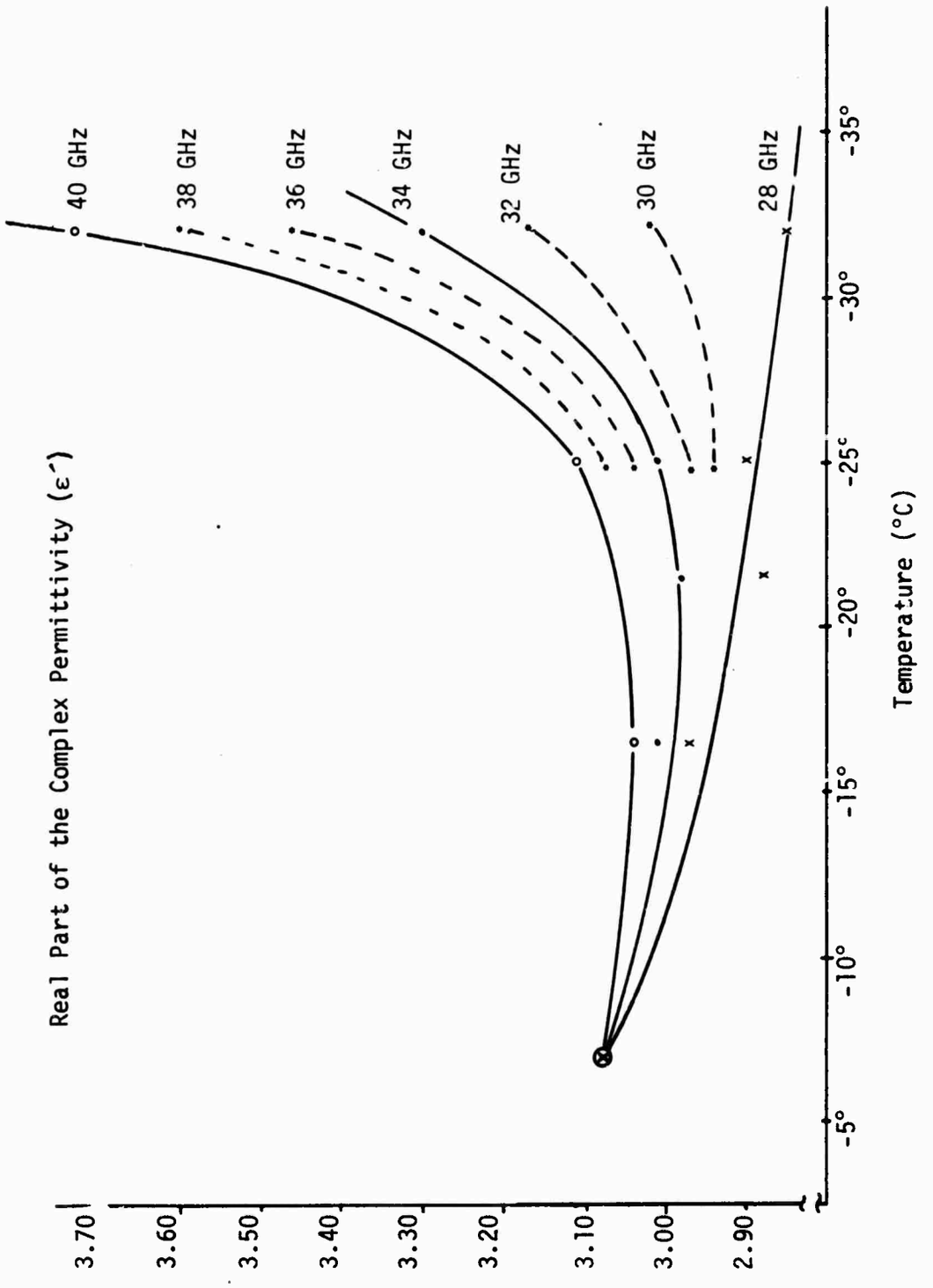

Figure 11. Change in the Real Part of the Complex Permittivity With Temperature and Frequency Averaged for all Salinities.

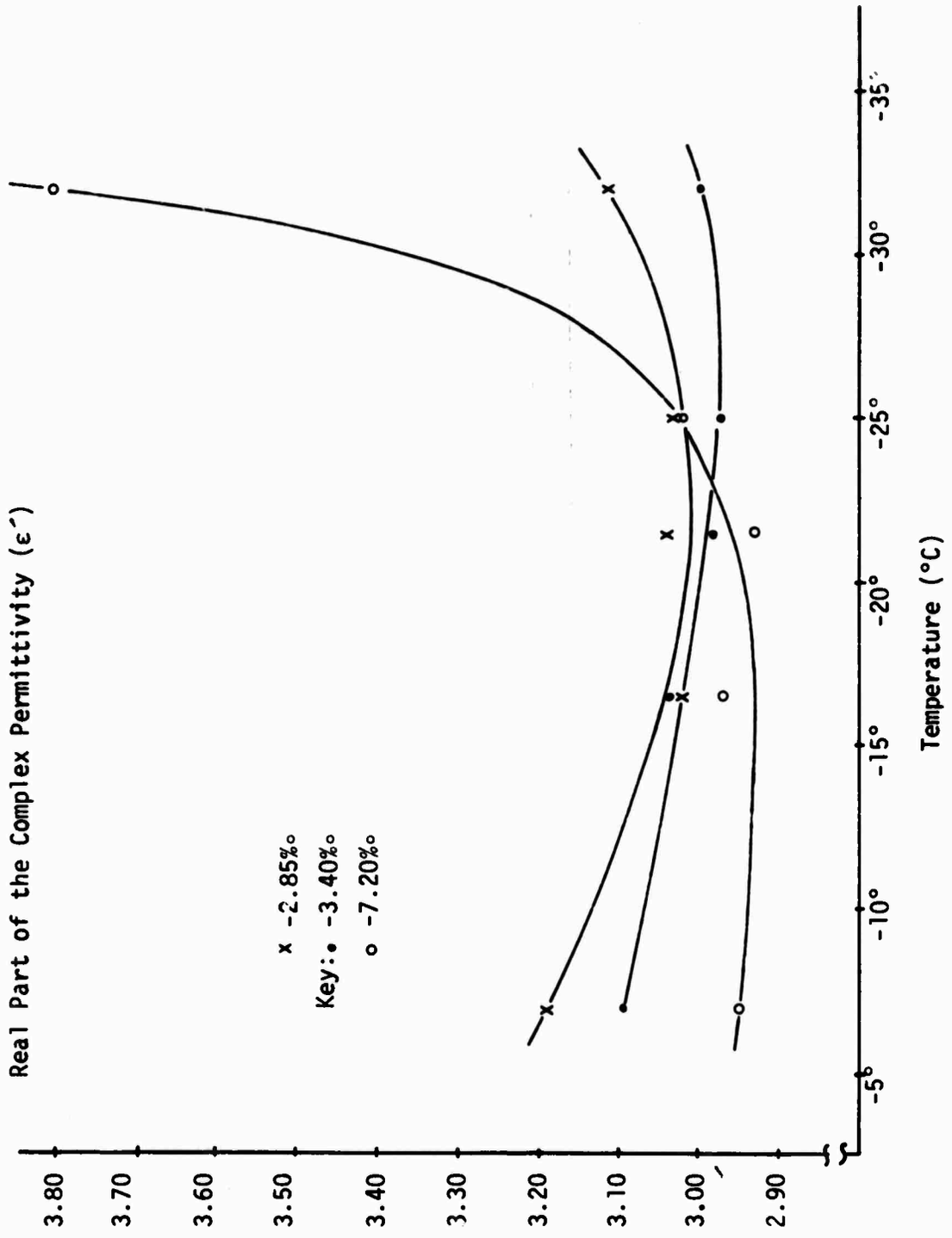

Figure 12. Change in the Real Part of the Complex Permittivity with Temperature and Salinity for a Constant Frequency of 34 Ghz.

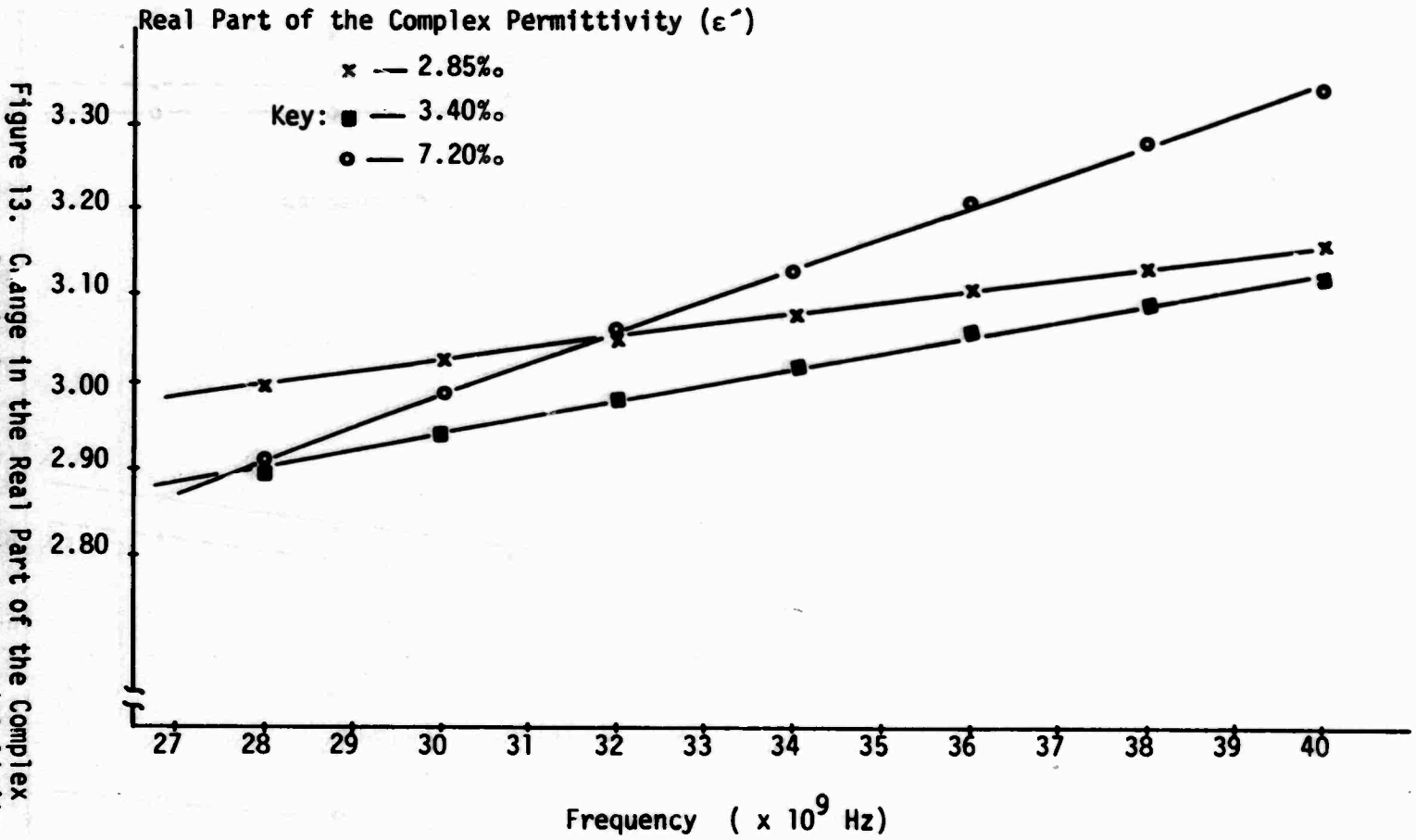

Figure 13. Change in the Real Part of the Complex Permittivity With Frequency and Salinity Averaged for all Temperatures.

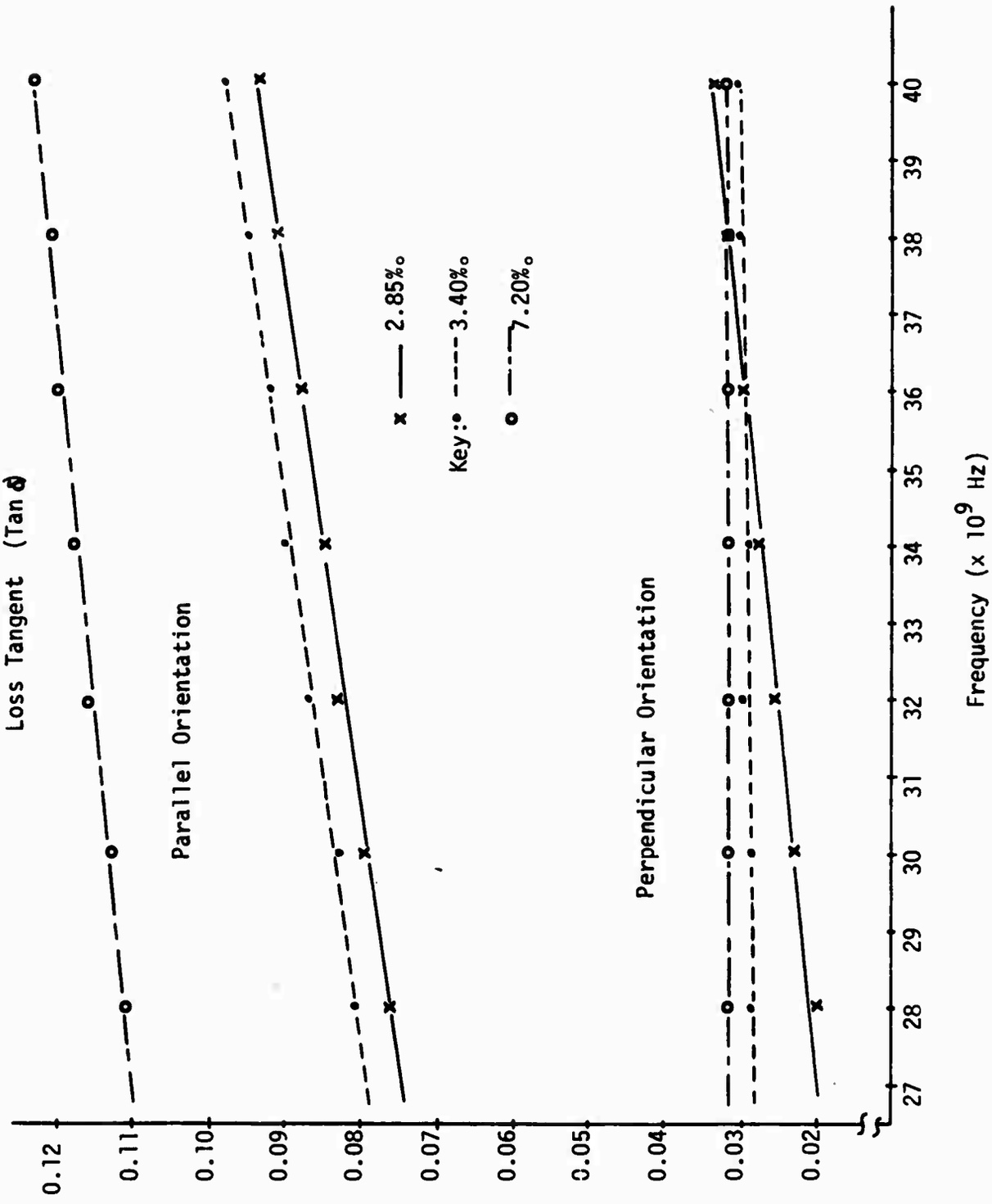

Figure 14. Change in Loss Tangent with Frequency, Salinity, and Orientation; Averaged for all Temperatures.

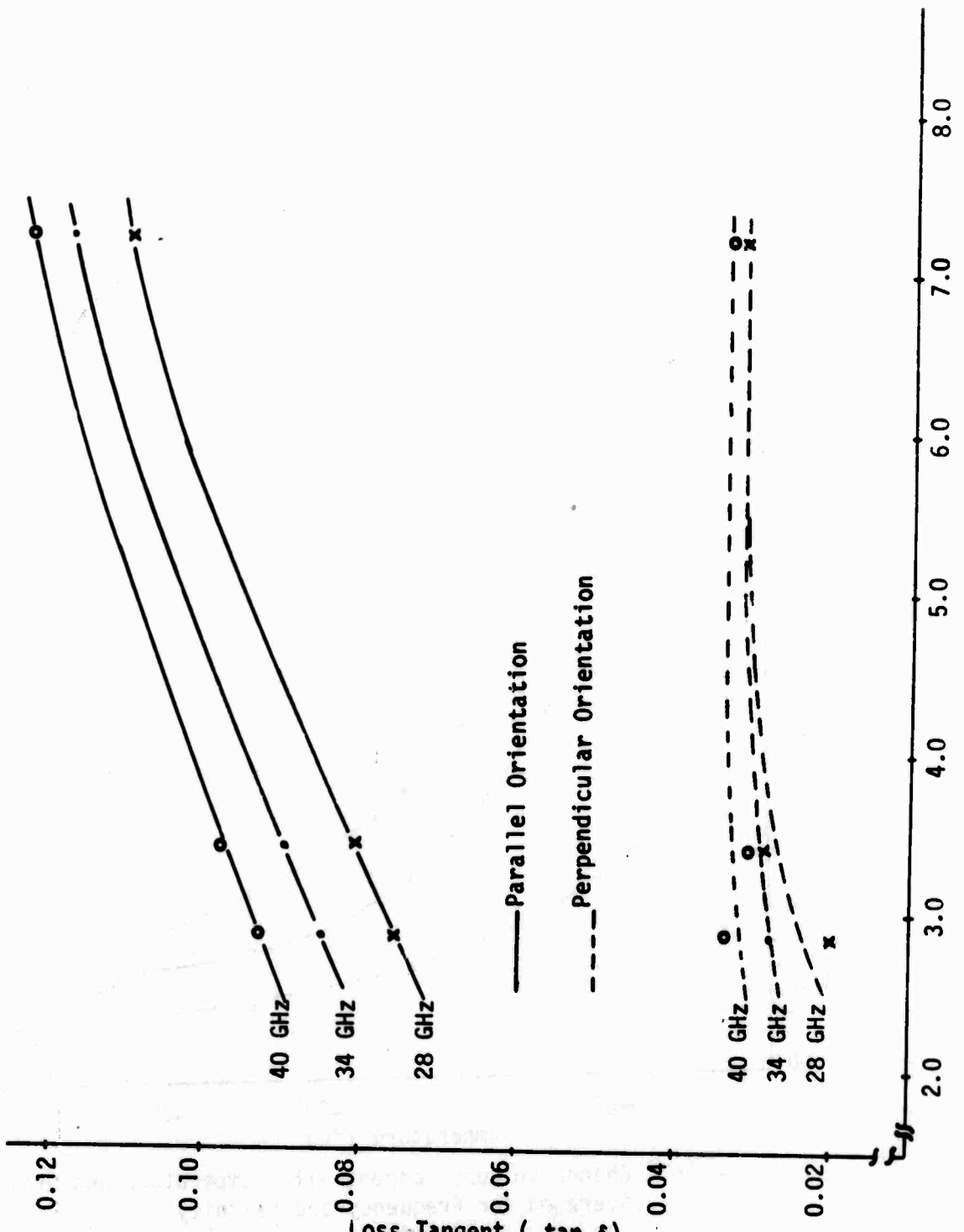

Figure 15. Change in Loss Tangent with Salinity, Frequency, and Orientation; Averaged for all Temperatures.

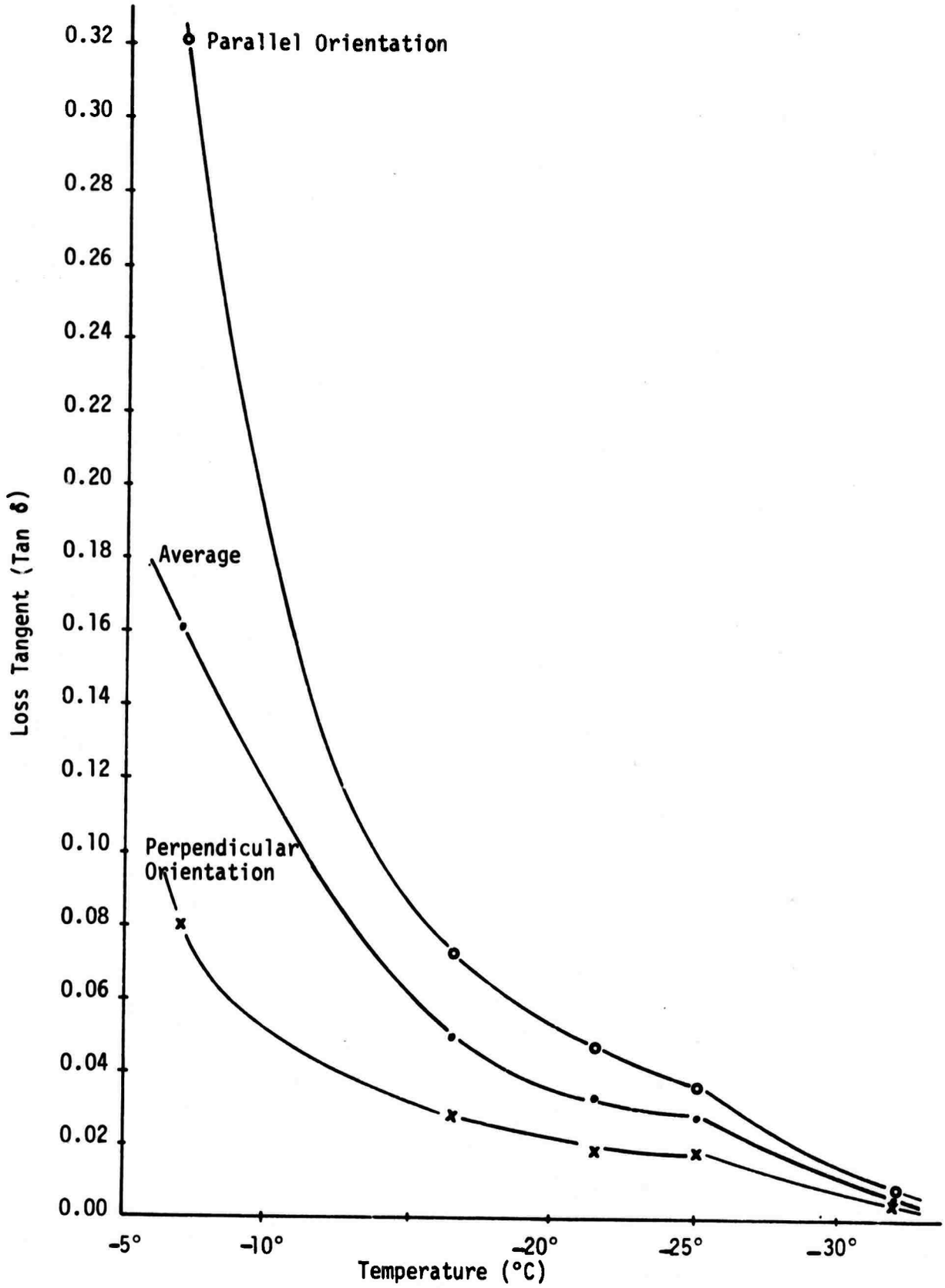

Figure 16. Change in Loss Tangent with Temperature and Orientation; Averaged for Frequency and Salinity.

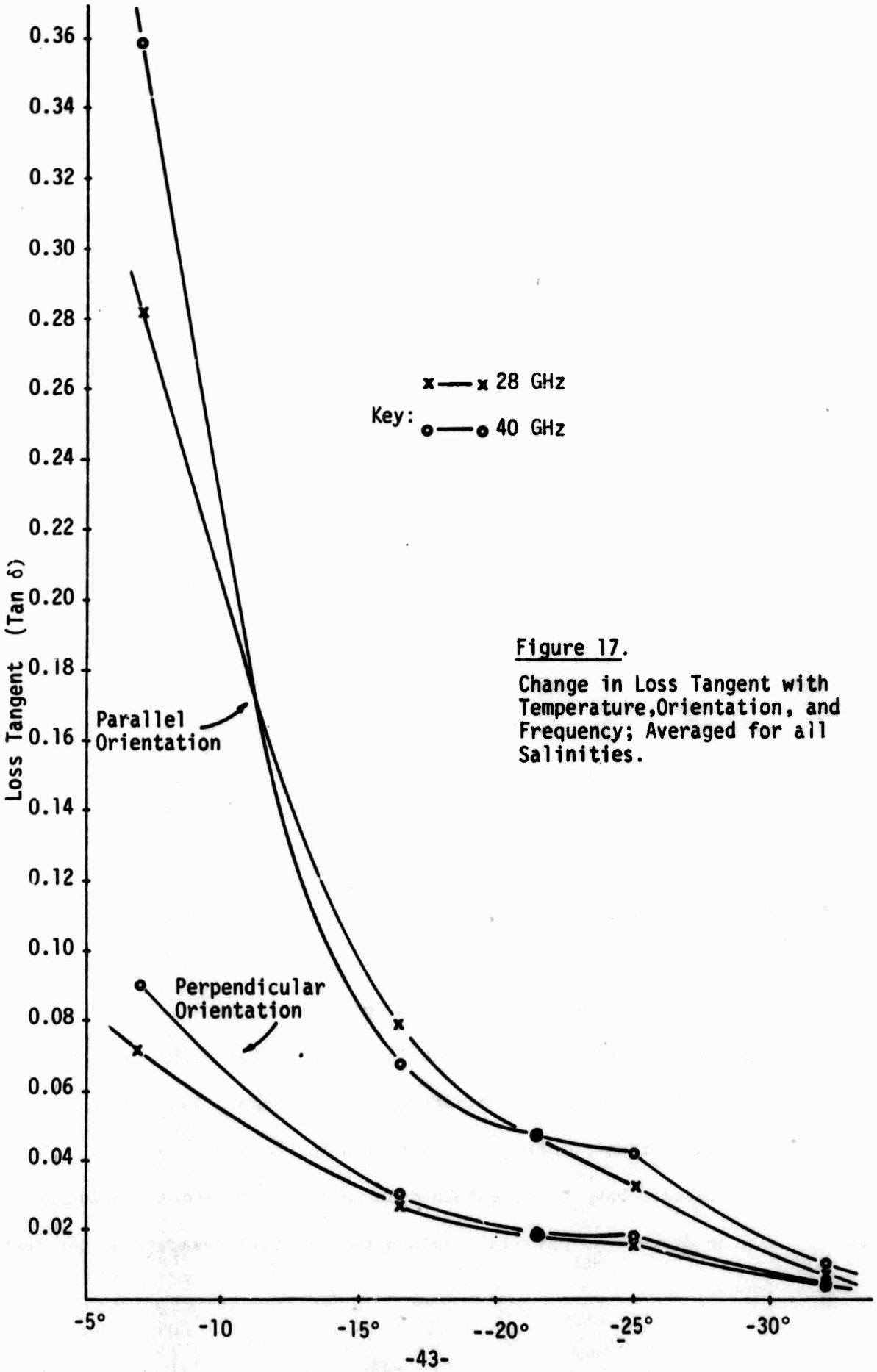

Figure 17.

Change in Loss Tangent with Temperature, Orientation, and Frequency; Averaged for all Salinities.

VI. DISCUSSION

An examination of the graphic presentation of the data for the real part of the dielectric constant (ε') shows that, though differences do exist for individual conditions, the effect of brine inclusion orientation is small and not detectable within the accuracy of these experiments. It has been stated that sea ice can be considered as a mixture of two dielectrics, ice and brine, and that the complex permittivity will be a function of the interaction of these two components. At the warmest temperature, -7°C, and highest salinity, 7.2 $^{o}/oo$, covered by these experiments the brine value was approximately 6% of the total volume of the sea ice (see Figure 2), compared to 2.5% for 2.85 $^{o}/oo$ sea ice at -7°C. The percent brine by volume drops to one tenth of these values at -32°C. [2] Figure 11 shows that the average value to the real part of the complex permittivity decreases with decrease in temperature, for the higher frequencies measured. Figure 12 shows that this effect is due primarily to the samples measured at 7.2 $^{o}/oo$ salinity. It should be noted that the errors in these measurements are independent of salinity and frequency. Further, the values represented in Figure 12 for 34 GHz also represent the averages for all frequencies. Figure 13 shows the overall increase of the real part with increase in frequency. These effects will have to be examined in more detail before conclusions can be drawn. No physical explanation for this observation has been found.

The most interesting result from this series of measurements is seen in the marked effect of brine inclusion orientation on the loss tangent in sea ice. An examination of the data presented in Figures A15 through A30 of the Appendix shows that without exception, the parallel orientation of brine inclusions with respect to the electric field in the wave guide caused the loss tangent to be greater than perpendicular orientation. It has been shown by a number of investigators that at frequencies above approximately 1 x 10^9 Hz dielectric losses due to ionic conduction are negligible and loss can be principally associated with dipole rotation of the molecules of the dielectric material.[12, 13, 14] In a crystalline substance such as pure ice, molecular rotation is restricted by the nature of the molecular bonding and dielectric loss is small. In liquid water, dipole rotation is significant and causes dielectric loss to be high in the frequencies of interest in this experiment. [12, 13, 14] It has been shown that the shape of the included medium in mixtures of dielectrics has an effect on the dielectric properties of the mixture.[14, 15] This theory should be examined further for the specific case of sea ice.

Figure 14 shows that the loss tangent of sea ice increases with frequency and that there is a pronounced difference between the different orientations for all salinities measured. Figure 15 shows that loss increased with salinity and again shows the increase with frequency. Figure 16 shows the large change in loss with temperature and orientation. Figure 17 shows this change with frequency as an added parameter.

Figure 18 shows a plot of ln(tan δ) as a function of 1/T, temperature being measured in degrees Kelvin. It would seem apparent from this presentation that a dramatic change occurs within the sea ice in the temperature range from -21.5°C to -25°C, since the slope of the straight line indicates the activation energy of the physical process which results in loss.

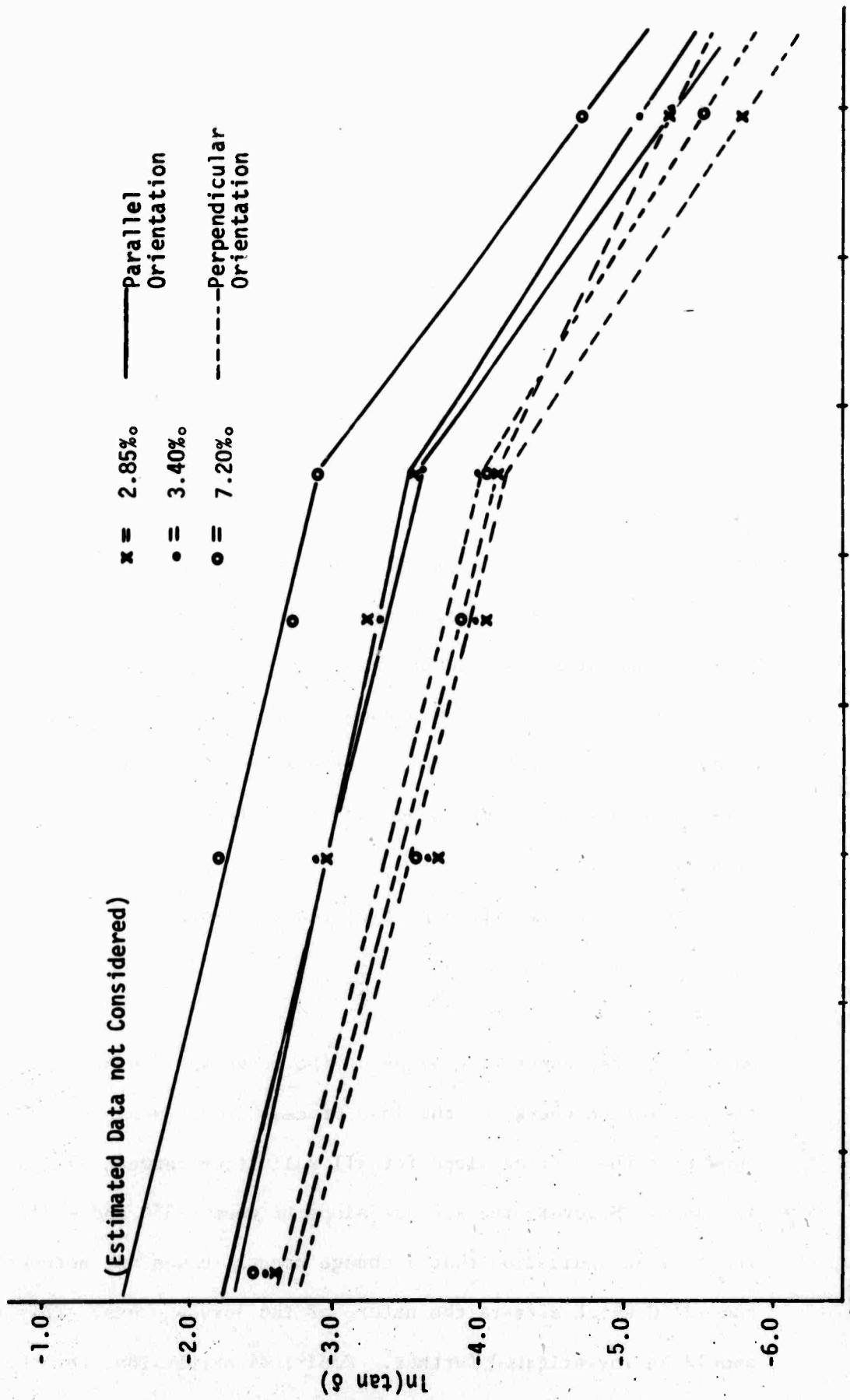

Figure 18. Change in the Natural Log of Loss Tangent With 1/T for Salinity and Orientation; Averaged for all Frequencies.

VII. CONCLUSIONS AND RECOMMENDATIONS

We can conclude that the average value of the real part of the relative complex permittivity for this band of frequencies is 3.08 $\pm$ 0.06. This compares favorably with limiting values for pure ice at high frequencies calculated by Auty and Cole to be 3.10 and by Lamb to be 3.17.[12] These values were extrapolated from experiments done at lower frequencies. Pure ice should be examined at the frequencies of this experiment for comparison. The increase in the real part seen in these measurements with the higher frequencies at low temperatures should be examined more closely.

These measurements show strong indications that the loss tangent of sea ice is a function of the orientation of the brine cell vertical axis. The physical process behind this effect should be examined more closely.

Figure 18 represents a plot of the expression

$$\ln (\tan \delta) = \ln A - \frac{E}{KT} \qquad (24)$$

where $-\frac{E}{K}$ represents the slope of the curve and can be related to the activation energy of the loss process in the sea ice. Calculations show that the average slope for all salinities between -7°C and -25°C is -5800. However, the average slope between -25°C and -32°C is -13,400. There is an indication that a change occurs in sea ice between -21°C and -25°C which affects the nature of the loss process. This effect should be investigated further. Empirical expressions for the loss

tangent of sea ice at approximately 5.0 °/oo can be derived from the information in Figure 18, for the two temperature ranges. For temperatures above -25°C this is

$$\ln (\tan \delta) = 20.13 - 5800 \frac{1}{T} \qquad (25)$$

For temperatures below -25°C this expression will be

$$\ln (\tan \delta) = 50.43 - 13400 \frac{1}{T} \qquad (26)$$

Temperature in these equations is expressed in degrees Kelvin. These expressions will need refinement for increased accuracy, but they should provide a good first approximation of the loss factor for sea ice below approximately -5°C and in the vicinity of 5 °/oo.

APPENDIX

TABLE AI. DATA POINTS FOR SEA ICE

OF SALINITY 2.85 °/oo

Temperature	Frequency (x 10^9 Hz)	ε'		Tan δ	
		perpendicular	parallel	perpendicular	parallel
-7°C	30.02	3.07		.074	
	33.58	3.47		.103	
	33.56	3.13		.049	
	37.18	3.09		.083	
	29.57		3.22		-
	29.60		2.20		-
	32.21		3.43		-
	32.30		2.88		-
	34.54		4.13		-
	35.06		3.29		-
	37.90		2.87		-
-16.5°C	29.23	2.81		.017	
	30.62	2.92		.026	
	34.15	2.93		.024	
	34.28	3.19		.032	
	37.98	3.01		.033	
	28.99		3.27		-
	30.16		2.83		.048
	30.92		3.07		.048
	31.34		3.02		.069
	32.68		3.26		.070
	33.81		2.77		-
	35.23		2.91		.063
	36.24		3.42		.069
	37.93		2.58		.052
	38.20		2.79		.044
	38.67		2.89		-
-21.5°C	29.28	2.76		.014	
	30.75	3.00		.020	
	34.25	2.82		.013	
	34.43	3.06		.025	
	38.11	3.22		.029	
	29.22		2.36		.037
	30.00		3.05		.037
	30.20		2.81		.034
	31.58		4.13		.044
	32.77		3.05		.041
	32.80		3.00		.036

(continued on the next page)

Table AI (continued): Data Points for Sea Ice of Salinity 2.85 °/oo

Temperature	Frequency ($x10^9$ Hz)				
-21.5°C	33.90		2.77		.042
	35.29		3.24		.049
	36.35		3.33		.058
	37.89		2.78		.043
	38.77		2.98		.037
-25°C	29.29	2.81		.009	
	30.79	3.05		.016	
	34.36	2.56		.012	
	34.36	3.06		.022	
	38.12	3.28		.024	
	27.81		2.93		.023
	29.11		3.17		.026
	30.11		3.00		.036
	30.32		2.98		.025
	31.50		2.91		.027
	32.83		3.23		.028
	32.87		3.01		.030
	33.98		2.86		.037
	35.35		3.07		.031
	35.62		3.25		.035
	36.41		3.33		.040
	37.96		2.85		.029
	38.36		3.20		.034
-32°C	27.94		3.20		.002
	29.23		3.62		.003
	30.46		2.74		.007
	30.62		3.24		.016
	31.65		2.54		.005
	32.93		3.77		.011
	33.43		3.34		.014
	34.08		3.47		.015
	35.50		2.43		.011
	35.62		3.25		.017
	36.51		2.77		.008
	38.23		2.98		.012
	38.36		3.20		.021

TABLE AII: Data Points for Sea Ice of Salinity 3.40 °/oo

Temperature	Frequency ($\times 10^9$ Hz)	ε'		Tan δ	
		perpendicular	parallel	perp.	par.
-7°C	28.10	2.86		-	
	29.55	2.91		.044	
	30.48	3.39		.081	
	31.00	3.31		-	
	32.03	3.23		.050	
	33.66	3.10		.086	
	33.90	3.02		-	
	34.50	3.13		.047	
	36.86	3.46		.106	
	36.90	3.11		-	
	36.94	3.53		.086	
	28.23		2.67		-
	28.90		2.75		-
	31.05		3.80		-
	32.30		3.18		-
	33.92		2.75		-
	35.80		2.80		-
	36.97		2.94		-
-16.5°C	30.05	3.15		.020	
	31.07	3.01		.031	
	31.40	3.10		-	
	32.51	3.13		.019	
	34.30	2.92		-	
	34.34	3.06		.029	
	35.04	2.96		.017	
	37.30	3.35		-	
	37.56	3.35		.017	
	37.61	3.22		.029	
	28.70		3.00		.053
	29.30		2.96		-
	31.60		3.06		.058
	32.80		2.79		-
	34.51		3.16		.053
	36.33		2.90		-
	37.97		2.97		.059
-21.5°C	30.15	2.88		.019	
	31.10	2.88		.023	
	31.50	2.97		-	
	32.65	3.16		.015	
	34.43	2.95		.021	
	34.50	2.98		-	
	35.14	3.15		.014	

(continued on the following page)

TABLE AII: Data Points for Sea Ice of Salinity 3.40 °/oo

(continued)

-21.5°C	37.40	3.11		-	
	37.67	3.04		.014	
	37.73	3.20		.019	
	28.81		3.01		.037
	29.30		2.95		-
	31.69		3.14		.037
	32.70		3.09		-
	34.60		3.09		.035
	36.25		2.63		-
	37.58		2.95		.038
-25°C	30.17	2.80		.017	
	31.21	3.01		.023	
	32.73	2.90		.012	
	34.50	3.00		.021	
	35.24	3.24		.011	
	37.77	2.96		.012	
	37.79	3.21		.021	
	28.79		3.09		.028
	29.40		3.03		-
	31.70		2.92		.029
	32.87		3.17		-
	34.64		3.17		.027
	37.67		2.72		.030
-32°C	30.35	2.57		.007	
	31.18	2.90		.011	
	32.91	3.17		.003	
	34.79	2.03		.005	
	38.09	4.81		.009	
	38.13	2.27		.003	
	28.93		3.18		.004
	31.79		3.07		.011
	34.79		2.76		.007
	37.80		3.19		.011

TABLE AIII: DATA POINTS FOR
SEA ICE OF SALINITY 7.20 °/oo

Temperature	Frequency (x10^9 Hz)	ε'		Tan δ	
		perpendicular	parallel	perpendicular	parallel
-7°C	28.73	3.18		.068	
	30.67	3.50		.070	
	30.80	2.78		.090	
	31.20	2.74		.068	
	32.39	3.11		.127	
	33.70	3.39		.080	
	34.97	2.80		.059	
	35.81	2.91		.161	
	36.70	2.68		.041	
-16.5°C	28.10	3.80		.029	
	31.06	2.26		.045	
	31.36	3.16		.027	
	31.46	2.54		.026	
	32.90	2.80		.028	
	34.17	3.84		.020	
	36.38	3.00		.035	
	37.30	2.24		.015	
	38.02	2.84		.031	
	28.58		2.80		-
	28.88		3.45		.101
	30.30		3.30		.053
	31.48		2.88		-
	31.79		2.66		.099
	34.42		2.84		-
	34.72		3.58		.072
	36.77		2.76		.043
	37.34		3.12		-
	37.55		3.27		.049
-21.5°C	28.16	3.69		.021	
	29.32	2.34		.031	
	31.10	2.17		.014	
	31.47	3.26		.021	
	31.50	2.54		.019	
	32.90	2.80		.022	
	34.19	3.99		.014	
	35.81	2.91		.023	
	36.38	3.00		.028	
	37.22	2.55		.008	
	28.76		2.79		.060
	28.99		2.87		.053
	31.66		2.88		.081
	32.00		2.69		.068

TABLE AIII: Data Points for Sea Ice of Salinity 7.20 °/oo

(continued)

-21.5°C	34.58		2.94		.075
	34.97		3.31		.063
	37.48		3.10		-
	37.86		3.20		.042
-25°C	28.16	3.69		.020	
	29.40	2.28		.017	
	31.12	2.24		.018	
	31.52	3.20		.013	
	31.50	3.10		.018	
	33.00	2.70		.018	
	34.05	4.03		.011	
	35.88	2.87		.016	
	36.60	3.00		.023	
	37.08	2.15		.010	
	28.82		2.74		.047
	29.44		2.74		.032
	31.72		2.96		.063
	32.44		3.48		.077
	34.66		2.85		.048
	35.00		3.93		.067
	37.57		3.20		.082
	37.81		3.10		.037
-32°C	31.65	3.07		.003	
	35.79	3.79		.004	
	29.45		3.21		.009
	32.38		2.79		.010
	35.00		5.90		.012
	37.40		4.15		.011

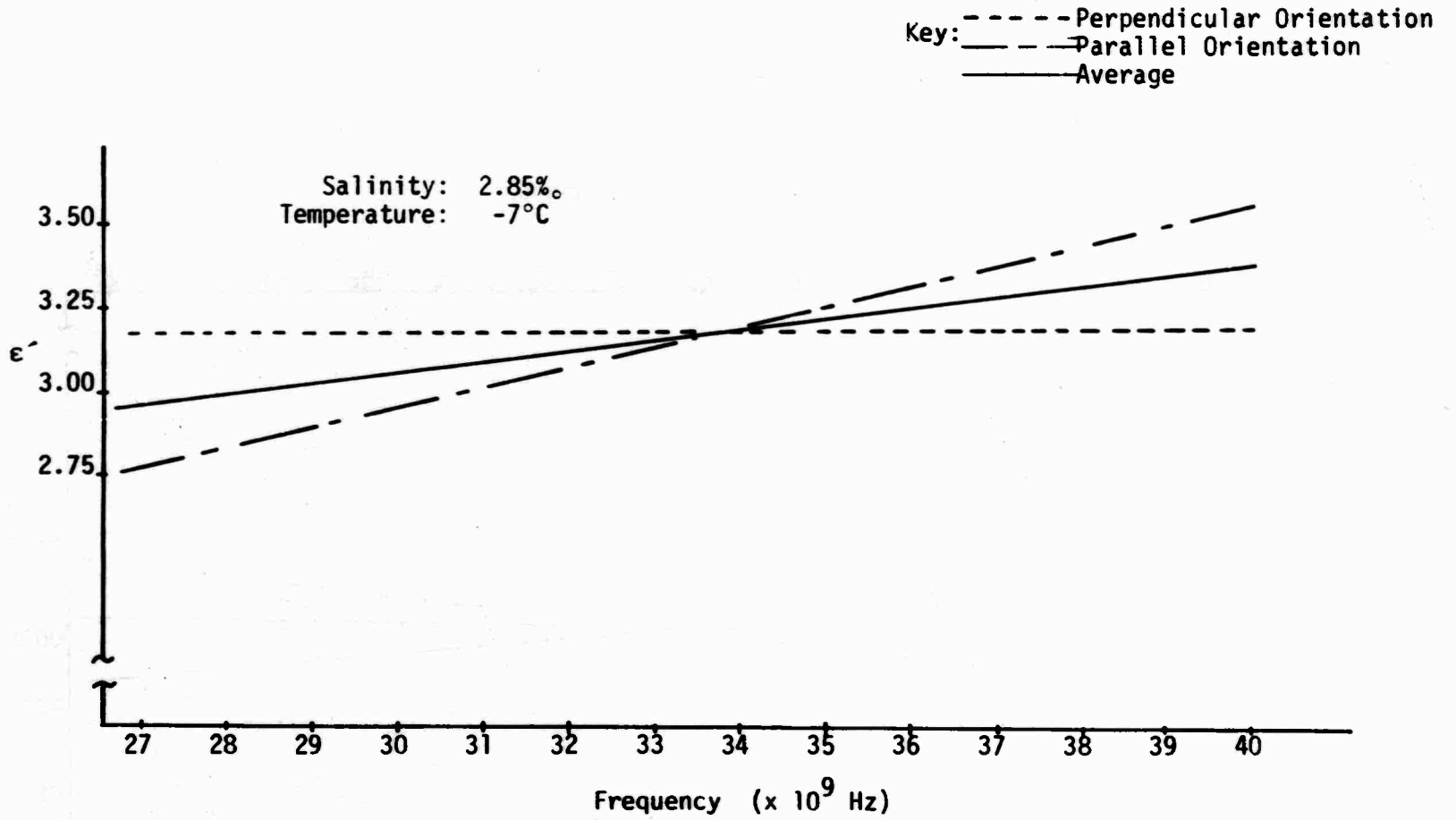

Figure. A-1: ε' vs Frequency

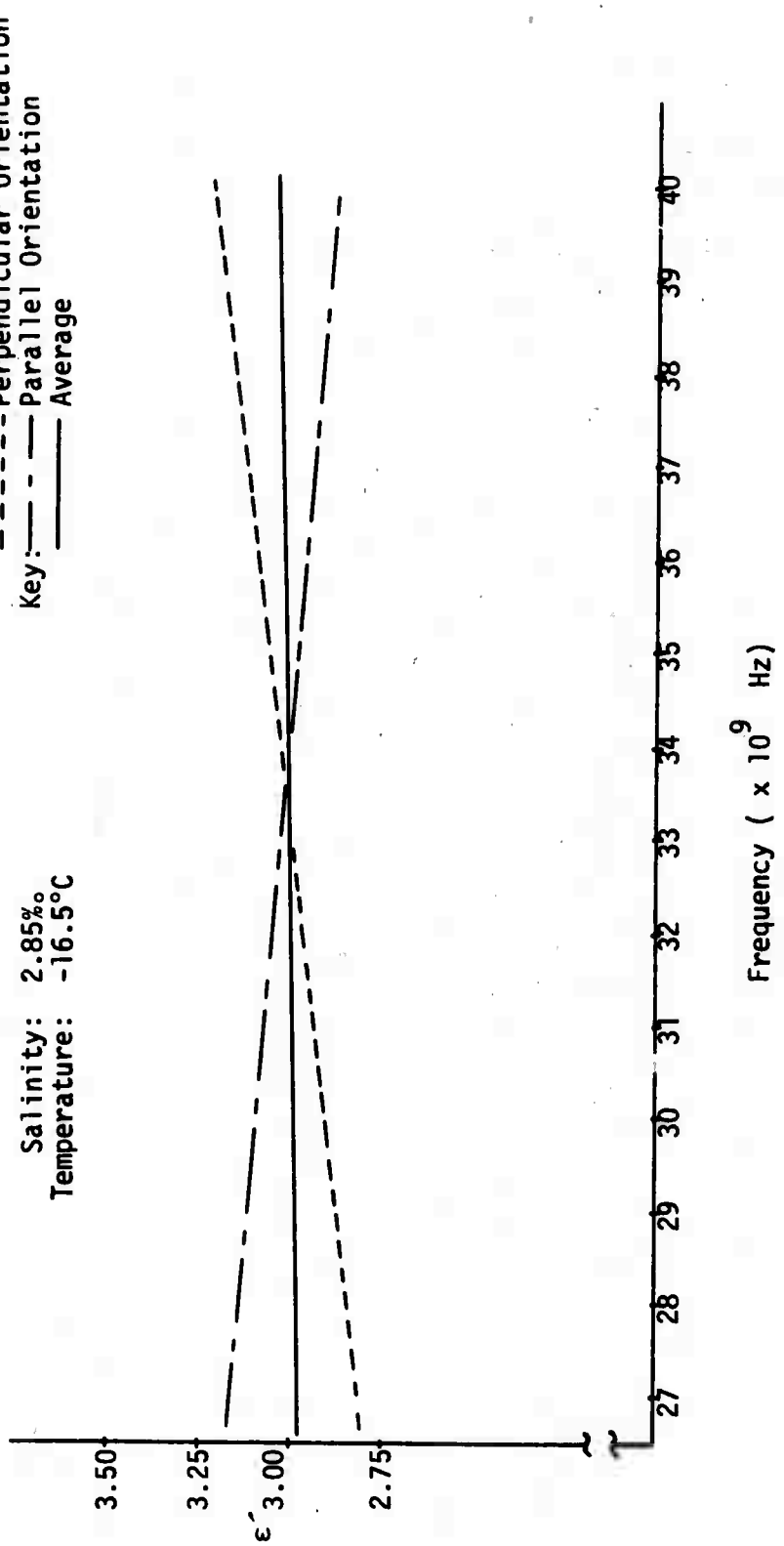

Figure A-2: ε´ versus Frequency

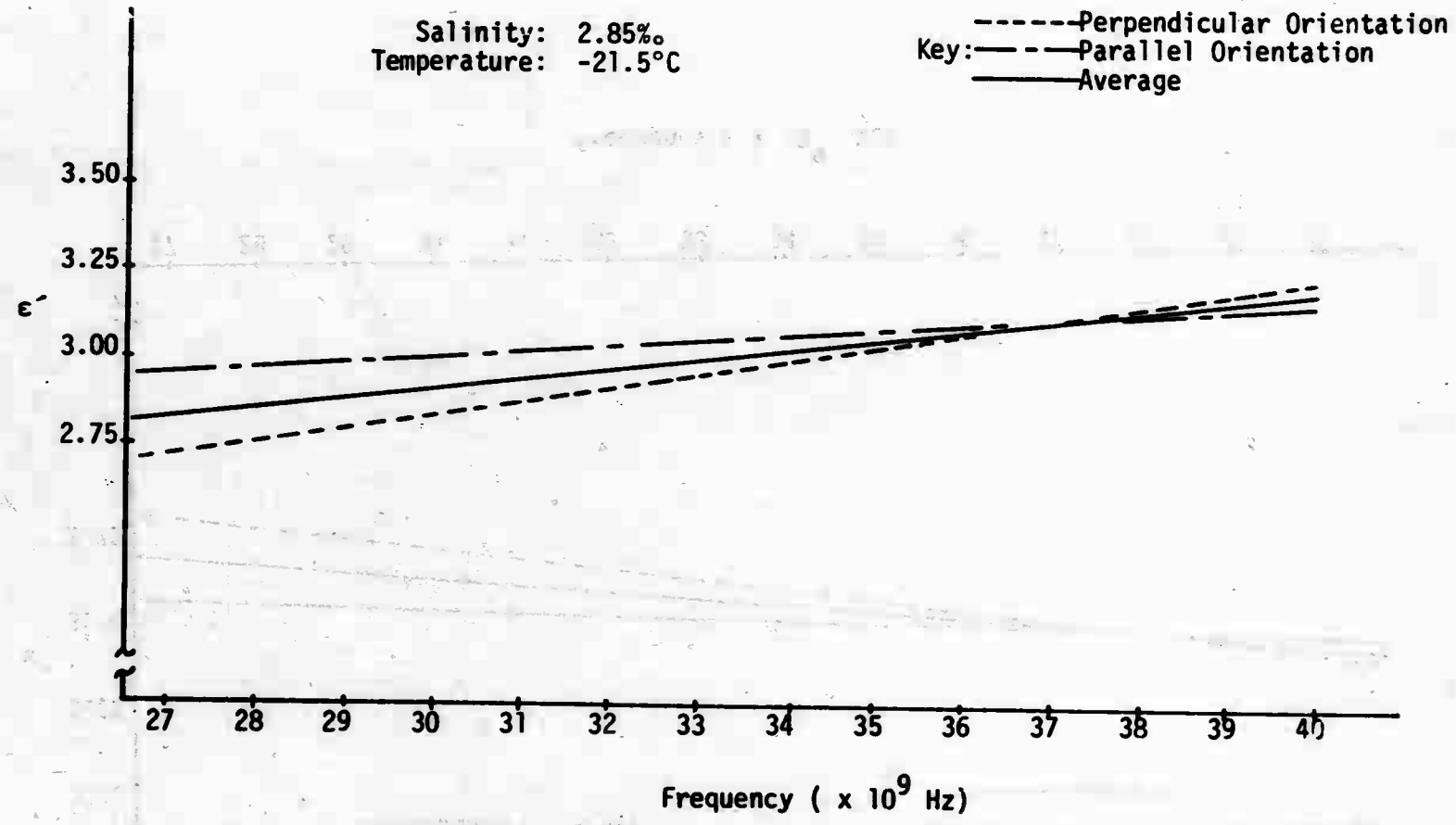

Figure A-3: ε´ versus Frequency

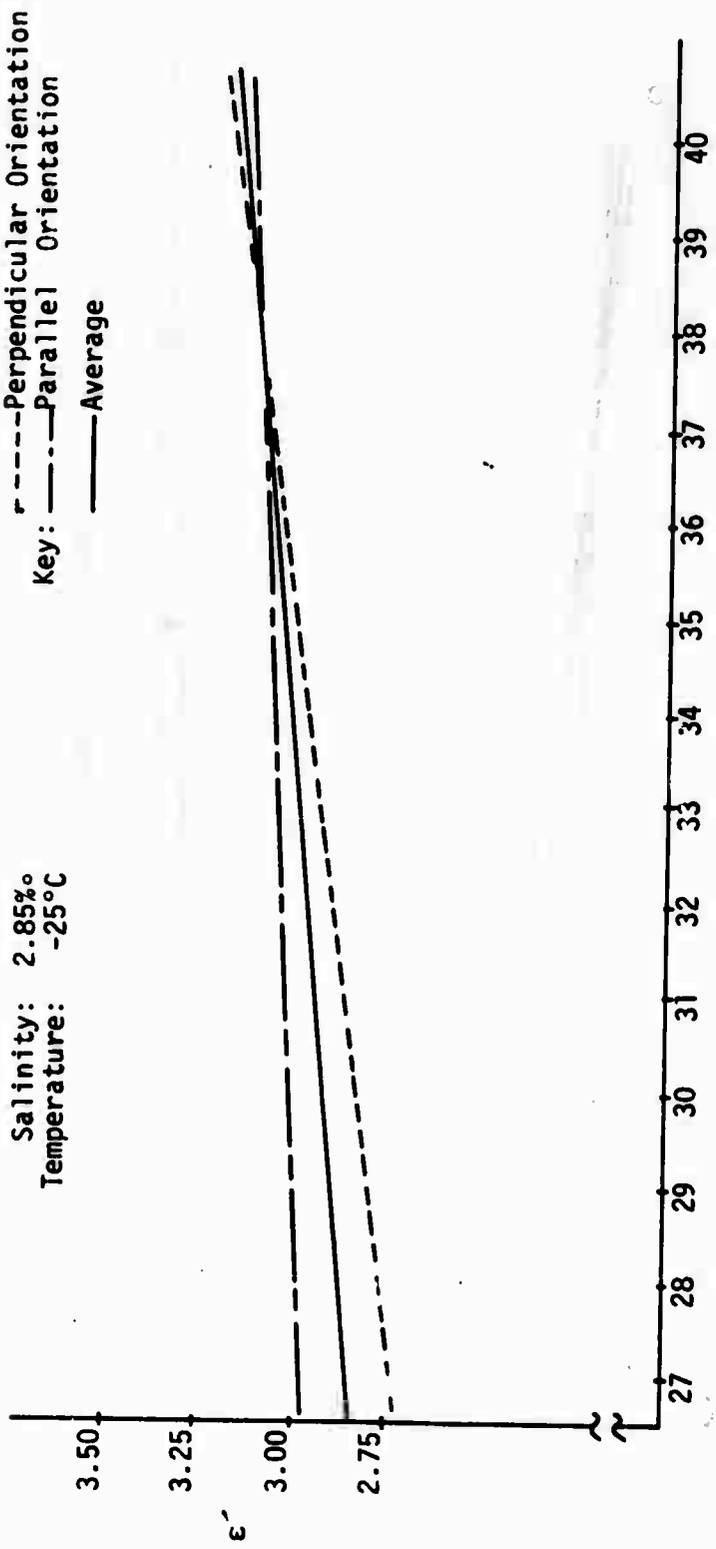

Figure A-4: ε′ versus Frequency

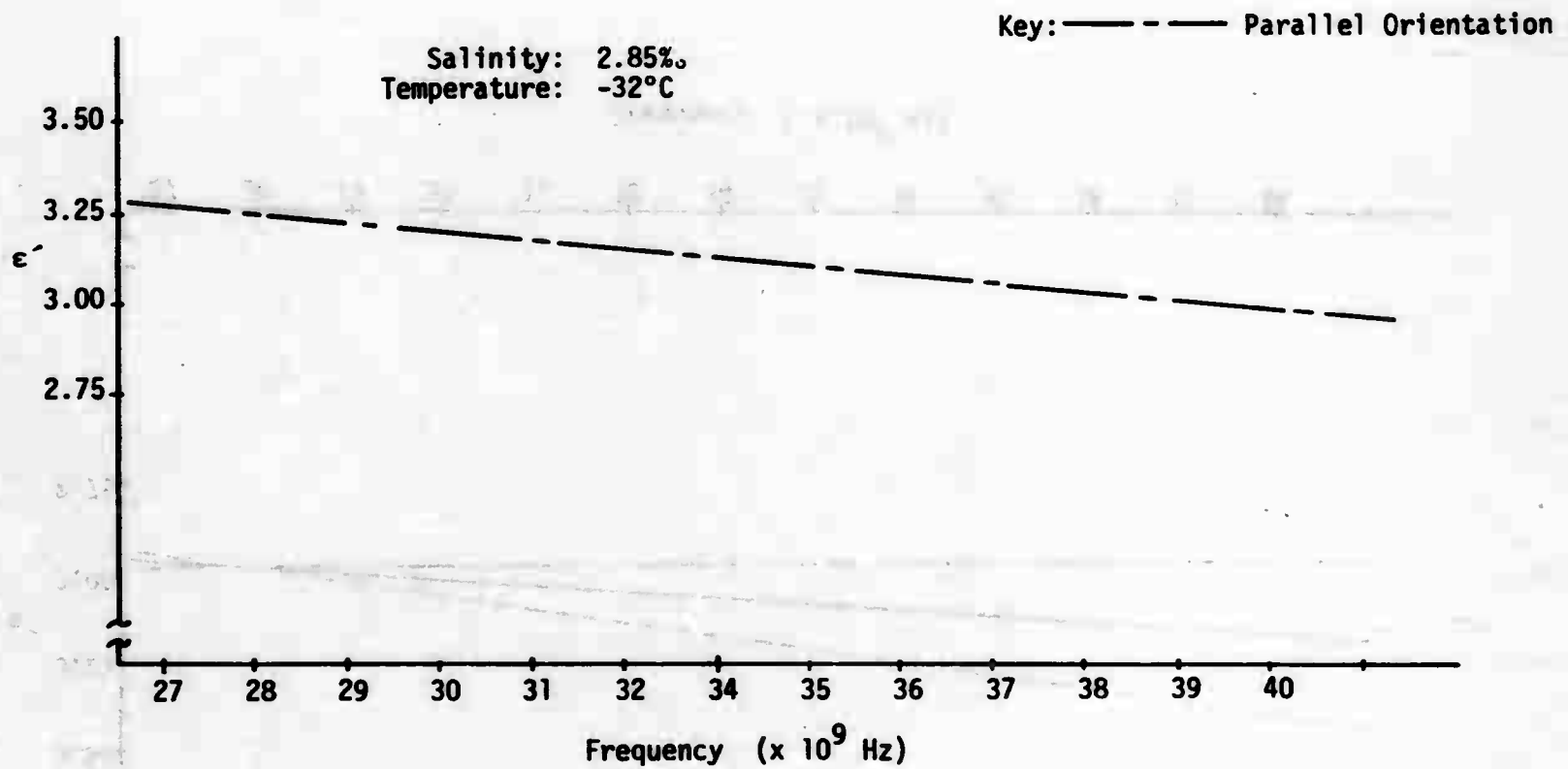

Figure A-5: ε´ versus Frequency

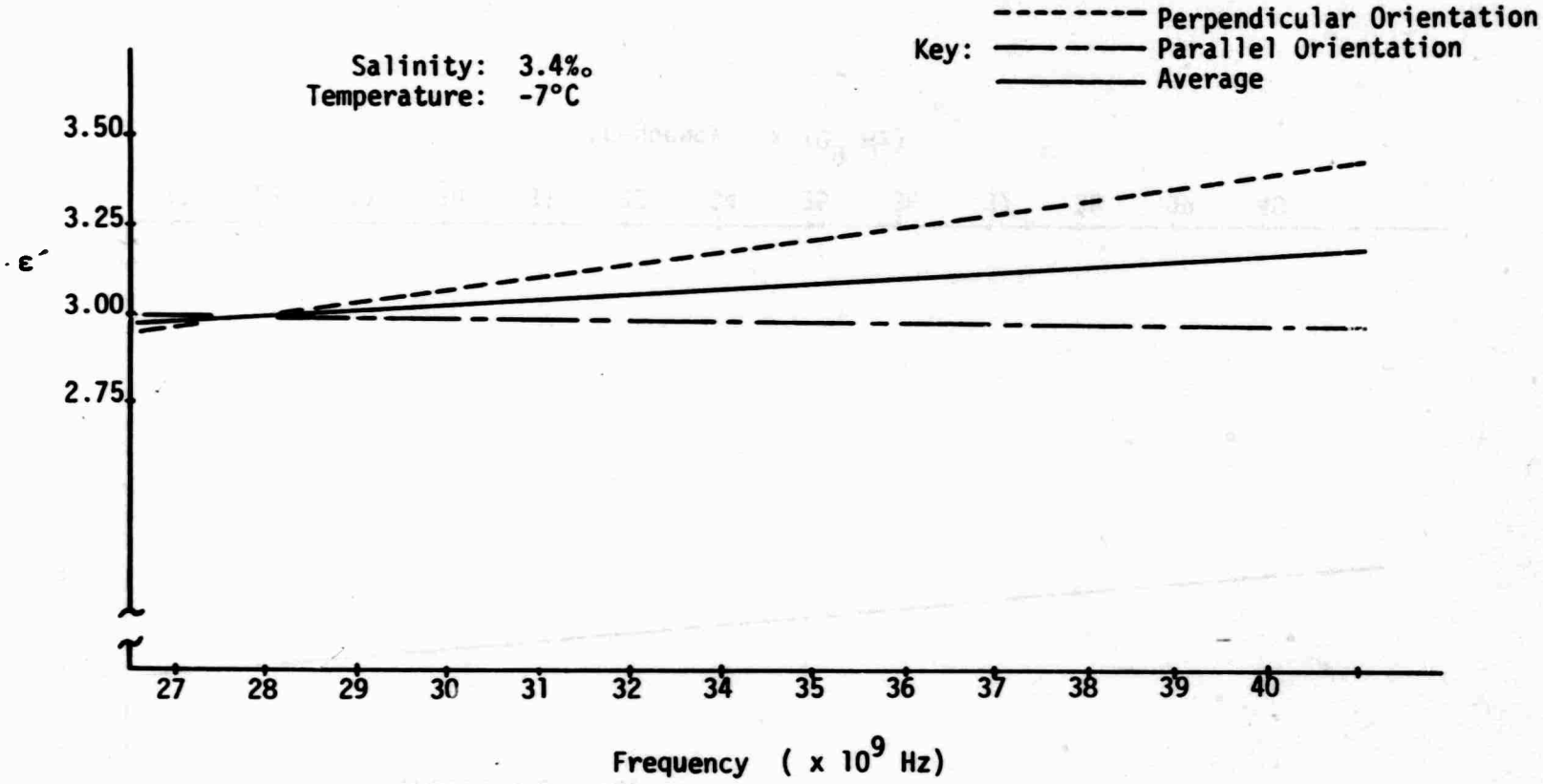

Figure A-6: ε´ vs. Frequency

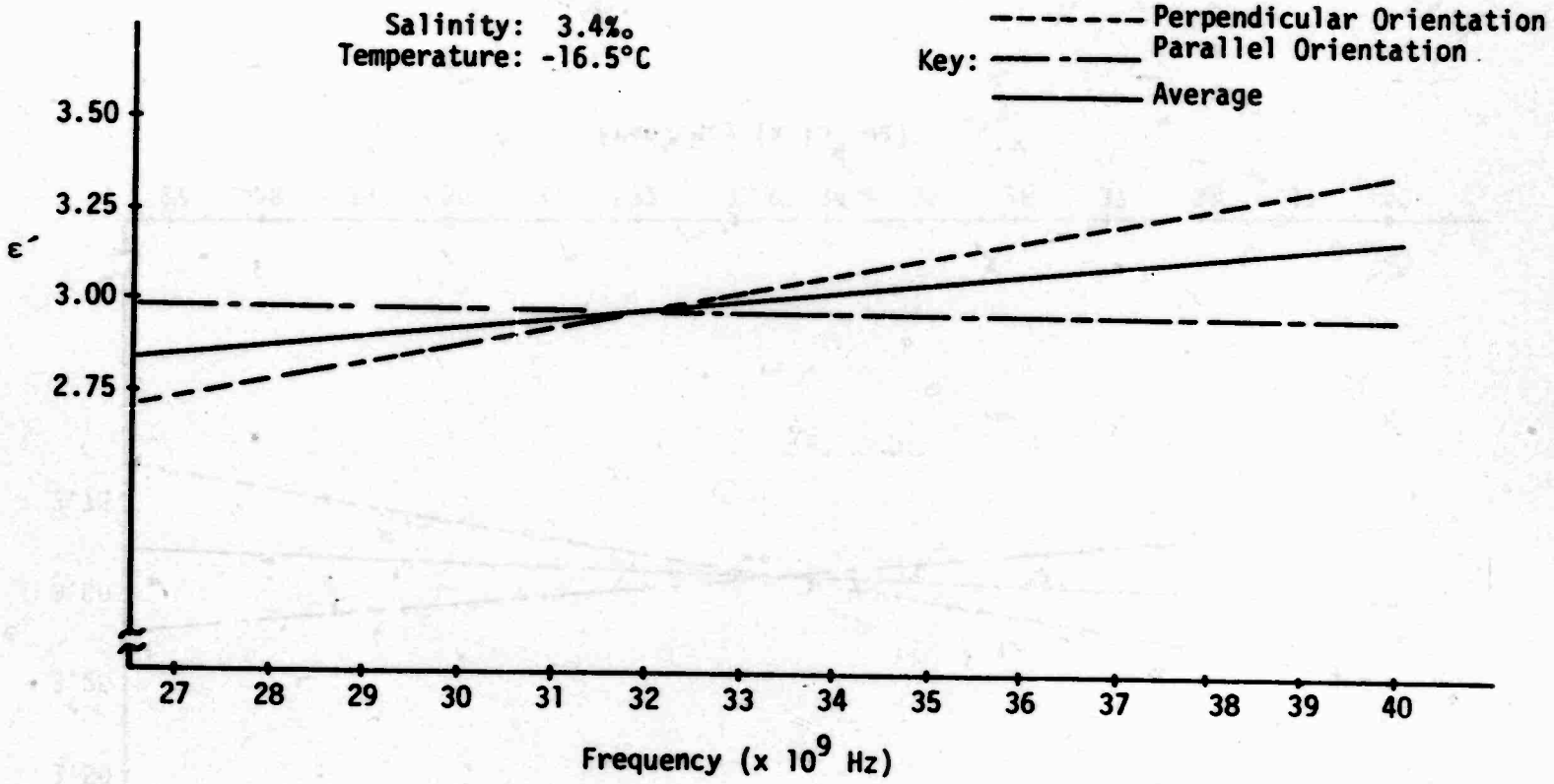

Figure A-7: ε´ versus Frequency

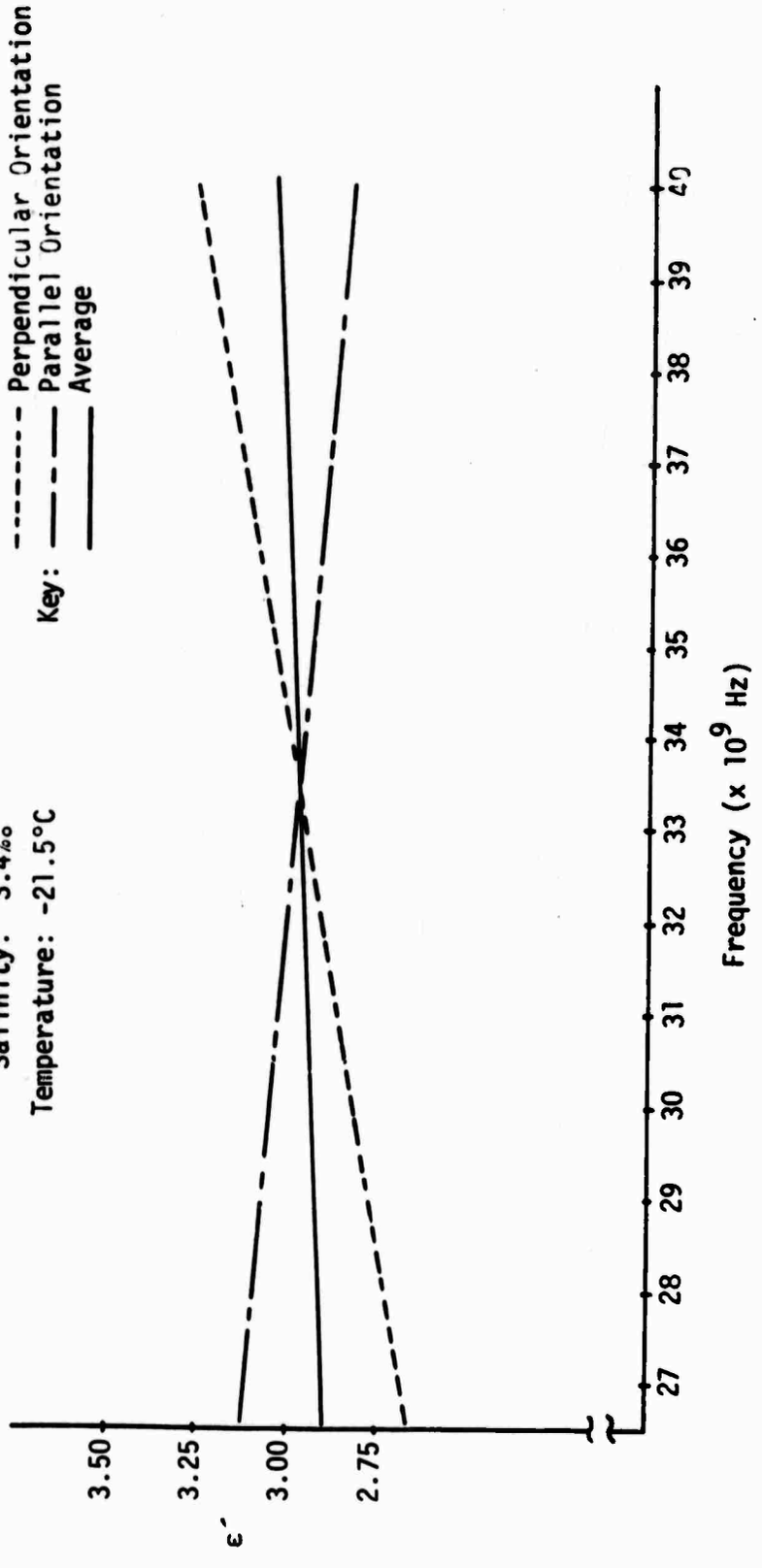

Figure A-8: ε´ versus Frequency

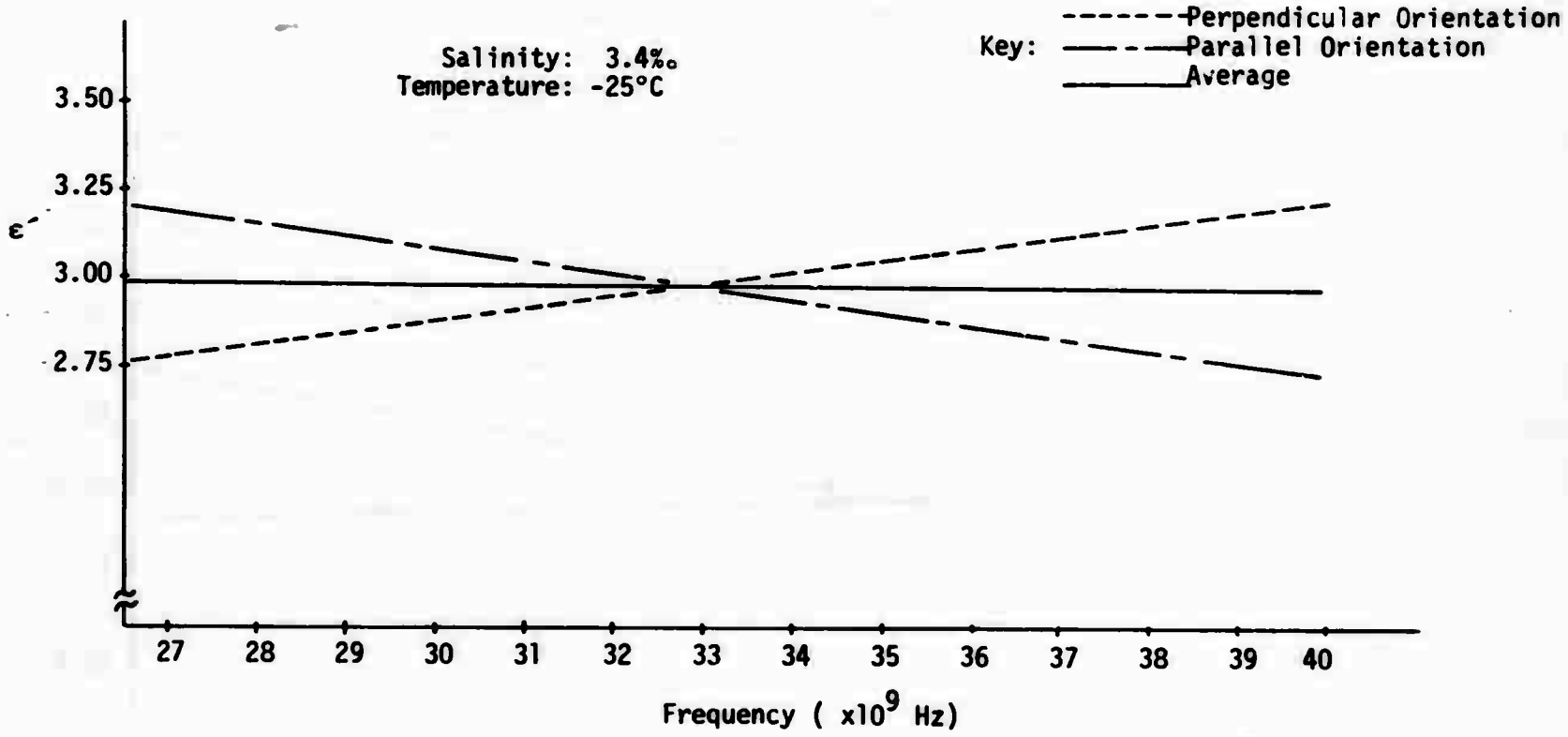

Figure A-9: ε' versus Frequency

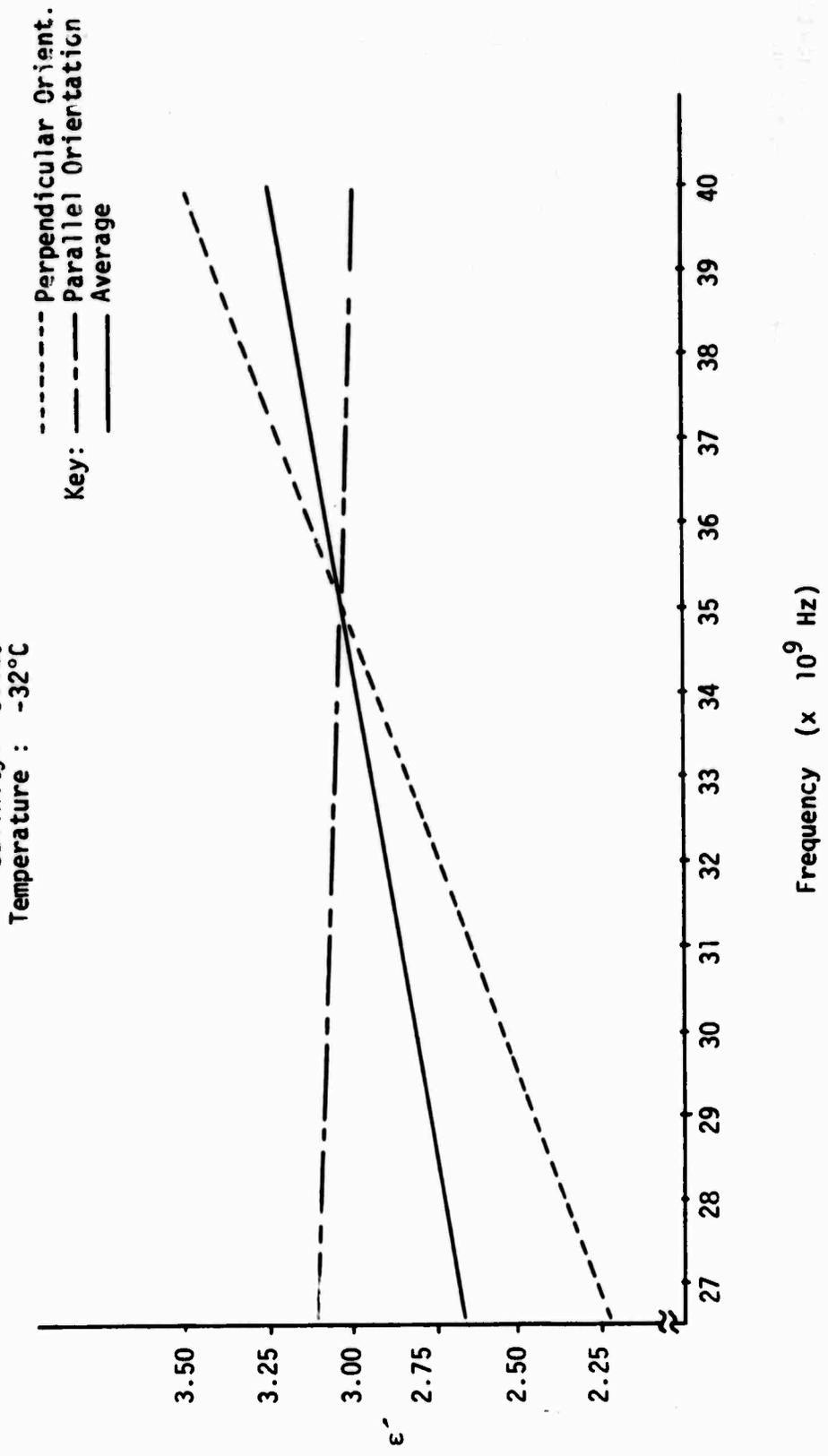

Figure A-10: ε´ vs. Frequency

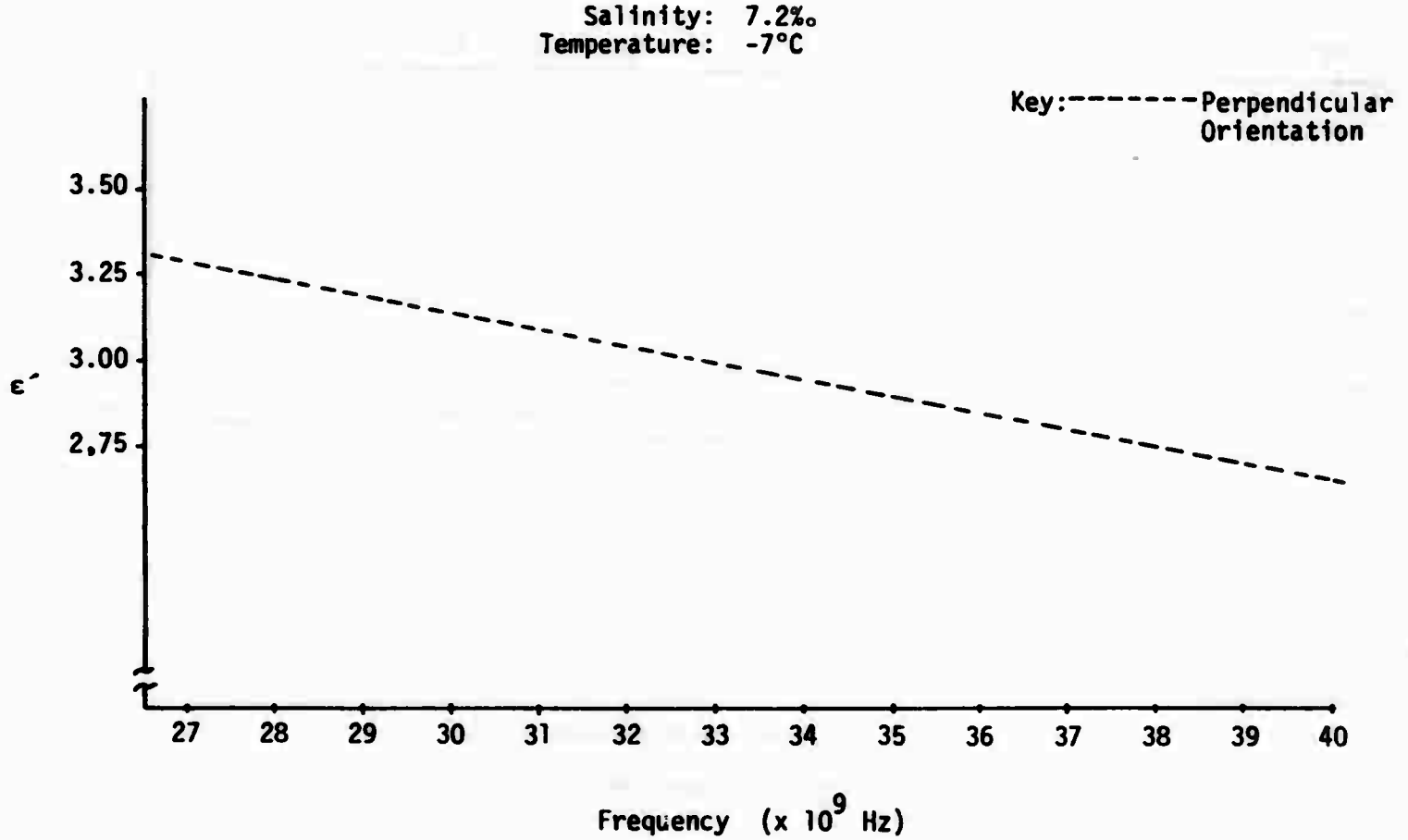

Figure A-11: ε' versus Frequency

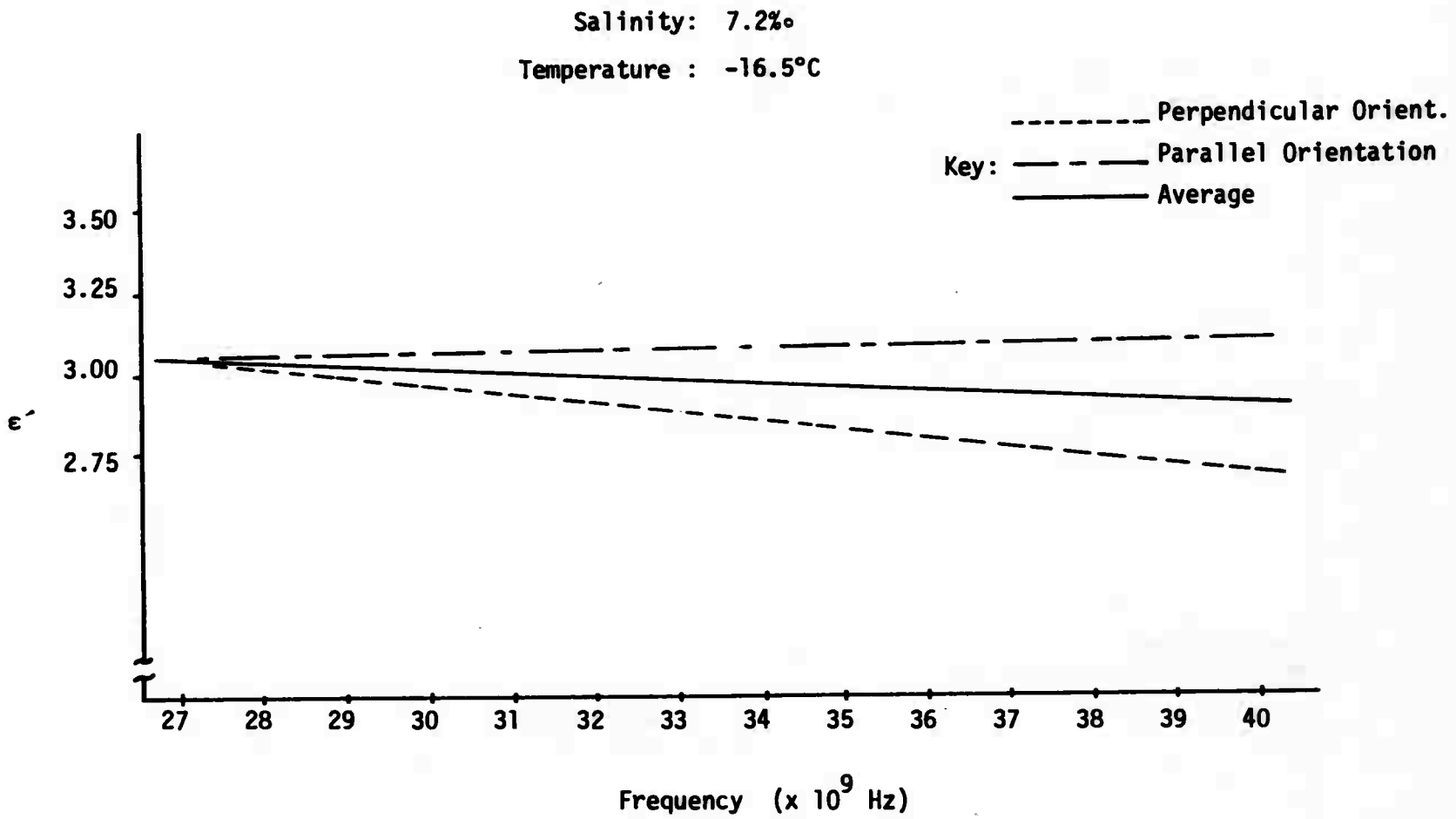

Figure A-12: ε´ versus Frequency

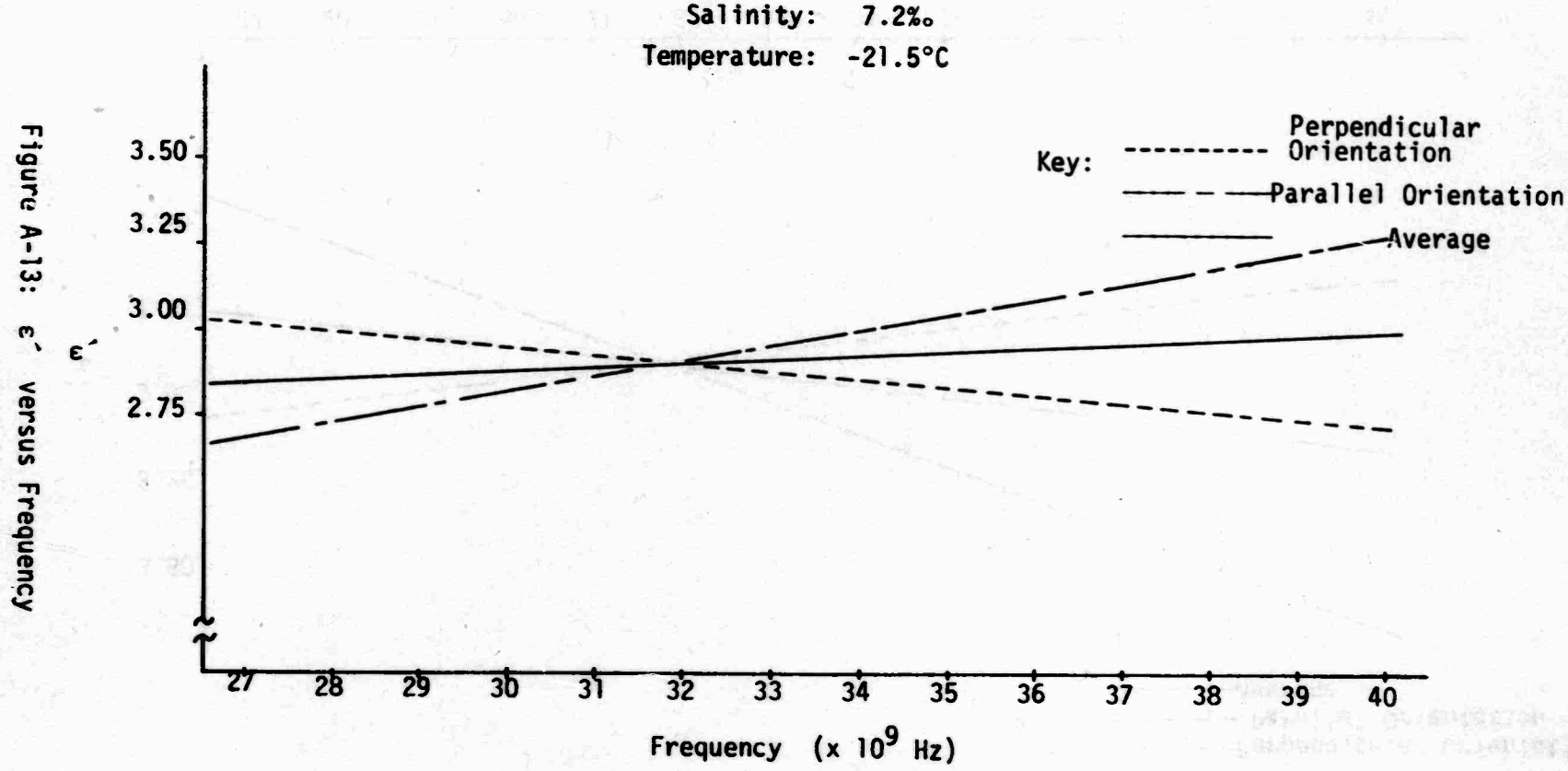

Figure A-13: ε' versus Frequency

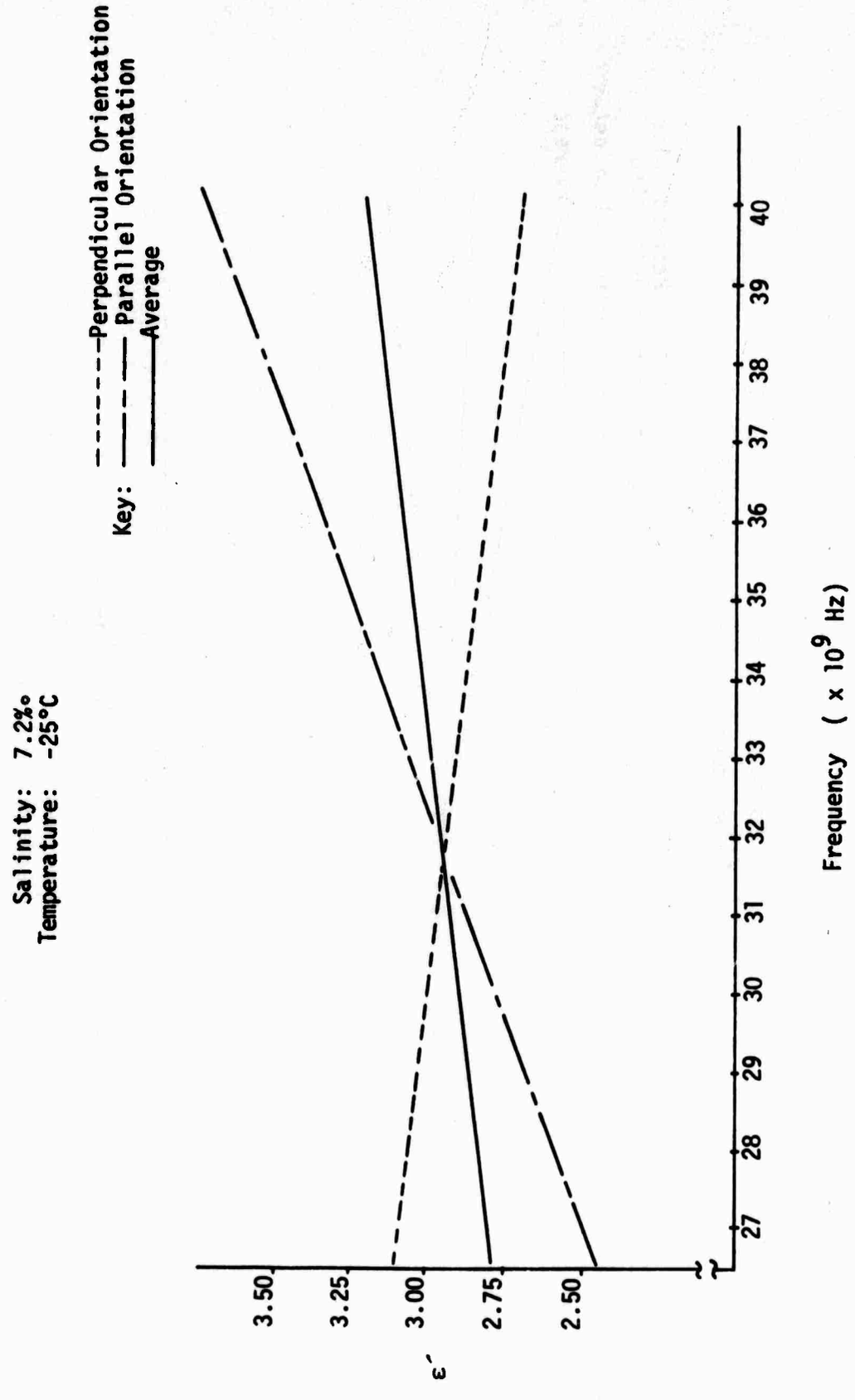

Figure A-14: ε´ versus Frequency

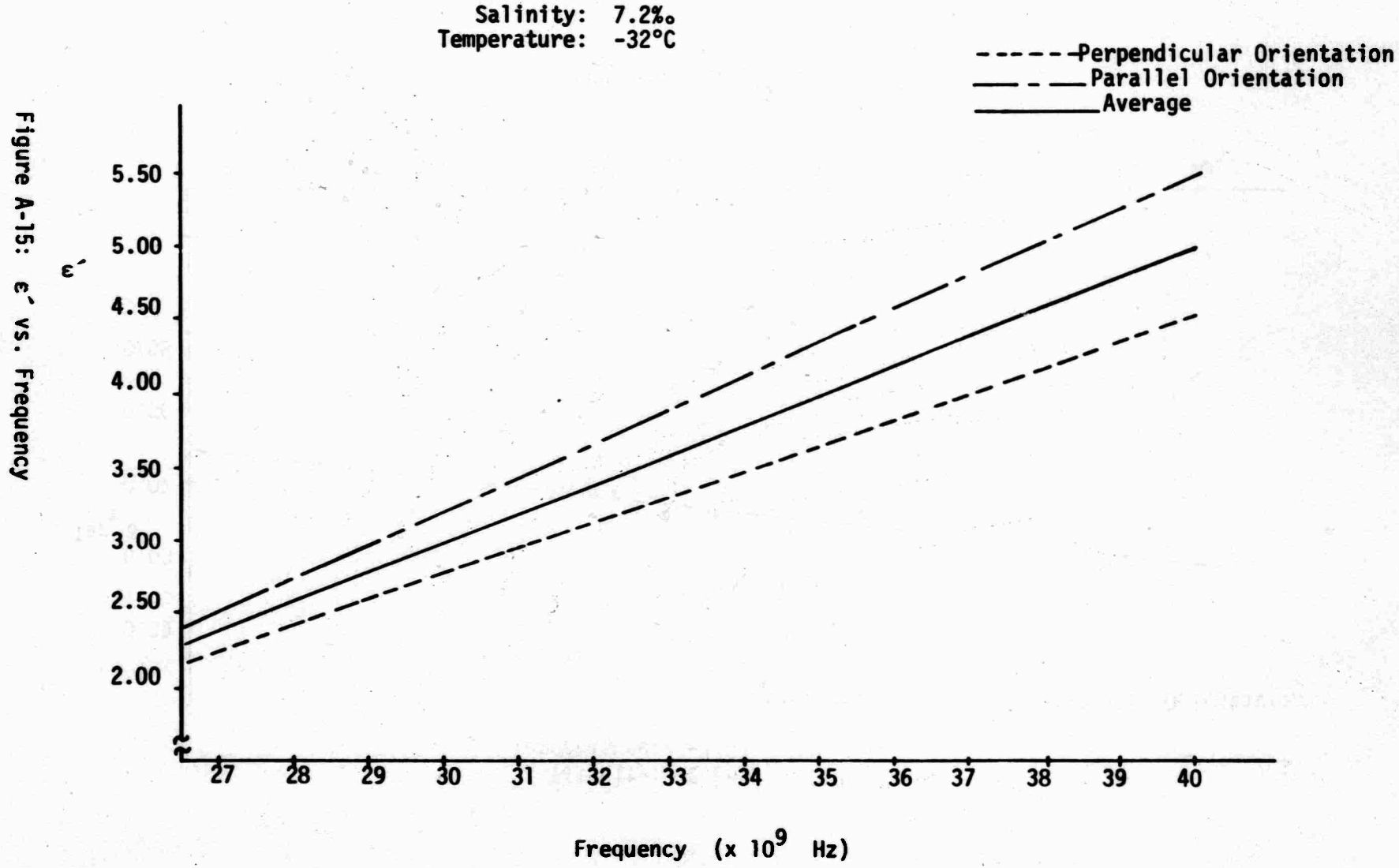

Figure A-15: ε′ vs. Frequency

Figure A-16: Tan δ versus Frequency

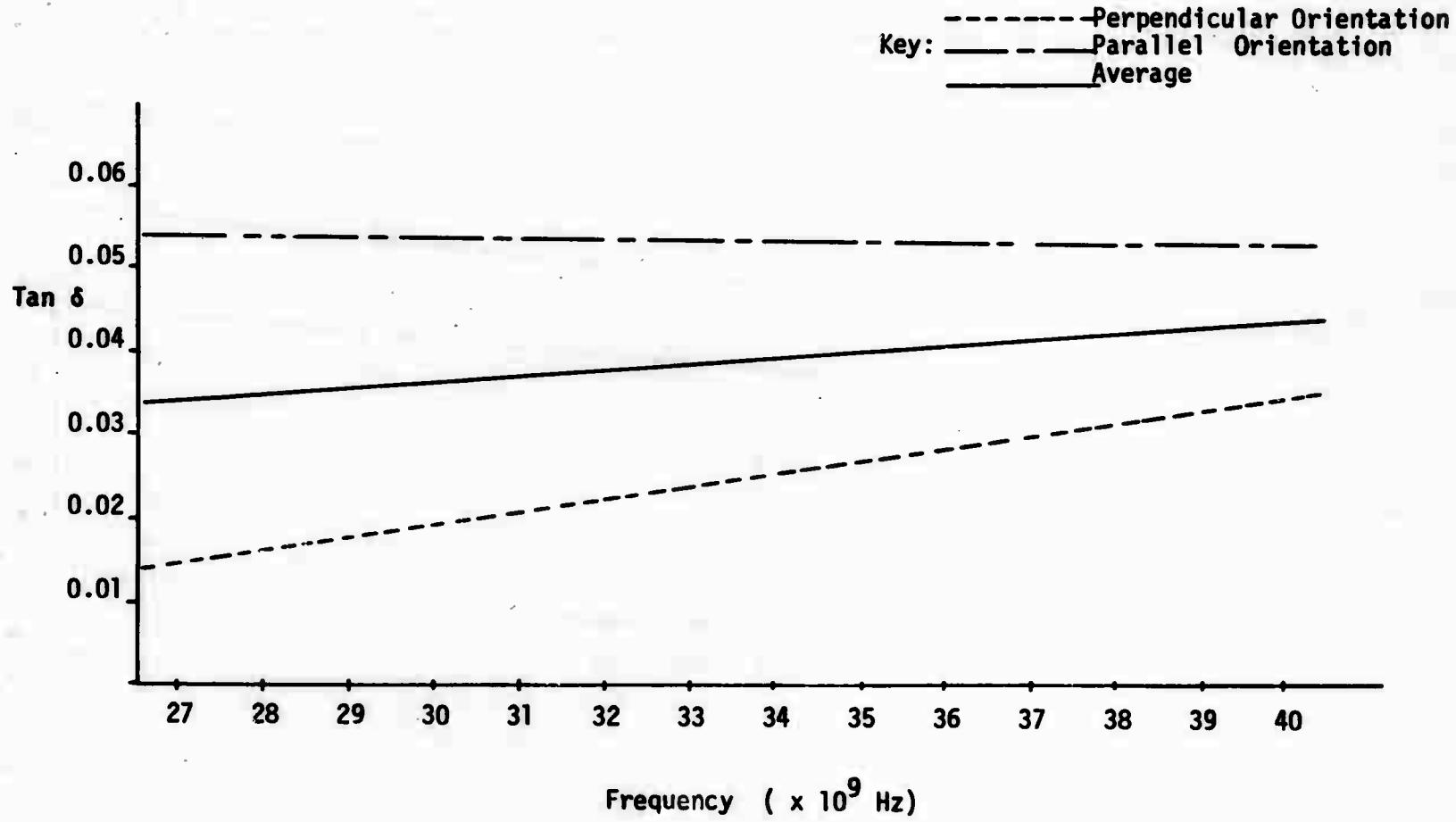

Figure A-17: Tan δ versus Frequency

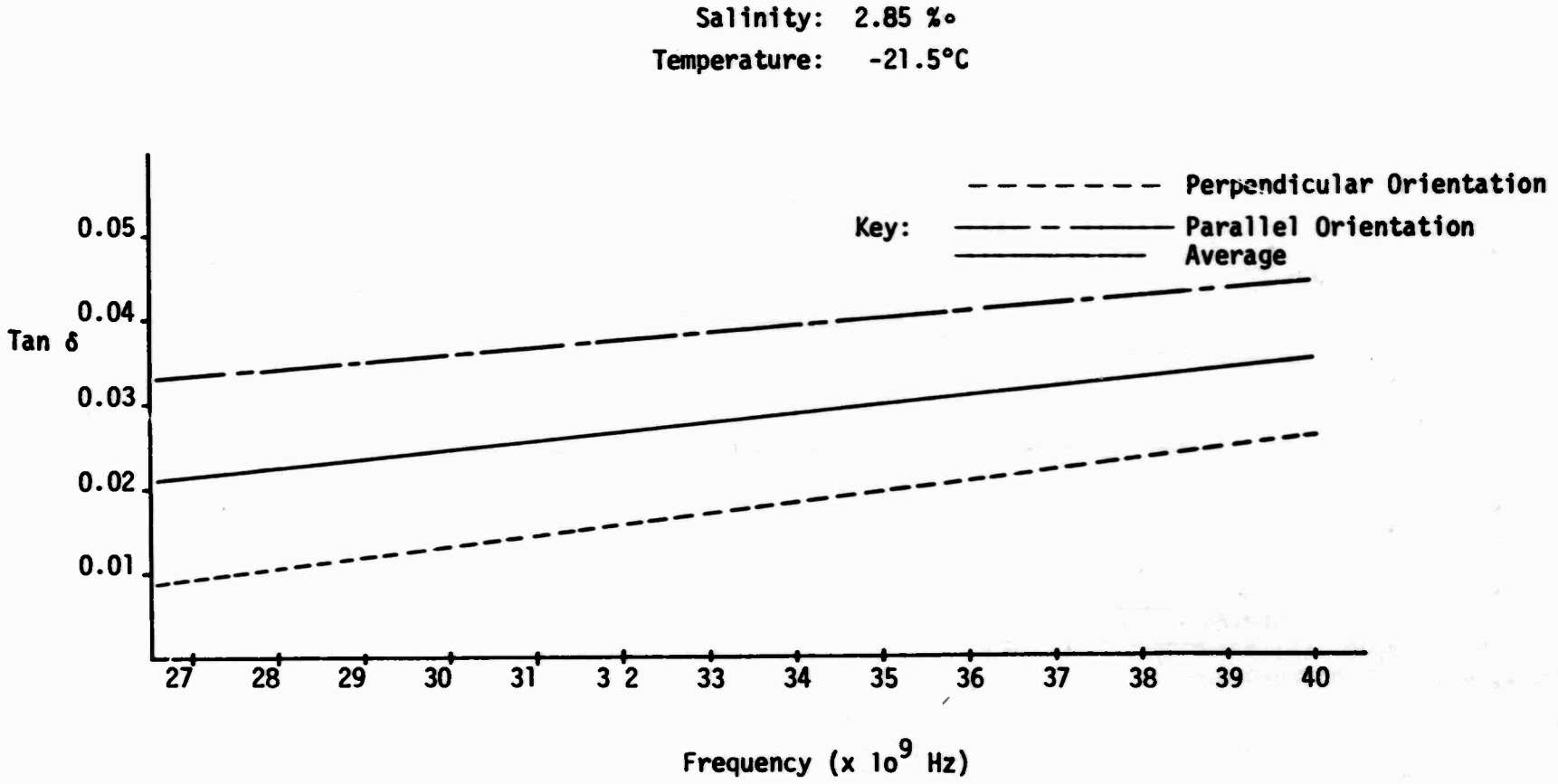

Figure A-18: Tan δ versus Frequency

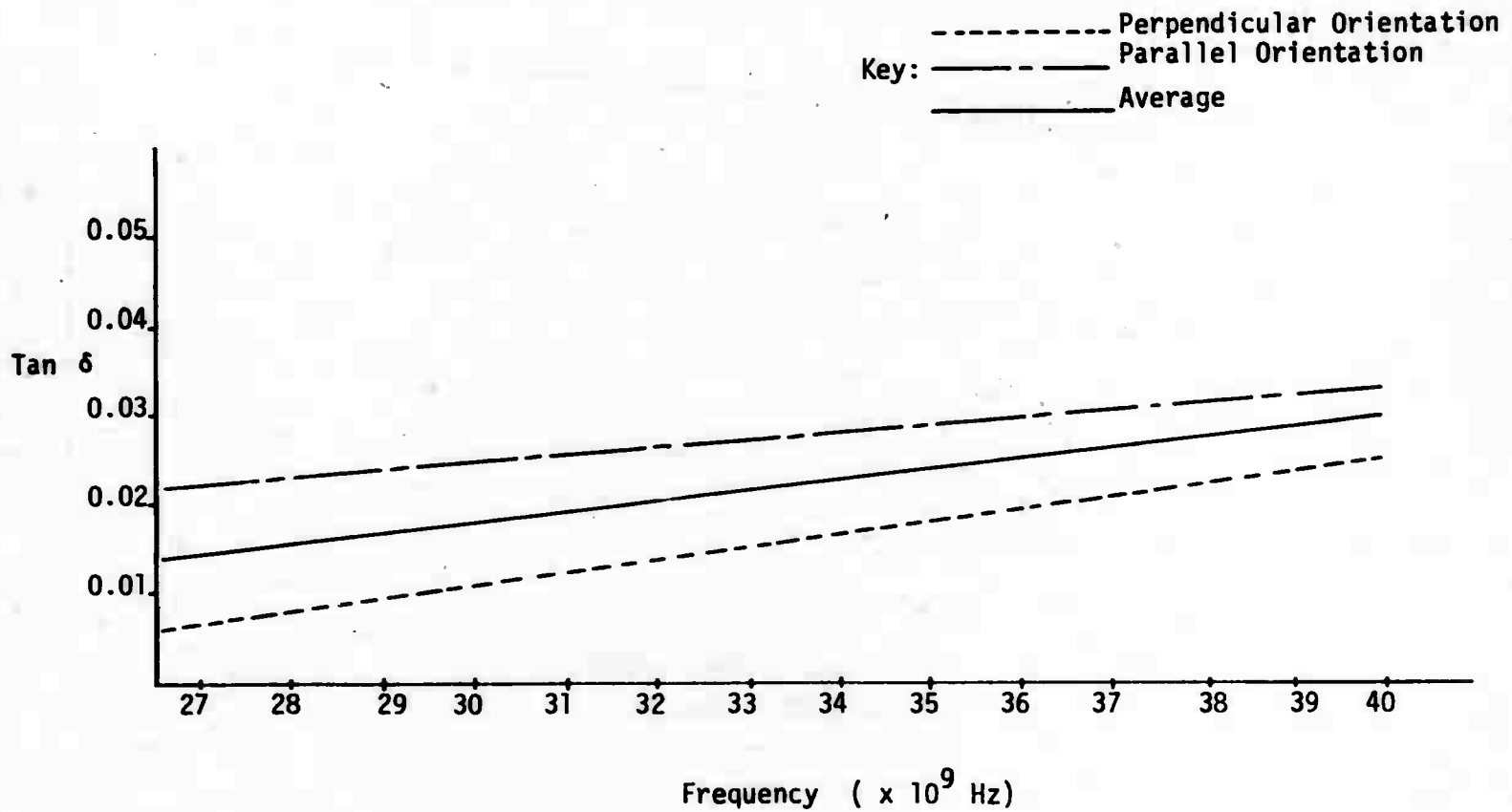

Figure A-19: Tan δ versus Frequency

Salinity: 2.85 ‰
Temperature: -32°C

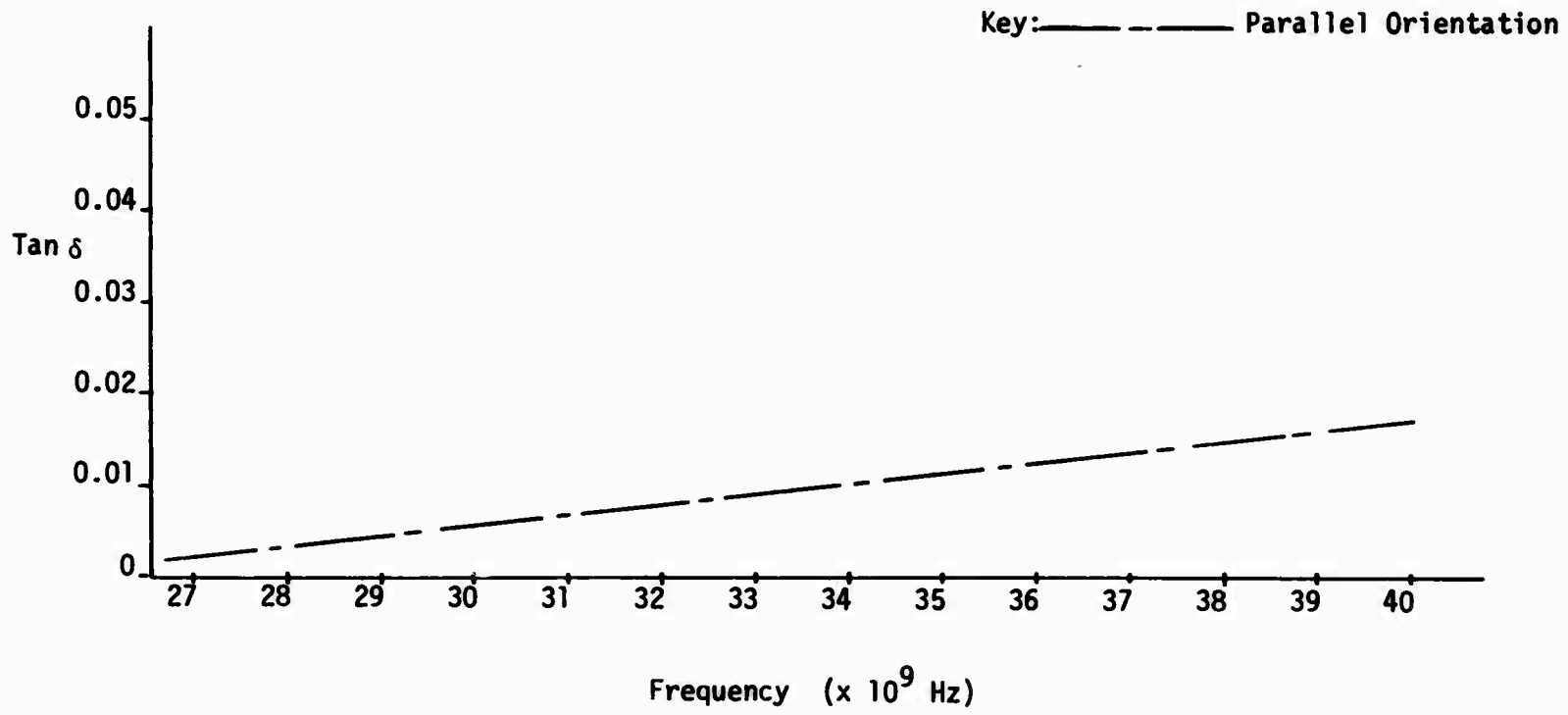

Figure A-20: Tan δ versus Frequency

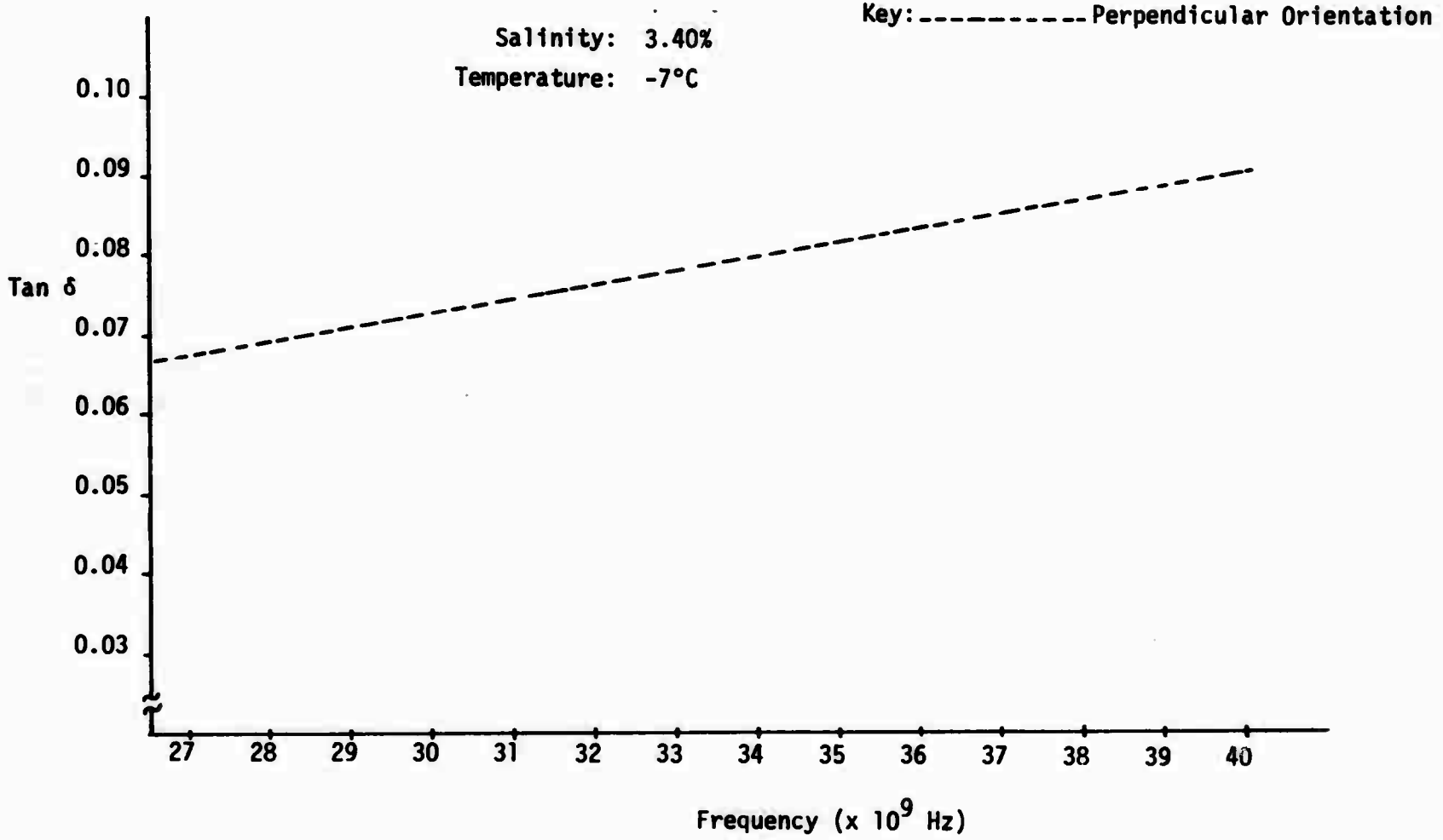

Figure A-21: Tan δ versus Frequency

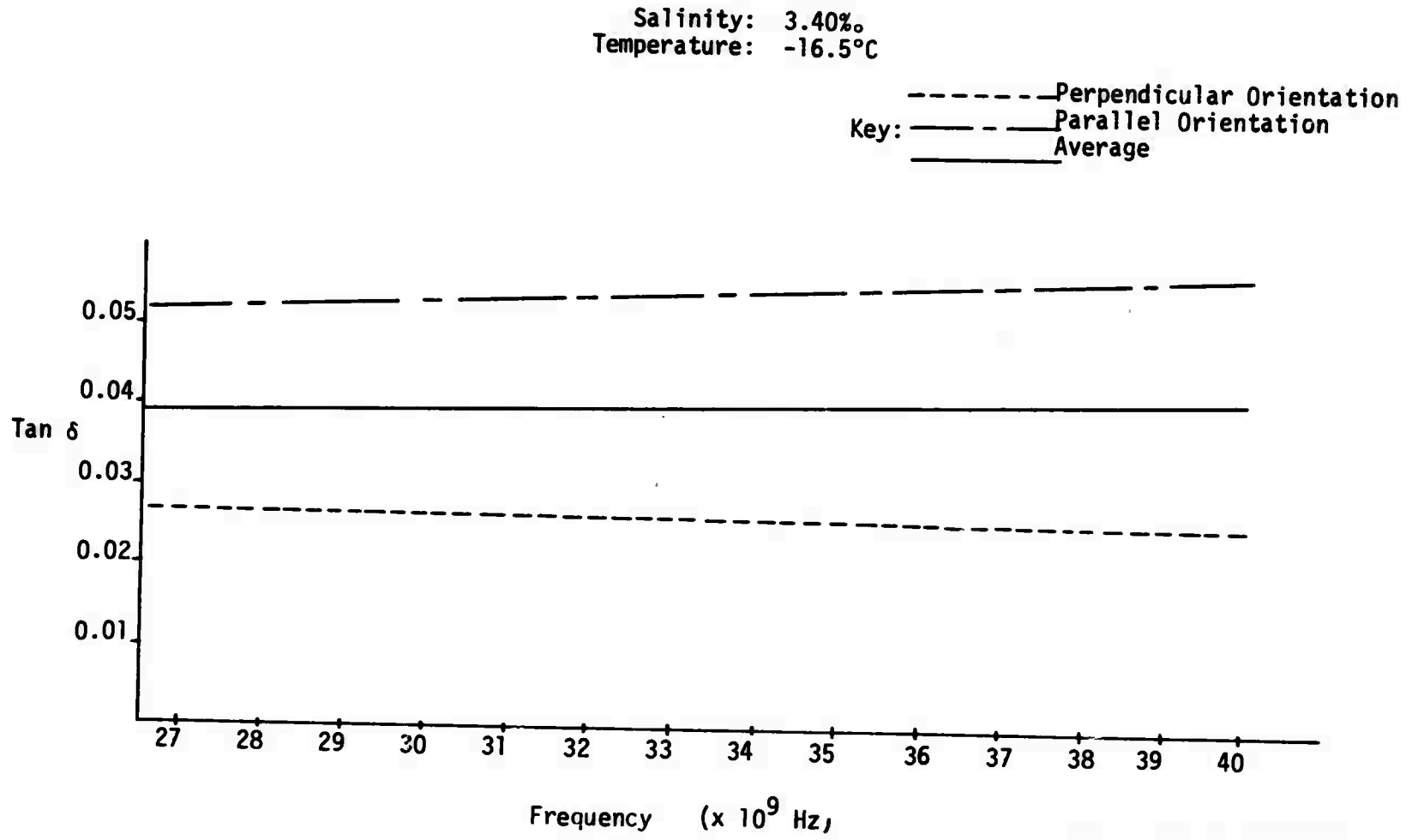

Figure A-22: Tan δ versus Frequency

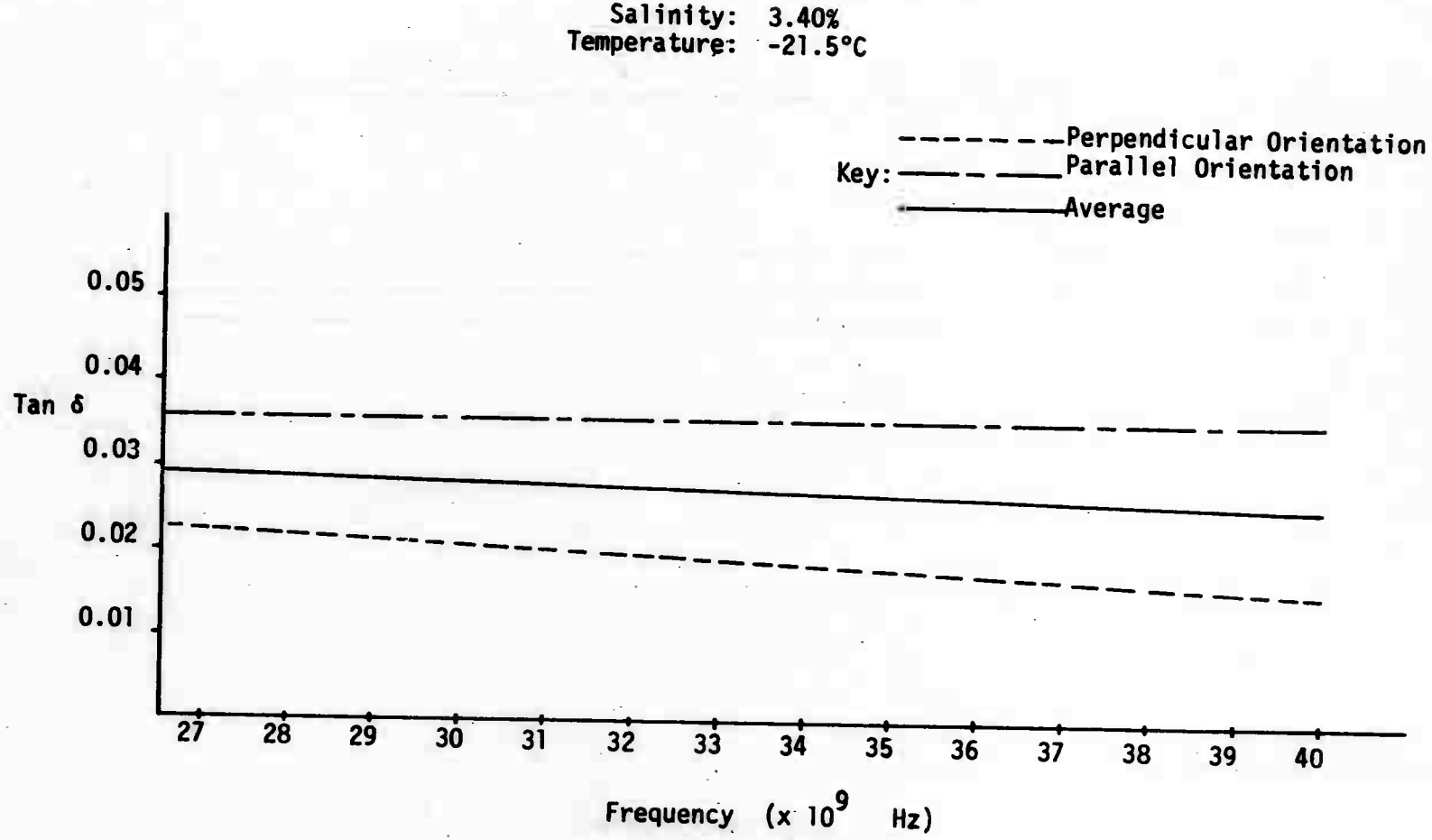

Figure A-23: Tan δ versus Frequency

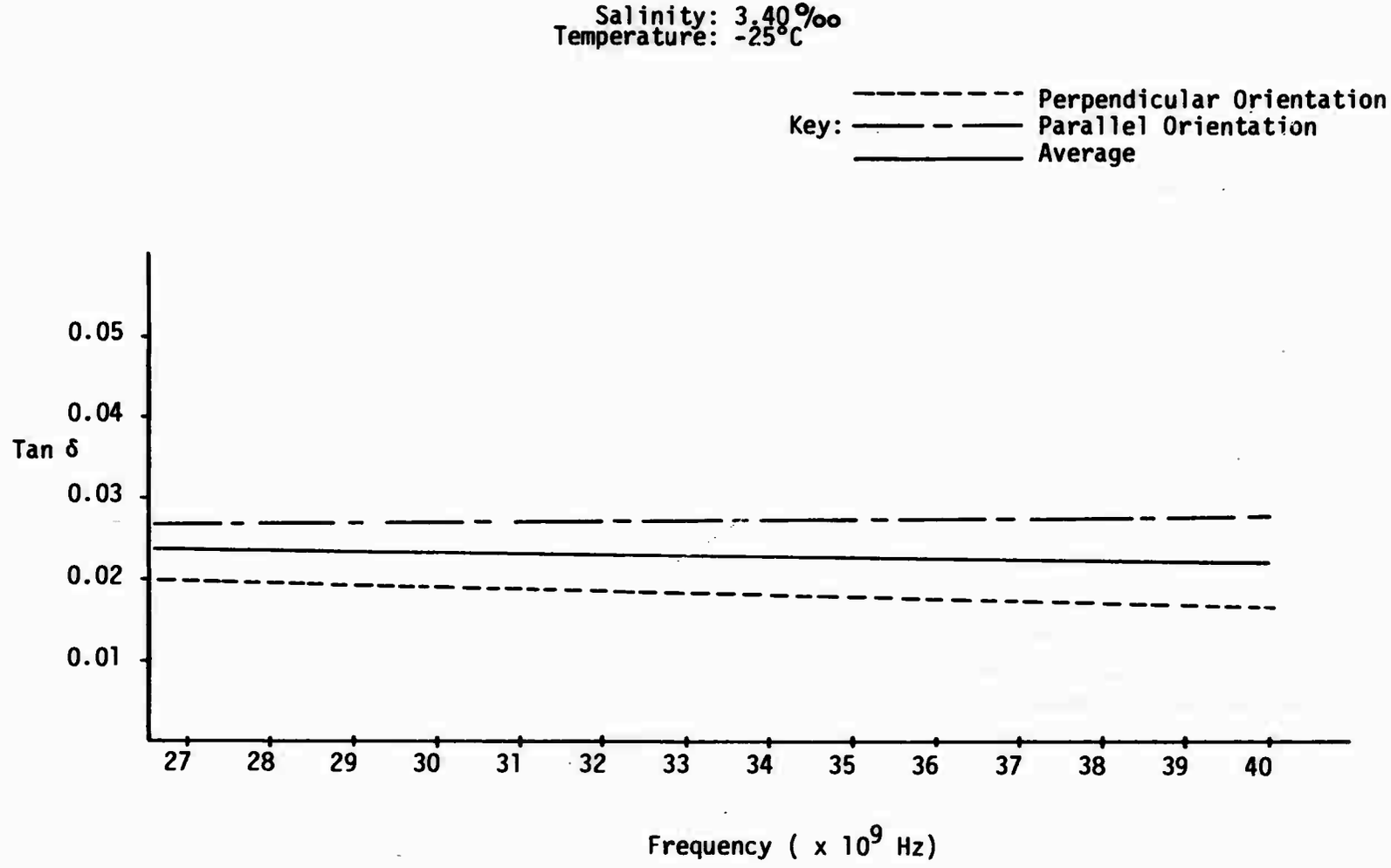

Figure A-24: Tan δ versus Frequency

Salinity:3.40 ‰
Temperature : -32°C

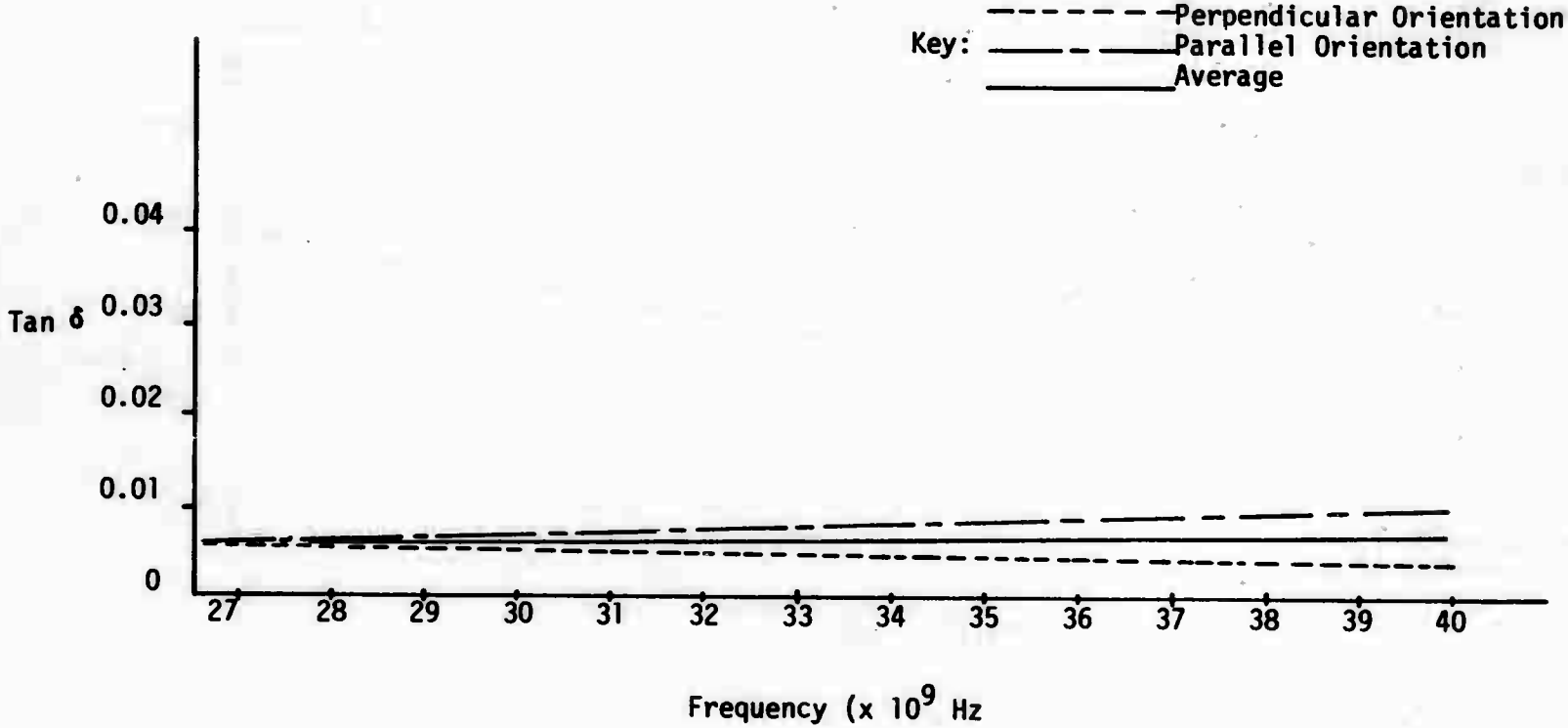

Figure A-25: Tan δ versus Frequency

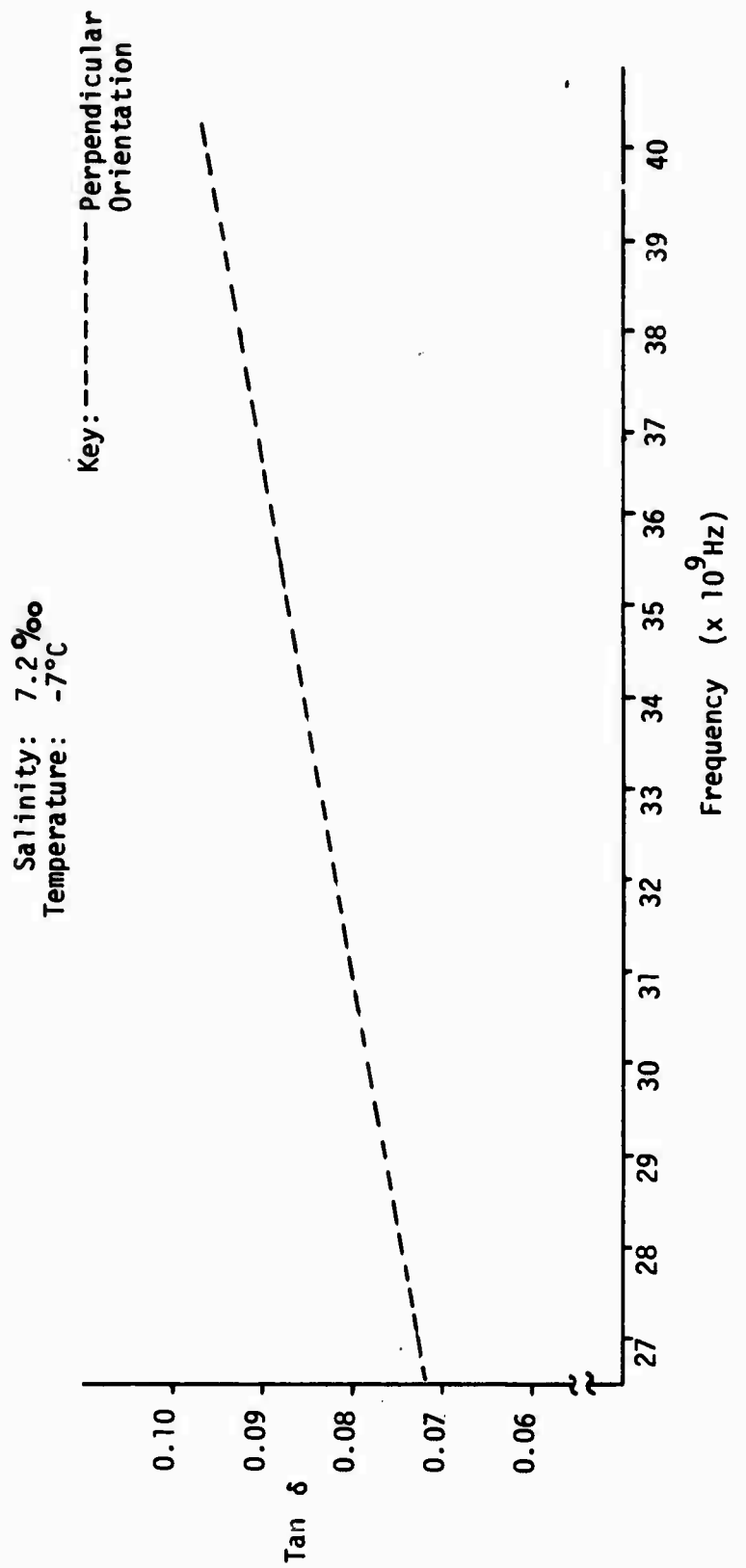

Figure A-26: Tan δ versus Frequency

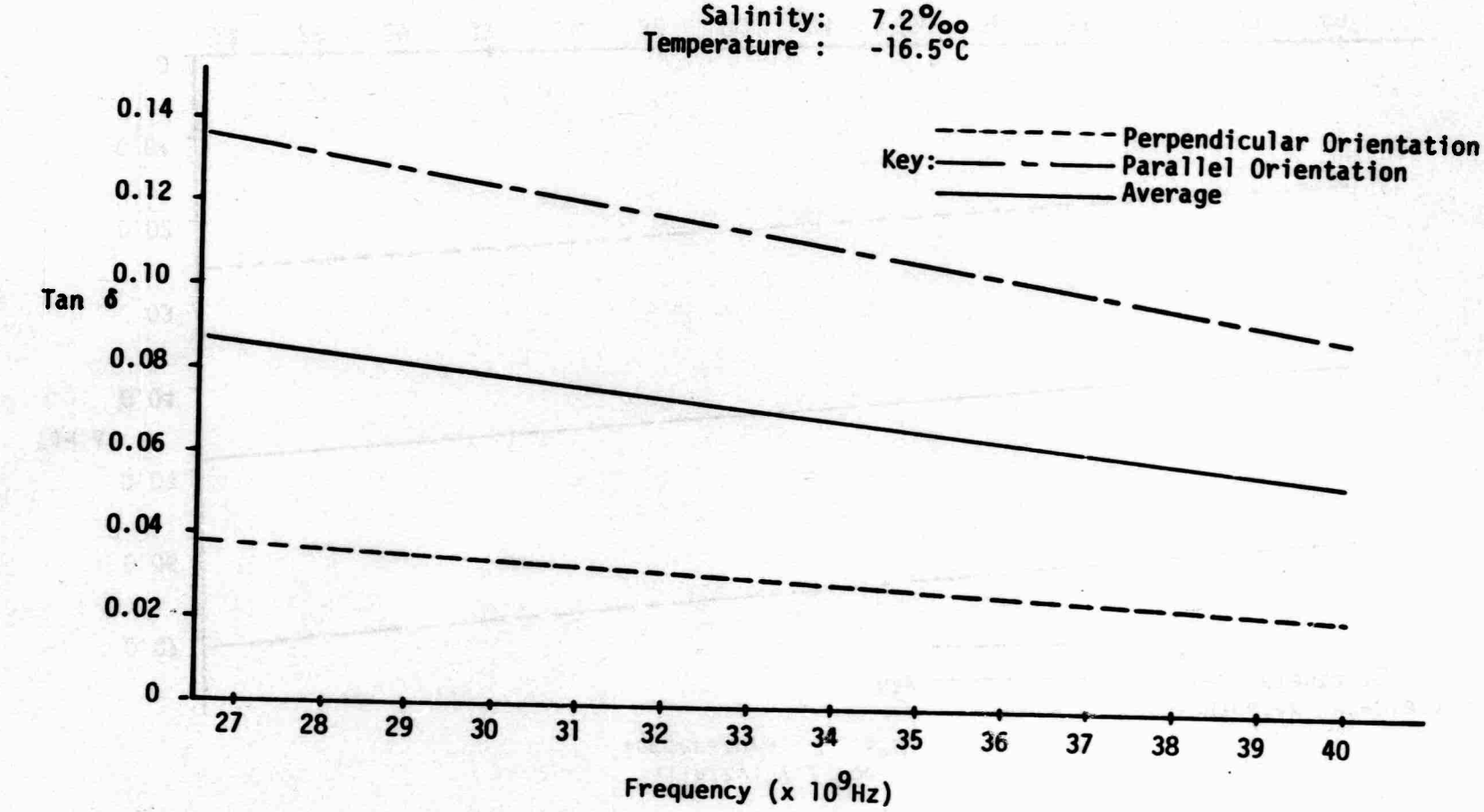

Figure A-27: Tan δ versus Frequency

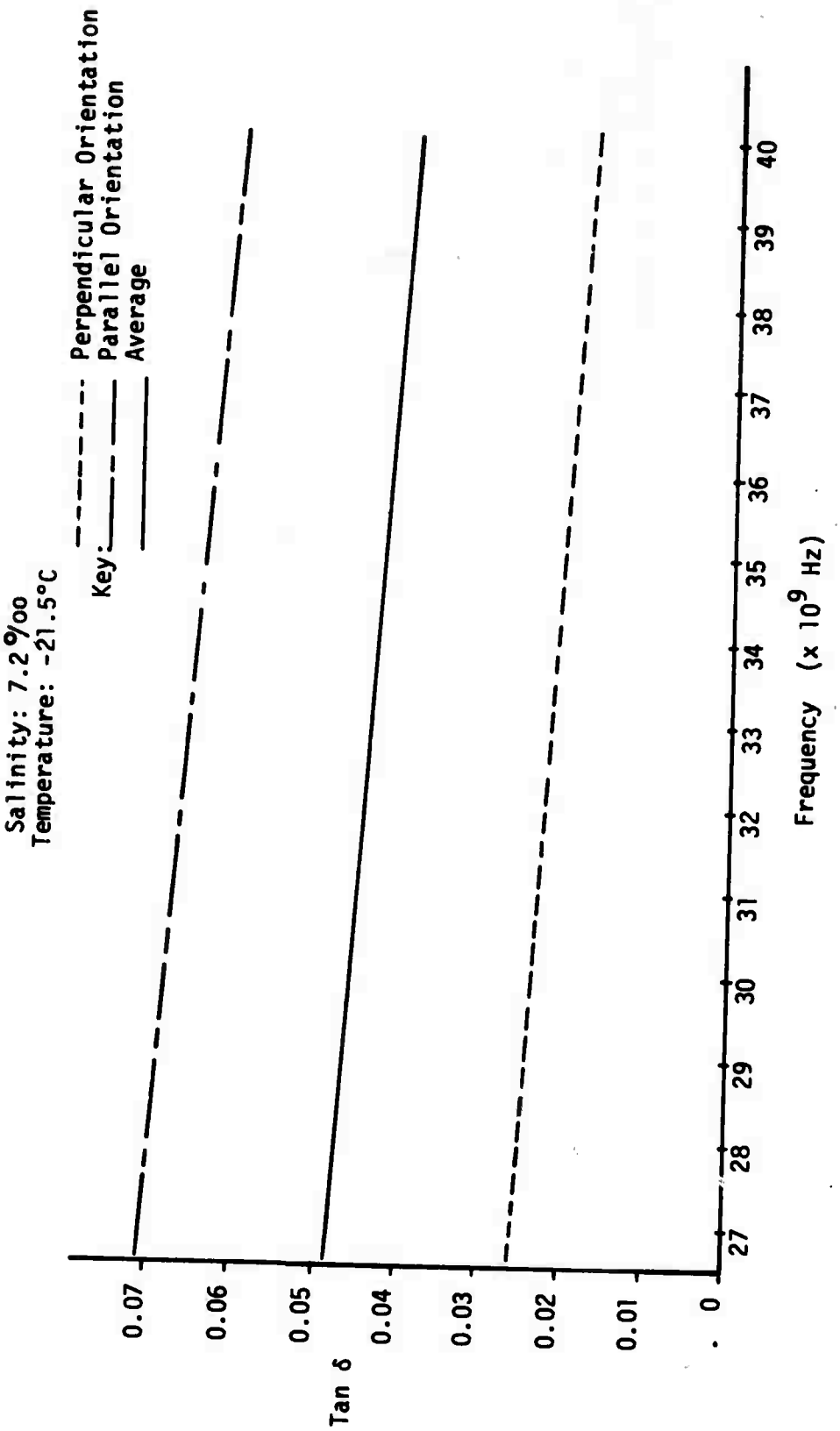

Figure A-28: Tan δ versus Frequency

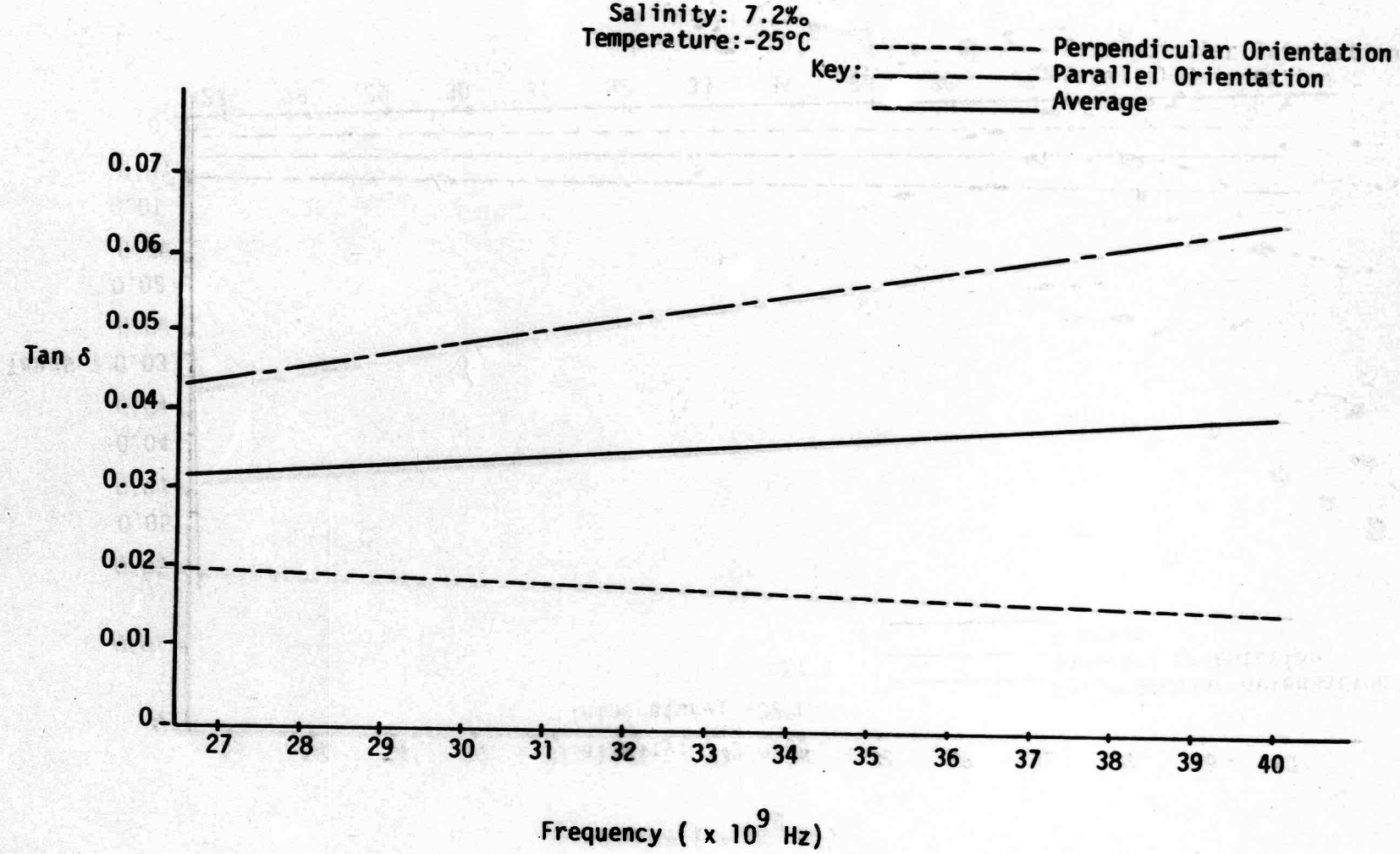

Figure A-29: Tan δ versus Frequency

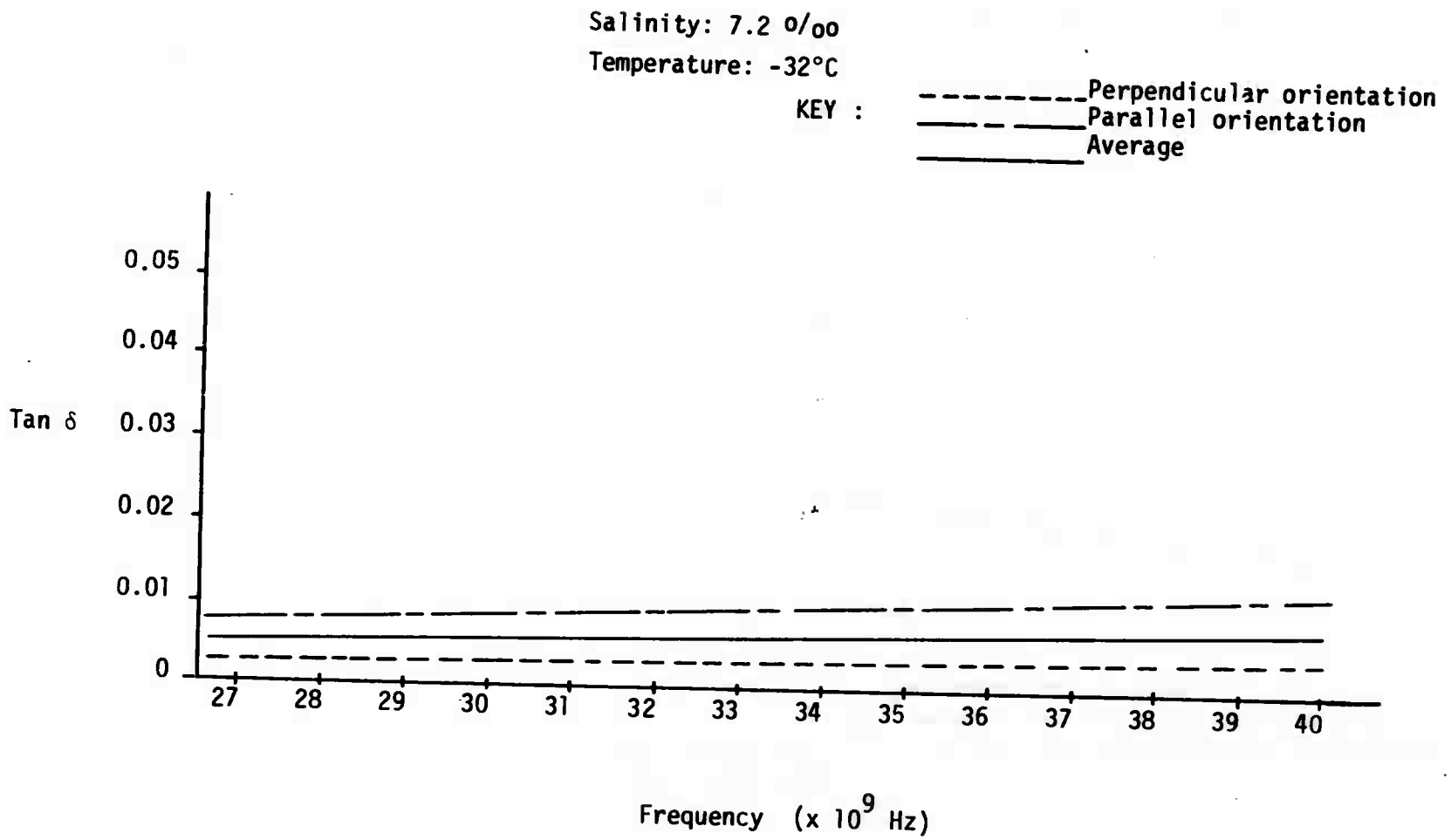

Figure A-30: Tan δ versus Frequency

REFERENCES

1. Lofgren, G. and Weeks, W.F., "Effect of growth parameters on substructure spacing in NaCl ice," Journal of Glaciology, 7, 153, (1969).
2. Weeks, W.F., "Studies of salt ice," USACRREL Research Report 80, (1961).
3. Weeks, W.F. and Assur, A., "Structural control of the vertical variation of the strength of sea and salt ice," USACRREL Research Report 113, (1964).
4. Hoekstra, R., Osterkamp, T.E., and Weeks, W.F., "The migration of liquid inclusions in single crystals," Journal of Geophysics Research, 70, 5035, (1965).
5. Weeks, W.F. and Lee O.S.,"The salinity distribution of young sea ice, " USACRREL Research Report 98, (1962).
6. Weeks, W.F. and Kovacs, A., "On pressure ridges," USACRREL Research Report for U.S. Coast Guard, January, 1970.
7. Auty, R.P. and Cole, R.H., "Dielectric properties of ice and solid D_2O," Journal of Chem. Physics, 20 (8), 1309, (1952).
8. Von Hippel, A.R., "Theory," Dielectric Materials and Applications. The Massachusetts Institute of Technology Press, Cambridge, Massachusetts, 1961.
9. Harvey, A.F., Microwave Engineering, New York, Academic Press Inc., 233, (1963).
10. Miller, G.B. and A. Moore,"Dielectric Parameters of Medium and Low Loss Liquids at Microwave Frequencies," Journal of Microwave Power, 3 (3), 114, (1968).
11. Tinga, W.R. and Edwards, E.M., "Dielectric measurements using swept frequency technique," Journal of Microwave Power, 3 (3), 114, (1968).
12. Evans, S., "Dielectric properties of ice and snow--a review," Journal of Glaciology, 5, 773, (1965).
13. Hoekstra, P. and P. Cappillino, "The Dielectric Properties of Sea Ice at UHF and Microwave Frequencies," U.S. Army Cold Regions Research and Engineering Laboratory, Hanover, New Hampshire, 1970

14. de Loor, G.P., "Dielectric Properties of Heterogeneous Mixtures Containing Water," Journal of Microwave Power, 3 (2), (1967).

15. Taylor, L.S., "Dielectric Properties of Mixtures," IEEE Transactions on Antennas and Propagation, Volume AP-13, Number 6, 943, (1965).